

ATTACHMENT I2

**WASTE ISOLATION PILOT PLANT
SHAFT SEALING SYSTEM
COMPLIANCE SUBMITTAL DESIGN REPORT**

(This page intentionally blank)

ATTACHMENT I2

**WASTE ISOLATION PILOT PLANT
SHAFT SEALING SYSTEM
COMPLIANCE SUBMITTAL DESIGN REPORT**

Adapted from:

SAND96-1326/1
Distribution Unlimited
Release Category UC-721
Printed August 1996

**Waste Isolation Pilot Plant
Shaft Sealing System
Compliance Submittal Design Report**

**Volume 1 of 2: Main Report
Appendices A and B**

**Repository Isolation Systems Department
Sandia National Laboratories
Albuquerque, NM 87185**

Abstract

This report describes a shaft sealing system design for the Waste Isolation Pilot Plant (WIPP), a proposed nuclear waste repository in bedded salt. The system is designed to limit entry of water and release of contaminants through the four existing shafts after the WIPP is decommissioned. The design approach applies redundancy to functional elements and specifies multiple, common, low-permeability materials to reduce uncertainty in performance. The system comprises 13 elements that completely fill the shafts with engineered materials possessing high density and low permeability. Laboratory and field measurements of component properties and performance provide the basis for the design and related evaluations. Hydrologic, mechanical, thermal, and physical features of the system are evaluated in a series of calculations. These evaluations indicate that the design guidance is addressed by effectively limiting transport of fluids within the shafts, thereby limiting transport of hazardous material to regulatory boundaries. Additionally, the use or adaptation of existing technologies for placement of the seal components combined with the use of available, common materials assure that the design can be constructed.

This report was modified to make it a part of the RCRA Facility Permit issued by the New Mexico Environment Department (NMED). The modifications included removal of Appendices C and D from the original document. Although they were important to demonstrate compliance with the performance standards in the hazardous waste regulations, they do not provide plans or procedures that will be implemented under the authority of the Permit. Appendices A, B and E are retained as Attachments to the Permit (Attachments I2-A, I2-B and I2-E). The Figures in

this report, which were interspersed in the text in the original document, have been moved to a common section following the References.

Acknowledgments

The work presented in this document represents the combined effort of a number of individuals at Sandia National Laboratories, Parsons Brinckerhoff (under contract AG-4909), INTERA (under contract AG-4910), RE/SPEC (under contract AG-4911), and Tech Reps. The Sandian responsible for the preparation of each section of the report and the lead individual(s) at firms under contract to Sandia that provided technical expertise are recognized below.

Section	Author(s)
Executive Summary	F.D. Hansen, Sandia
Section 1, Introduction	J.R. Tillerson, Sandia
Section 2, Site Geologic, Hydrologic, & Geochemical Setting	A.W. Dennis and S.J. Lambert, Sandia
Section 3, Design Guidance	A.W. Dennis, Sandia
Section 4, Design Description	A.W. Dennis, Sandia
Section 5, Material Specifications	F.D. Hansen, Sandia
Section 6, Construction Techniques	E.H. Ahrens, Sandia
Section 7, Structural Analyses of Shaft Seals	L.D. Hurtado, Sandia; M.C. Loken and L.L. Van Sambeek, RE/SPEC
Section 8, Hydrologic Evaluation of the Shaft Seal System	M.K. Knowles, Sandia; V.A. Kelley, INTERA
Section 9, Conclusions	J.R. Tillerson and A.W. Dennis, Sandia
Appendix A, Material Specifications	F.D. Hansen, Sandia
Appendix B, Shaft Sealing Construction Procedures	E.H. Ahrens, Sandia, with the assistance of Parsons Brinckerhoff Construction and Scheduling staff
Appendix C, Fluid Flow Analyses	M.K. Knowles, Sandia; V.A. Kelley, INTERA

Appendix D, Structural Analyses L.D. Hurtado, Sandia; M.C. Loken and L.L. Van
Sambeek, RE/SPEC

Appendix E, Design Drawings A.W. Dennis, Sandia; C.D. Mann, Parsons
Brinckerhoff, with the assistance of the Parsons
Brinckerhoff Design staff

Design reviews provided by Malcolm Gray, Atomic Energy Canada Ltd., Whiteshell Laboratory; Stephen Phillips, Phillips Mining, Geotechnical & Grouting, Inc.; and John Tinucci, Itasca Consulting Group, Inc. are appreciated, as are document reviews provided by Don Galbraith, U.S. Department of Energy Carlsbad Area Office; William Thompson, Carlsbad Area Office Technical Assistance Contractor; Robert Stinebaugh, Palmer Vaughn, Deborah Coffey, and Wendell Weart, Sandia.

T.P. Peterson and S.B. Kmetz, Tech Reps, served as technical editors of this document.

Table of Contents

Abstract	I2-i
Acknowledgments	I2-ii
Executive Summary	I2-1
Introduction	I2-1
Site Setting	I2-1
Design Guidance	I2-2
Design Description	I2-2
Structural Analysis	I2-4
Concluding Remarks	I2-7
1. Introduction	I2-8
1.1 Purpose of Compliance Submittal Design Report	I2-8
1.2 WIPP Description	I2-8
1.3 Performance Objective for WIPP Shaft Seal System	I2-8
1.4 Sealing System Design Development Process	I2-8
1.5 Organization of Document	I2-10
1.6 Systems of Measurement	I2-11
2. Site Geologic, Hydrologic, and Geochemical Setting	I2-12
2.1 Introduction	I2-12
2.2 Site Geologic Setting	I2-12
2.2.1 Regional WIPP Geology and Stratigraphy	I2-12
2.2.2 Local WIPP Stratigraphy	I2-13
2.2.3 Rock Mechanics Setting	I2-13
2.3 Site Hydrologic Setting	I2-14
2.3.1 Hydrostratigraphy	I2-14
2.3.2 Observed Vertical Gradients	I2-18
2.4 Site Geochemical Setting	I2-19
2.4.1 Regional and Local Geochemistry in Rustler Formation and Shallower Units	I2-19
2.4.2 Regional and Local Geochemistry in the Salado Formation	I2-21
3. Design Guidance	I2-24
3.1 Introduction	I2-24
3.2 Design Guidance and Design Approach	I2-24
4. Design Description	I2-26
4.1 Introduction	I2-26
4.2 Existing Shafts	I2-26
4.3 Sealing System Design Description	I2-29
4.3.1 Salado Seals	I2-30
4.3.1.1 Compacted Salt Column	I2-30
4.3.1.3 Upper, Middle, and Lower Concrete-Asphalt Waterstops	I2-32
4.3.1.4 Asphalt Column	I2-32

4.3.1.5 Shaft Station Monolith	12-33
4.3.2 Rustler Seals	12-33
4.3.2.1 Rustler Compacted Clay Column	12-33
4.3.2.2 Rustler Concrete Plug	12-34
4.3.3 Near-Surface Seals	12-34
4.3.3.1 Near-Surface Upper Compacted Earthen Fill	12-34
4.3.3.2 Near-Surface Concrete Plug	12-34
4.3.3.3 Near-Surface Lower Compacted Earthen Fill	12-34
5. Material Specification	12-35
5.1 Longevity	12-36
5.2 Materials	12-37
5.2.1 Mass Concrete	12-37
5.2.2 Compacted Clay	12-38
5.2.3 Asphalt	12-39
5.2.4 Compacted Salt Column	12-39
5.2.5 Cementitious Grout	12-40
5.2.6 Earthen Fill	12-41
5.3 Concluding Remarks	12-41
6. Construction Techniques	12-42
6.1 Multi-Deck Stage	12-42
6.2 Salado Mass Concrete (Shaft Station Monolith and Shaft Plugs)	12-42
6.3 Compacted Clay Columns (Salado and Rustler Formations)	12-43
6.4 Asphalt Waterstops and Asphaltic Mix Columns	12-43
6.5 Compacted WIPP Salt	12-43
6.6 Grouting of Shaft Walls and Removal of Liners	12-44
6.7 Earthen Fill	12-44
6.8 Schedule	12-45
7. Structural Analyses of Shaft Seals	12-46
7.1 Introduction	12-46
7.2 Analysis Methods	12-46
7.3 Models of Shaft Seals Features	12-46
7.3.1 Seal Material Models	12-46
7.3.2 Intact Rock Lithologies	12-47
7.3.3 Disturbed Rock Zone Models	12-47
7.4 Structural Analyses of Shaft Seal Components	12-47
7.4.1 Salado Mass Concrete Seals	12-47
7.4.1.1 Thermal Analysis of Concrete Seals	12-47
7.4.1.2 Structural Analysis of Concrete Seals	12-48
7.4.1.3 Thermal Stress Analysis of Concrete Seals	12-48
7.4.1.4 Effect of Dynamic Compaction on Concrete Seals	12-48
7.4.1.5 Effect of Clay Swelling Pressures on Concrete Seals	12-49
7.4.2 Crushed Salt Seals	12-49
7.4.2.1 Structural Analysis of Compacted Salt Seal	12-49

7.4.2.2 Pore Pressure Effects on Reconsolidation of Crushed Salt Seals	12-49
7.4.3 Compacted Clay Seals	12-50
7.4.4 Asphalt Seals	12-50
7.4.4.1 Thermal Analysis	12-50
7.4.4.2 Structural Analysis	12-50
7.4.4.3 Shrinkage Analysis	12-50
7.5 Disturbed Rock Zone Considerations	12-51
7.5.1 General Discussion of DRZ	12-51
7.5.2 Structural Analyses	12-51
7.5.2.1 Salado Salt	12-51
7.5.2.2 Salado Anhydrite Beds	12-51
7.5.2.3 Near-Surface and Rustler Formations	12-51
7.6 Other Analyses	12-52
7.6.1 Asphalt Waterstops	12-52
7.6.2 Shaft Pillar Backfilling	12-52
8. Hydrologic Evaluation of the Shaft Seal System	12-53
8.1 Introduction	12-53
8.2 Performance Models	12-53
8.3 Downward Migration of Rustler Groundwater	12-53
8.3.1 Analysis Method	12-54
8.3.2 Summary of Results	12-54
8.4 Gas Migration and Consolidation of Compacted Salt Column	12-55
8.4.1 Analysis Method	12-56
8.4.2 Summary of Results	12-56
8.5 Upward Migration of Brine	12-58
8.6 Intra-Rustler Flow	12-58
9. Conclusions	12-59
10. References	12-61
Appendix I2-A	Material Specifications A-1
Appendix I2-B	Shaft Sealing Construction Procedures B-1
Appendix C*	Fluid Flow Analyses C-1
Appendix D*	Structural Analyses D-1
Appendix I2-E	Design Drawings E-1

* Appendices C and D are not included in the facility Permit.

***FIGURES**

Figure I2-1	View of the WIPP underground facility
Figure I2-2	Location of the WIPP in the Delaware Basin
Figure I2-3	Chart showing major stratigraphic divisions, southeastern New Mexico
Figure I2-4	Generalized stratigraphy of the WIPP site showing repository level
Figure I2-5	Arrangement of the Air Intake Shaft sealing system
Figure I2-6	Multi-deck stage illustrating dynamic compaction
Figure I2-7	Multi-deck stage illustrating excavation for asphalt waterstop
Figure I2-8	Drop pattern for 6-m-diameter shaft using a 1.2-m-diameter tamper
Figure I2-9	Plan and section views of downward spin pattern of grout holes
Figure I2-10	Plan and section views of upward spin pattern of grout holes
Figure I2-11	Example of calculation of an effective salt column permeability from the depth-dependent permeability at a point in time
Figure I2-12	Effective permeability of the compacted salt column using the 95% certainty line

*NOTE: All Figures are attached following References

Tables

Table I2-1	Salado Brine Seepage Intervals ⁽¹⁾
Table I2-2	Permeability and Thickness of Hydrostratigraphic Units in Contact with Seals
Table I2-3	Freshwater Head Estimates in the Vicinity of the Air Intake Shaft
Table I2-4	Chemical Formulas, Distributions, and Relative Abundance of Minerals in the Rustler and Salado Formations (after Lambert, 1992)
Table I2-5	Major Solutes in Selected Representative Groundwater from the Rustler Formation and Dewey Lake Redbeds, in mg/L (after Lambert, 1992)
Table I2-6	Variations in Major Solutes in Brines from the Salado Formation, in mg/L (after Lambert, 1992)
Table I2-7	Shaft Sealing System Design Guidance
Table I2-8	Drawings Showing Configuration of Existing WIPP Shafts (Drawings are in Appendix I2-E)
Table I2-9	Summary of Information Describing Existing WIPP Shafts
Table I2-10	Drawings Showing the Sealing System for Each Shaft (Drawings are in Appendix I2-E)
Table I2-11	Drawings Showing the Shaft Station Monoliths (Drawings are in Appendix I2-E)
Table I2-12	Summary of Results from Performance Model

Acronyms

1		
2	AIS	Air Intake Shaft
3	AMM	asphalt mastic mix
4	CFR	Code of Federal Regulations
5	DOE	Department of Energy
6	DRZ	disturbed rock zone
7	EPA	Environmental Protection Agency
8	HMAC	hot mix asphalt concrete
9	MDCF	Multimechanism Deformation Coupled Fracture
10	MD	Munson-Dawson
11	NMED	New Mexico Environment Department
12	NMVP	No Migration Variance Petition
13	PA	performance assessment
14	PTM	Plug Test Matrix
15	QA	quality assurance
16	SMC	Salado Mass Concrete
17	SPVD	Site Preliminary Design Validation
18	SSSPT	Small Scale Seal Performance Test
19	SWCF	Sandia WIPP Central Files
20	TRU	transuranic
21	WIPP	Waste Isolation Pilot Plant

Executive Summary

Introduction

This report documents a shaft seal system design developed as part of a submittal to the Environmental Protection Agency (**EPA**) and the New Mexico Environment Department (**NMED**) that will demonstrate regulatory compliance of the Waste Isolation Pilot Plant (**WIPP**) for disposal of transuranic waste. The shaft seal system limits entry of water into the repository and restricts the release of contaminants. Shaft seals address fluid transport paths through the opening itself, along the interface between the seal material and the host rock, and within the disturbed rock surrounding the opening. The entire shaft seal system is described in this Permit Attachment and its three appendices, which include seal material specifications, construction methods, rock mechanics analyses, fluid flow evaluations, and the design drawings. The design represents a culmination of several years of effort that has most recently focused on providing to the EPA and NMED a viable shaft seal system design. Sections of this report and the appendices explore function and performance of the WIPP shaft seal system and provide well documented assurance that such a shaft seal system could be constructed using available materials and methods. The purpose of the shaft seal system is to limit fluid flow within four existing shafts after the repository is decommissioned. Such a seal system would not be implemented for several decades, but to establish that regulatory compliance can be achieved at that future date, a shaft seal system has been designed that exhibits excellent durability and performance and is constructable using existing technology. The design approach is conservative, applying redundancy to functional elements and specifying various common, low-permeability materials to reduce uncertainty in performance. It is recognized that changes in the design described here will occur before construction and that this design is not the only possible combination of materials and construction strategies that would adequately limit fluid flow within the shafts.

Site Setting

One of the Department of Energy's (**DOE's**) site selection criteria is a favorable geologic setting which minimizes fluid flow as a transport mechanism. Groundwater hydrology in the proximity of the WIPP site is characterized by geologic strata with low transmissivity and low hydrologic gradients, both very positive features with regard to sealing shafts. For purposes of performance evaluations, hydrological analyses divide lithologies and requirements into the Rustler Formation (and overlying strata) and the Salado Formation, comprised mostly of salt. The principal design concern is fluid transport phenomena of seal materials and lithologies within the Salado Formation. The rock mechanics setting is an important consideration in terms of system performance. Rock properties affect hydrologic response of the shaft seal system. The stratigraphic section contains lithologies that exhibit brittle and ductile behavior. A zone of rock around the shafts is disturbed owing to the creation of the opening. The disturbed rock zone (**DRZ**) is an important design consideration because it possesses higher permeability than intact rock. Host rock response and its potential to fracture, flow, and heal around WIPP shaft openings are relevant to the performance of the shaft seal system.

Design Guidance

Use of both engineered and natural barriers to isolate wastes from the accessible environment is required by 20.4.1.500 NMAC (incorporating 40 CFR §§264.111 and 264.601) and 40 CFR §191.14(d). The use of engineered barriers to prevent or substantially delay movement of water, hazardous constituents, or radionuclides toward the accessible environment is required by 20.4.1.500 NMAC (incorporating 40 CFR §§264.111 and 264.601) and 40 CFR §194.44. Hazardous constituent release performance standards are specified in Permit Module V and 20.4.1.500 NMAC (incorporating 40 CFR §§264.111(b), 264.601(a), and 264 Subpart F). Radionuclide release limits are specified in 40 CFR §191 for the entire repository system (EPA, 1996a; 1996b). Design guidance for the shaft seal system addresses the need for the WIPP to comply with system requirements and to follow accepted engineering practices using demonstrated technology. Design guidance is categorized below:

- limit hazardous constituents reaching regulatory boundaries,
- restrict groundwater flow through the sealing system,
- use materials possessing mechanical and chemical compatibility,
- protect against structural failure of system components,
- limit subsidence and prevent accidental entry, and
- utilize available construction methods and materials.

Discussions of the design presented in the text of this report and the details presented in the appendices respond to these qualitative design guidelines. The shaft seal system design was completed under a Quality Assurance program that includes review by independent, qualified experts to assure the best possible information is provided to the DOE on selection of engineered barriers (40 CFR §194.27). Technical reviewers examined the complete design including conceptual, mathematical, and numerical models and computer codes (40 CFR §194.26). The design reduces the impact of uncertainty associated with any particular element by using multiple sealing system components and by using components constructed from different materials.

Design Description

The shaft sealing system comprises 13 elements that completely fill the shaft with engineered materials possessing high density and low permeability. Salado Formation components provide the primary regulatory barrier by limiting fluid transport along the shaft during and beyond the 10,000-year regulatory period. Components within the Rustler Formation limit commingling between brine-bearing members, as required by state regulations. Components from the Rustler to the surface fill the shaft with common materials of high density, consistent with good engineering practice. A synopsis of each component is given below.

Shaft Station Monolith. At the bottom of each shaft a salt-saturated concrete monolith supports the local roof. A salt-saturated concrete, called Salado Mass Concrete (**SMC**), is specified and is placed using a conventional slickline construction procedure where the concrete is batched at the surface. SMC has been tailored to match site conditions. The salt-handling shaft and the waste-handling shaft have sumps which also will be filled with salt-saturated concrete as part of the monolith.

1 **Clay Columns.** A sodium bentonite is used for three compacted clay components in the Salado
2 and Rustler Formations. Although alternative construction specifications are viable, labor-
3 intensive placement of compressed blocks is specified because of proven performance. Clay
4 columns effectively limit brine movement from the time they are placed to beyond the
5 10,000-year regulatory period. Stiffness of the clay is sufficient to promote healing of fractures in
6 the surrounding rock salt near the bottom of the shafts, thus removing the proximal DRZ as a
7 potential pathway. The Rustler clay column limits brine communication between the Magenta
8 and Culebra Members of the Rustler Formation.

9 **Concrete-Asphalt Waterstop Components.** Concrete-asphalt waterstop components
10 comprise three elements: an upper concrete plug, a central asphalt waterstop, and a lower
11 concrete plug. Three such components are located within the Salado Formation. These
12 concrete-asphalt waterstop components provide independent shaft cross-section and DRZ
13 seals that limit fluid transport, either downward or upward. Concrete fills irregularities in the
14 shaft wall, while use of the salt-saturated concrete assures good bonding with salt. Salt creep
15 against the rigid concrete components establishes a compressive stress state and promotes
16 early healing of the salt DRZ surrounding the concrete plugs. The asphalt intersects the shaft
17 cross section and the DRZ.

18 **Compacted Salt Column.** Each shaft seal includes a column of compacted WIPP salt with 1.5
19 percent weight water added to the natural material. Construction demonstrations have shown
20 that mine-run WIPP salt can be dynamically compacted to a density equivalent to approximately
21 90% of the average density of intact Salado salt. The remaining void space is removed through
22 consolidation caused by creep closure. The salt column becomes less permeable as density
23 increases. The location of the compacted salt column near the bottom of the shaft assures the
24 fastest achievable consolidation of the compacted salt column after closure of the repository.
25 Analyses indicate that the salt column becomes an effective long-term barrier in under 100
26 years.

27 **Asphalt Column.** An asphalt-aggregate mixture is specified for the asphalt column, which
28 bridges the Rustler/Salado contact and provides a seal essentially impermeable to brine for the
29 shaft cross-section and the shaft wall interface. All asphalt is placed with a heated slickline.

30 **Concrete Plugs.** A concrete plug is located just above the asphalt column and keyed into the
31 surrounding rock. Mass concrete is separated from the cooling asphalt column with a layer of
32 fibercrete, which permits work to begin on the overlying clay column before the asphalt has
33 completely cooled. Another concrete plug is located near the surface, extending downward from
34 the top of the Dewey Lake Redbeds.

35 **Earthen Fill.** The upper shaft is filled with locally available earthen fill. Most of the fill is
36 dynamically compacted (the same method used to construct the salt column) to a density
37 approximating the surrounding lithologies. The uppermost earthen fill is compacted with a
38 sheepsfoot roller or vibratory plate compactor.

Structural Analysis

Structural issues pertaining to the shaft seal system have been evaluated. Mechanical, thermal, physical, and hydrological features of the system are included in a broad suite of structural calculations. Conventional structural mechanics applications would normally calculate load on system elements and compare the loads to failure criteria. Several such conventional calculations have been performed and show that the seal elements exist in a favorable, compressive stress state that is low in comparison to the strength of the seal materials. Thermal analyses have been performed to examine the effects of concrete heat of hydration and heat transfer for asphalt elements. Coupling between damaged rock and fluid flow and between the density and permeability of the consolidating salt column is evaluated within the scope of structural calculations. The appendices provide descriptions of various structural calculations conducted as part of the design study. The purpose of each calculation varies; however, the calculations generally address one or more of the following concerns: (1) stability of the component, (2) influences of the component on hydrological properties of the seal and surrounding rock, or (3) construction methods. Stability calculations address:

- potential for thermal cracking of concrete;
- structural loads on seal components resulting from salt creep, gravity, swelling clay, dynamic compaction, or possible repository-generated gas pressures.

Structural calculations defining input conditions to hydrological calculations include:

- spatial extent of the DRZ within the Salado Formation salt beds as a function of depth, time, and seal material;
- fracturing and DRZ development within Salado Formation interbeds;
- shaft-closure induced consolidation of compacted salt columns; and
- impact of pore pressures on salt consolidation.

Construction analyses examine:

- placement and structural performance of asphalt waterstops, and
- potential subsidence reduction through backfilling the shaft station areas.

Structural calculations model shaft features including representation of the host rock and its damaged zone as well as the seal materials themselves. Two important structural calculations discussed below are unique to shaft seal applications.

DRZ Behavior. The development and subsequent healing of a DRZ that forms in the rock mass surrounding the WIPP shafts is a significant concern in the seal design. It is well known that a DRZ will develop in rock salt adjacent to the shaft upon excavation. Placement of rigid components in the shaft promotes healing within the salt DRZ as seal elements restrain inward creep and reduce the stress difference. Two computer models to calculate development and

1 extent of the salt DRZ are used. The first model uses a ratio of stress invariants to predict
2 fracture; the second approach uses a damage stress criterion. The temporal and spatial extent
3 of the DRZ along the entire shaft length is evaluated. Several analyses are performed to
4 examine DRZ behavior of the rock salt surrounding the shaft. The time-dependent DRZ
5 development and subsequent healing in the Salado salt surrounding each of the four seal
6 materials are considered. All seal materials below a depth of about 300 m provide sufficient
7 rigidity to heal the DRZ, a phenomenon that occurs quickly around rigid components near the
8 shaft bottom. An extensive calculation is made of construction effects on the DRZ during
9 placement of the asphalt-concrete waterstops. The time-dependent development of the DRZ
10 within anhydrite and polyhalite interbeds of the Salado Formation is calculated. For all
11 interbeds, the factor of safety against shear or tensile fracturing increases with depth into the
12 rock surrounding the shaft wall. These results indicate that a continuous DRZ will not develop in
13 nonsalt Salado rocks. Rock mechanics analysis also determines which of the near surface
14 lithologies fracture in the proximity of the shaft. Results from these rock mechanics analyses are
15 used as input conditions for the fluid-flow analyses.

16 **Compacted Salt Behavior.** Unique application of crushed salt as a seal component required
17 development of a constitutive model for salt reconsolidation. The model developed includes a
18 nonlinear elastic component and a creep consolidation component. The nonlinear elastic
19 modulus is density-dependent, based on laboratory test data performed on WIPP crushed salt.
20 Creep consolidation behavior of crushed salt is based on three candidate models whose
21 parameters are obtained from model fitting to hydrostatic and shear consolidation test data
22 gathered for WIPP crushed salt. The model for consolidating crushed salt is used to predict
23 permeability of the salt column. The seal system prevents fluid transport to the consolidating
24 salt column to ensure that pore pressure does not unacceptably inhibit the reconsolidation
25 process. Calculations made to estimate fractional density of the crushed salt seal as a function
26 of time, depth, and pore pressure show consolidation time increases as pore pressure
27 increases, as expected. At a constant pore pressure of one atmosphere, compacted salt will
28 increase from its initial fractional density of 90% to 96% within 40, 80, and 120 years after
29 placement at the bottom, middle, and top of the salt component, respectively. At a fractional
30 density of 96%, the permeability of reconsolidating salt is approximately 10^{-18} m^2 . A pore
31 pressure of 2 MPa increases times required to achieve a fractional density of 96% to 92 years,
32 205 years, and 560 years at the bottom, middle, and top of the crushed salt column,
33 respectively. A pore pressure of 4 MPa would effectively prevent reconsolidation of the crushed
34 salt within 1,000 years. Fluid flow calculations show only minimal transport of fluids to the salt
35 column, so pore pressure equilibrium in the consolidating salt does not occur before low
36 permeabilities ($\sim 10^{-18} \text{ m}^2$) are achieved.

37 **Hydrologic Evaluations**

38 The ability of the shaft seal system to satisfy design guidance is determined by the performance
39 of the actual seal components within the physical setting in which they are constructed.
40 Important elements of the physical setting are hydraulic gradients of the region, properties of the
41 lithologic units surrounding a given seal component, and potential gas generation within the
42 repository. Hydrologic evaluations focus on processes that could result in fluid flow through the
43 shaft seal system and the ability of the seal system to limit any such flow. Transport of
44 radiological or hazardous constituents will be limited if the carrier fluids are similarly limited.
45 Physical processes that could impact seal system performance have been incorporated into four

models. These models evaluate: (1) downward migration of groundwater from the Rustler Formation, (2) gas migration and reconsolidation of the crushed salt seal component, (3) upward migration of brines from the repository, and (4) flow between water-bearing zones in the Rustler Formation.

Downward Migration of Rustler Groundwater. The shaft seal system is designed to limit groundwater flowing into and through the shaft sealing system. The principal source of groundwater to the seal system is the Culebra Member of the Rustler Formation. No significant sources of groundwater exist within the Salado Formation; however, brine seepage has been noted at a number of the marker beds and is included in the models. Downward migration of Rustler groundwater is limited to ensure that liquid saturation of the compacted salt column does not impact the consolidation process and to limit quantities of brine reaching the repository horizon. Consolidation of the compacted salt column will be most rapid immediately following seal construction. Simulations conducted for the 200-year period following closure demonstrate that, during this initial period, downward migration of Rustler groundwater is insufficient to impact the consolidation process. Rock mechanics analyses show that this period encompasses the reconsolidation process. Lateral migration of brine through the marker beds is quantified in the analysis and shown to be inconsequential. At steady-state, the flow rate is most dependent on permeability of the system. Potential flow paths within the seal system consist of the seal material, an interface with the surrounding rock, and the host rock DRZ. Low permeability is specified for the engineered materials, and construction methods ensure a tight interface. Thus the flow path most likely to impact performance is the DRZ. Effects of the DRZ and sensitivity of the seal system performance to both engineered and host rock barriers show that the DRZ is successfully mitigated by the proposed design.

Gas Migration and Salt Column Consolidation. A multi-phase flow model of the lower seal system evaluates the performance of components extending from the middle concrete-asphalt waterstop located at the top of the salt column to the repository horizon for 200 years following closure. During this time period, the principal fluid sources to the model consist of potential gas generated by the waste and lateral brine migration within the Salado Formation. The predicted downward migration of a small quantity of Rustler groundwater (discussed above) is included in this analysis. Effects of gas generation are evaluated for three different repository repressurization scenarios, which simulate pressures as high as 14 MPa. Model results predict that high repository pressures do not produce appreciable differences in the volume of gas migration over the 200-year simulation period. Relatively low gas flow is a result of the low permeability and rapid healing of the DRZ around the lower concrete-asphalt waterstop.

Upward Migration of Brine. The Salado Formation is overpressurized with respect to the measured heads in the Rustler, and upward migration of contaminated brines could occur through an inadequately sealed shaft. Results from the model discussed above demonstrate that the crushed salt seal will reconsolidate to a very low permeability within 100 years following repository closure. Structural results show that the DRZ surrounding the long-term clay and crushed salt seal components will completely heal within the first several decades. Model calculations predict that very little brine flows from the repository to the Rustler/Salado contact.

Intra-Rustler Flow. Based on head differences between the various members of the Rustler Formation, nonhydrostatic conditions exist within the Rustler Formation. Therefore, the potential exists for vertical flow within water-bearing strata within the Rustler. The two units with the

1 greatest transmissivity within the Rustler are the Culebra and the Magenta dolomites, which
2 have the greatest potential for interflow. The relatively low undisturbed permeabilities of the
3 mudstone and anhydrite units separating the Culebra and the Magenta naturally limit crossflow.
4 However, the construction and subsequent closure of the shaft provide a potentially permeable
5 vertical conduit connecting water-bearing units. The primary motivation for limiting formation
6 crossflow within the Rustler is to prevent mixing of formation waters within the Rustler, as
7 required by State of New Mexico statute. Commonly, such an undertaking would limit migration
8 of higher dissolved solids (high-density) groundwater into lower dissolved solids groundwater. In
9 the vicinity of the WIPP site, the Culebra has a higher density groundwater than the Magenta,
10 and the potential for fluid migration between the two most transmissive units is from the unit with
11 the lower total dissolved solids to the unit with the higher dissolved solids. This calculation
12 shows that potential flow rates between the Culebra and the Magenta are insignificant. Under
13 expected conditions, intra-Rustler flow is expected to be of such a limited quantity that (1) it will
14 not affect either the hydraulic or chemical regime within the Culebra or the Magenta and (2) it
15 will not be detrimental to the seal system itself.

16 **Concluding Remarks**

17 The principal conclusion is that an effective, implementable shaft seal system has been
18 designed for the WIPP. Design guidance is addressed by limiting any transport of fluids within
19 the shaft, thereby limiting transport of hazardous material to regulatory boundaries. The
20 application or adaptation of existing technologies for placement of seal components combined
21 with the use of available, common materials provide confidence that the design can be
22 constructed. The structural setting for seal elements is compressive, with shear stresses well
23 below the strength of seal materials. Because of the favorable hydrologic regime coupled with
24 the low intrinsic permeability of seal materials, long-term stability of the shaft seal system is
25 expected. Credibility of these conclusions is bolstered by the basic design approach of using
26 multiple components to perform each sealing function and by using extensive lengths within the
27 shafts to effect a sealing system. The shaft seal system adequately meets design requirements
28 and can be constructed.

1. Introduction

1.1 Purpose of Compliance Submittal Design Report

This report documents the detailed design of the shaft sealing system for the Waste Isolation Pilot Plant (WIPP). The design documented in this report builds on the concepts and preliminary evaluations presented in the Sealing System Design Report issued in 1995 (DOE, 1995). The report contains a detailed description of the design and associated construction procedures, material specifications, analyses of structural and fluid flow performance, and design drawings. The design documented in this report forms the basis for the shaft sealing system which will be constructed under the authority of the hazardous waste facility Permit issued by NMED and as required by 20.4.1.500 NMAC (incorporating 40 CFR §§264.111(b) and 264.601(a)).

1.2 WIPP Description

The WIPP is designed as a full-scale, mined geological repository for the safe management, storage, and disposal of transuranic (TRU) radioactive wastes and TRU mixed wastes generated by US government defense programs. The facility is located near Carlsbad, New Mexico, in the southeastern portion of the state. The underground facility (Figure I2-1) consists of a series of shafts, drifts, panels, and disposal rooms. Four shafts, ranging in diameter from 3.5 to 6.1 m, connect the disposal horizon to the surface. Sealing of these four shafts is the focus of this report.

The disposal horizon is at a depth of approximately 655 m in bedded halite within the Salado Formation. The Salado is a sequence of bedded evaporites approximately 600 m thick that were deposited during the Permian Period, which ended about 225 million years ago. Salado salt has been identified as a good geologic medium to host a nuclear waste repository because of several favorable characteristics. The characteristics present at the WIPP site include very low permeability, vertical and lateral stratigraphic extent, tectonic stability, and the ability of salt to creep and ultimately entomb material placed in excavated openings. Creep closure also plays an important role in the shaft sealing strategy.

The WIPP facility must be determined to be in compliance with applicable regulations prior to the disposal of waste. After the facility meets the regulatory requirements, disposal rooms will be filled with containers holding TRU wastes of various forms. Wastes placed in the drifts and disposal rooms will be at least 150 m from the shafts. Regulatory requirements include use of both engineered and natural barriers to limit migration of hazardous constituents from the repository to the accessible environment. The shaft seals are part of the engineered barriers.

1.3 Performance Objective for WIPP Shaft Seal System

Each of the four shafts from the surface to the underground repository must be sealed to limit hazardous material release to the accessible environment and to limit groundwater flow into the repository. Although the seals will be permanent, the regulatory period applicable to the repository system analyses is 10,000 years.

1.4 Sealing System Design Development Process

This report presents a conservative approach to shaft sealing system design. Shaft sealing system performance plays a crucial role in meeting regulatory radionuclide and hazardous constituents release requirements. Although all engineering materials have uncertainties in properties, a combination of available, low-permeability materials can provide an effective

1 sealing system. To reduce the impact of system uncertainties and to provide a high level of
2 assurance of compliance, numerous components are used in this sealing system. Components
3 in this design include long columns of clay, densely compacted crushed salt, a waterstop of
4 asphaltic material sandwiched between massive low-permeability concrete plugs, a column of
5 asphalt, and a column of earthen fill. Different materials perform identical functions within the
6 design, thereby adding confidence in the system performance through redundancy.

7 The design is based on common materials and construction methods that utilize available
8 technologies. When choosing materials, emphasis was given to permeability characteristics and
9 mechanical properties of seal materials. However, the system is also chemically and physically
10 compatible with the host formations, enhancing long-term performance.

11 Recent laboratory experiments, construction demonstrations, and field test results have been
12 added to the broad and credible database and have supported advances in modeling capability.
13 Results from a series of multi-year, in situ, small-scale seal performance tests show that
14 bentonite and concrete seals maintain very low permeabilities and show no deleterious effects
15 in the WIPP environment. A large-scale dynamic compaction demonstration established that
16 crushed salt can be successfully compacted. Laboratory tests show that compacted crushed
17 salt consolidates through creep closure of the shaft from initial conditions achieved in dynamic
18 compaction to a dense salt mass with regions where permeability approaches that of in situ salt.
19 These technological advances have allowed more credible analysis of the shaft sealing system.

20 The design was developed through an interactive process involving a design team consisting of
21 technical specialists in the design and construction of underground facilities, materials behavior,
22 rock mechanics analysis, and fluid flow analysis. The design team included specialists drawn
23 from the staff of Sandia National Laboratories, Parsons Brinckerhoff Quade and Douglas, Inc.
24 (contract number AG-4909), INTERA, Inc. (contract number AG-4910), and RE/SPEC Inc.
25 (contract number AG-4911), with management by Sandia National Laboratories. The
26 contractors developed a quality assurance program consistent with the Sandia National
27 Laboratories Quality Assurance Program Description for the WIPP project. All three contractors
28 received quality assurance support visits and were audited through the Sandia National
29 Laboratories audit and assessment program. Quality assurance (QA) documentation is
30 maintained in the Sandia National Laboratories WIPP Central Files. Access to project files for
31 each contractor can be accomplished using the contract numbers specified above. In addition to
32 the contractor support, technical input was obtained from consultants in various technical
33 specialty areas.

34 Formal preliminary and final design reviews have been conducted on the technical information
35 documented in the report. In addition, technical, management, and QA reviews have been
36 performed on this report. Documentation is in the WIPP Central File.

37 It is recognized that additional information, such as on specific seal material or formation
38 characteristics, on the sensitivity of system performance to component properties, on placement
39 effectiveness, and on long-term performance, could be used to simplify the design and perhaps
40 reduce the length or number of components. Such design optimization and associated
41 simplifications are left to future research that may be used to update the compliance evaluations
42 completed between now and the time of actual seal emplacement.

1.5 Organization of Document

This report contains an Executive Summary, 10 sections, and 5 appendices. The body of the report does not generally contain detailed backup information; this information is incorporated by reference or in the appendices.

The Executive Summary is a synopsis of the design and the supporting discussions related to seal materials, construction procedures, structural analyses, and fluid flow analyses. Introductory material in Section 1 sets the stage for and provides a “road map” to the remainder of the report.

Site characteristics that detail the setting into which the seals would be placed are documented in Section 2. These characteristics include the WIPP geology and stratigraphy for both the region and the shafts as well as a brief discussion of rock mechanics considerations of the site that impact the sealing system. Regional and local characteristics of the hydrologic and geochemical settings are also briefly discussed.

Section 3 presents the design guidance used for development of the shaft sealing system design. Seal-related guidance from applicable regulations is briefly described. The design guidance is then provided along with the design approach used to implement the guidance. The guidance forms the basis both for the design and for evaluations of the sealing system presented in other sections.

The shaft sealing system is documented in Section 4; detailed drawings for the design are provided in Appendix I2-E. The seal components, their design, and their functions are discussed for the Salado, the Rustler, and the overlying formations.

The sealing materials are described briefly in Section 5, with more detail provided in the materials specifications (Appendix I2-A). The materials used in the various seal components are discussed along with the reasons they are expected to function as intended. Material properties including permeability, strength, and mechanical constitutive response are given for each material. Brief discussions of expected compatibility, performance, construction techniques, and other characteristics relevant to the WIPP setting are also given.

Section 6 contains a brief description of the construction techniques proposed for use. General site and sealing preparation activities are discussed, including construction of a multi-deck stage for use throughout the placement of the components. Construction procedures to be used for the various types of components are then summarized based on the more detailed discussions provided in Appendix I2-B.

Section 7 summarizes structural analyses performed to assess the ability of the shaft sealing system to function in accordance with the design guidance provided in Section 3 and to provide input to hydrological calculations. The methods and computer programs, the models used to simulate the behavior of the seal materials and surrounding salt, and the results of the analyses are discussed. Particular emphasis is placed on the evaluations of the behavior of the disturbed rock zone. Details of the structural analyses are presented in Appendix D of Appendix I2 in the permit application (Appendix D is not included in the Permit). Section 8 summarizes fluid flow analyses performed to assess the ability of the shaft sealing system to function in accordance with the design guidance provided in Section 3. Hydrologic evaluations are focused on

processes that could result in fluid flow through the shaft seal system and the ability of the seal system to limit such flow. Processes evaluated are downward migration of groundwater from the overlying formation, gas migration and reconsolidation of the crushed salt component, upward migration of brines from the repository, and flow between water-bearing zones in the overlying formation. Hydrologic models are described and the results are discussed as they relate to satisfying the design guidance, with extensive reference to Appendix C of Appendix I2 in the permit application that documents details of the flow analyses (Appendix C is not included in the Permit). Conclusions drawn about the performance of the WIPP shaft sealing system are described in Section 9. The principal conclusion that an effective, implementable design has been presented is based on the presentations in the previous sections. A reference list that documents principal references used in developing this design is then provided.

The three appendices that follow provide details related to the following subjects:

Appendix I2-A — Material Specification

Appendix I2-B — Shaft Sealing Construction Procedures

Appendix I2-E — Design Drawings (separate volume)

1.6 Systems of Measurement

Two systems of measurement are used in this document and its appendices. Both the System International d'Unites (SI) and English Gravitational (*fps* units) system are used. This usage corresponds to common practice in the United States, where SI units are used for scientific studies and *fps* units are used for facility design, construction materials, codes, and standards. Dual dimensioning is used in the design description and other areas where this use will aid the reader.

2. Site Geologic, Hydrologic, and Geochemical Setting

The site characteristics relevant to the sealing system are discussed in this section. The location and geologic setting of the WIPP are discussed first to provide background. The geology and stratigraphy, which affect the shafts, are then discussed. The hydrologic and geochemical settings, which influence the seals, are described last.

2.1 Introduction

The WIPP site is located in an area of semiarid rangeland in southeastern New Mexico. The nearest major population center is Carlsbad, 42 km west of the WIPP. Two smaller communities, Loving and Malaga, are about 33 km to the southwest. Population density close to the WIPP is very low: fewer than 30 permanent residents live within a 16-km radius.

2.2 Site Geologic Setting

Geologically the WIPP is located in the Delaware Basin, an elongated depression that extends from just north of Carlsbad southward into Texas. The Delaware Basin is bounded by the Capitan Reef (see Figure I2-2). The basin covers over 33,000 km² and is filled with sedimentary rocks to depths of 7,300 m (Hills, 1984). Rock units of the Delaware Basin (representing the Permian System through the Quaternary System) are listed in Figure I2-3.

Minimal tectonic activity has occurred in the region since the Permian Period (Powers et al., 1978). Faulting during the late Tertiary Period formed the Guadalupe and Delaware Mountains along the western edge of the basin. The most recent igneous activity in the area occurred during the mid-Tertiary Period about 35 million years ago and is evidenced by a dike in the subsurface 16 km northwest of the WIPP. Major volcanic activity last occurred more than 1 billion years ago during Precambrian time (Powers et al., 1978). None of these processes affected the Salado Formation at the WIPP. Therefore, seismic-related design criteria are not included in the current seal systems design guidelines.

2.2.1 Regional WIPP Geology and Stratigraphy

The Delaware Basin began forming with crustal subsidence during the Pennsylvanian Period approximately 300 million years ago. Relatively rapid subsidence over a period of about 14 million years resulted in the deposition of a sequence of deep-water sandstones, shales, and limestones rimmed by shallow-water limestone reefs such as the Capitan Reef (see Figure I2-2). Subsidence slowed during the late Permian Period. Evaporite deposits of the Castile Formation and the Salado Formation (which hosts the WIPP underground workings) filled the basin and extended over the reef margins. The evaporites, carbonates, and clastic rocks of the Rustler Formation and the Dewey Lake Redbeds were deposited above the Salado Formation near the end of the Permian Period. The Santa Rosa and Gatuña Formations were deposited after the close of the Permian Period.

From the surface downward to the repository horizon the stratigraphic units are the Quaternary surface sand sediments, Gatuña Formation, Santa Rosa Formation, Dewey Lake Redbeds, Rustler Formation, and Salado Formation. Three principal stratigraphic units (the Dewey Lake Redbeds, the Rustler Formation, and the Salado Formation) comprise all but the upper 15 to 30 m (50 to 100 ft) of the geologic section above the WIPP facility.

The Dewey Lake Redbeds consist of alternating layers of reddish-brown, fine-grained sandstone and siltstone cemented with calcite and gypsum (Vine, 1963). The Rustler Formation

lies below the Dewey Lake Redbeds; this formation, the youngest of the Late Permian evaporite sequence, includes units that provide potential pathways for radionuclide migration from the WIPP. The five units of the Rustler, from youngest to oldest, are: (1) the Forty-niner Member, (2) the Magenta Dolomite Member, (3) the Tamarisk Member, (4) the Culebra Dolomite Member, and (5) an unnamed lower member.

The 250-million-year-old Salado Formation lies below the Rustler Formation. This unit is about 600 m thick and consists of three informal members. From youngest to oldest, they are: (1) an upper member (unnamed) composed of reddish-orange to brown halite interbedded with polyhalite, anhydrite, and sandstone, (2) a middle member (the McNutt Potash Zone) composed of reddish-orange and brown halite with deposits of sylvite and langbeinite; and (3) a lower member (unnamed) composed of mostly halite with lesser amounts of anhydrite, polyhalite, and glauberite, with some layers of fine clastic material. These lithologic layers are nearly horizontal at the WIPP, with a regional dip of less than one degree. The WIPP repository is located in the unnamed lower member of the Salado Formation, approximately 655 m (2150 ft) below the ground surface.

2.2.2 Local WIPP Stratigraphy

The generalized stratigraphy of the WIPP site, with the location of the repository, is shown in Figure I2-4. To establish the geologic framework required for the design of the WIPP facility shaft sealing system, an evaluation was performed to assess the geologic conditions existing in and between the shafts, where the individual shaft sealing systems will eventually be emplaced (DOE, 1995: Appendix I2-A). The study evaluated shaft stratigraphy, regional groundwater occurrence, brine occurrence in the exposed Salado Formation section, and the consistency between recorded data and actual field data.

Four shafts connect the WIPP underground workings to the surface, the (1) Air Intake Shaft (AIS), (2) Exhaust Shaft, (3) Salt Handling Shaft, and (4) Waste Shaft. Stratigraphic correlation and evaluation of the unit contacts show that lithologic units occur at approximately the same levels in all four shaft locations. Some stratigraphic contact elevations vary because of regional structure and stratigraphic thinning and thickening of units. However, the majority of the stratigraphic contacts used to date are suitable for engineering design reference because they intersect all four shafts.

2.2.3 Rock Mechanics Setting

The WIPP stratigraphy includes rock types that exhibit both brittle and ductile behaviors. The majority of the stratigraphy intercepted by the shafts consists of the Salado Formation, which is predominantly halite. The primary mechanical behavior of halitic rocks is creep. Except near free surfaces (such as the shaft wall), the salt rocks will remain tight and undisturbed despite the long-term creep deformation they sustain. The other rock types within the Salado Formation are anhydrites and polyhalites. These two rock types are typically brittle, stiff, and exhibit high strength in laboratory tests. The structural strength of particular anhydritic rock layers, however, depends on the thickness of the layers, which range from thin (<1 m) to fairly thick (10 m or more). Brittle failure of these noncreeping rocks can occur as they restrain, or attempt to restrain, the creep of the salt above and below the stiff layer. Although thick layers can resist the induced stresses, thin layers are fractured in tension by the salt creep. Because the deformation in the bounding salt is time dependent, the damage in the brittle rock is also time dependent.

Above the Salado Formation, the Rustler Formation stratigraphy consists of relatively strong limestones and siltstones. The shaft excavation is the only significant disturbance to these rocks. Any subsurface subsidence (deformation) or loading induced by the presence of the repository are negligible in a rock mechanics sense.

Regardless of rock type, the shafts create a disturbed zone in the surrounding rock. Microfracturing will occur in the rock adjacent to the shaft wall, where confining stresses are low or nonexistent. The extent of the zone depends on the rock strength and the prevailing stress state, which is depth dependent. In the salt rocks, microfracturing occurs to form the disturbed zone both at the time of excavation and later as dilatant creep deformations occur. In the brittle rocks, the disturbance occurs at the time of excavation and does not worsen with time. The extent of disturbed zones in the salt and brittle rocks can be calculated, as will be described in Section 7 and Appendix D in the permit application.

Preventing the salt surrounding the shafts from creeping causes reintroduction of stresses that reverse the damage process and cause healing (Van Sambeek et al., 1993). The seal system design relies on this principle for sealing the disturbed zone in salt. In the brittle rocks, grouting of the damage is a viable means of reducing the interconnected fractures that increase the permeability of the rock.

2.3 Site Hydrologic Setting

The WIPP shafts penetrate approximately 655 m (2150 ft) of sediments and rocks. From a hydrogeologic perspective, relevant information includes the permeability of the water-bearing units, the thickness of the water-bearing units, and the observed vertical pressure (head) gradients expected to exist after shaft construction and ambient pressure recovery. This section will discuss these three aspects of the site hydrogeology. The geochemistry of the pore fluids adjacent to the shaft system is also important hydrogeologic information and will be provided in Section 2.4.

2.3.1 Hydrostratigraphy

The WIPP shafts penetrate Quaternary surface sediments, the Gatuña Formation, the Santa Rosa Formation, the Dewey Lake Redbeds, the Rustler Formation, and the Salado Formation. The Rustler Formation contains the only laterally-persistent water-bearing units in the WIPP vicinity. As a result, flow-field characterization, regional flow-modeling, and performance assessment off-site release scenarios focus on the Rustler Formation. The hydrogeology of the stratigraphic units in contact with the upper portion of the AIS sealing system is fairly well known from detailed hydraulic testing of the Rustler Formation at well H-16 located 17 m from the AIS (Beauheim, 1987). The H-16 borehole was drilled in July and August 1987 to monitor the hydraulic responses of the Rustler members to the drilling and construction of the AIS. During the drilling of H-16, each member of the Rustler Formation was cored. In addition, detailed drill-stem, pulse, and slug hydraulic tests were performed in H-16 on the members of the Rustler. Through the detailed testing program at H-16, the permeability of each of the Rustler members was estimated. Detailed mapping of the AIS by Holt and Powers (1990) and other investigators provided information on the location of wet zones and weeps within the Salado Formation. This information will be summarized below. The reader, unless particularly interested in this subject, should proceed to Section 2.3.2.

Water-bearing zones have been observed in units above the Rustler Formation in the WIPP site vicinity. However, drilling in the Dewey Lake Redbeds has not identified any continuous saturated units at the WIPP site. Water-bearing units within stratigraphic intervals above the Rustler are typically perched saturated zones of very low yield. Thin perched groundwater intervals have been encountered in WIPP wells H-1, H-2, and H-3 (Mercer and Orr, 1979). The only Dewey Lake Redbed wells that have sufficient yields for watering livestock are the James Ranch wells, the Pocket well, and the Fairfield well (Brinster, 1991). These wells are located to the south of the WIPP and are not in the immediate vicinity of the WIPP shafts.

The Dewey Lake Redbeds overlie the Rustler Formation. The Rustler is composed of five members defined by lithology. These are, in ascending order, the unnamed lower member, the Culebra dolomite, the Tamarisk, the Magenta dolomite, and the Forty-niner (see Figure I2-4). Of these five members, the unnamed lower member, the Culebra, and the Magenta are the most transmissive units in the Rustler. The Tamarisk and the Forty-niner are aquitards within the Rustler and have very low permeabilities relative to the three members listed above.

To the east of the shafts in Nash Draw, the Rustler/Salado contact has been observed to be permeable and water-bearing. This contact unit has been referred to as the "brine aquifer" (Mercer, 1983). The brine aquifer is not reported to exist in the vicinity of the shafts. The hydraulic conductivity of the Rustler/Salado contact in the vicinity of the shafts is reported to be approximately 4×10^{-11} m/s, which is equivalent to a permeability of 6×10^{-18} m² using reference brine fluid properties (Brinster, 1991). The unnamed lower member was hydraulic tested at well H-16 in close proximity to the AIS. The maximum permeability of the unnamed lower member was interpreted to be 2.2×10^{-18} m² and was attributed to the unnamed lower member claystone by Beauheim (1987), which correlates to the transition and bioturbated clastic zones of Holt and Powers (1990).

The Culebra Dolomite Member is the most transmissive member of the Rustler Formation in the vicinity of the WIPP site and is the most transmissive saturated unit in contact with the shaft sealing system. The Culebra is an argillaceous dolomicrite which contains secondary porosity in the form of abundant vugs and fractures. The permeability of the Culebra varies greatly in the vicinity of the WIPP and is controlled by the condition of the secondary porosity (fractures). The permeability of the Culebra in the vicinity of the shafts is approximately 2.1×10^{-14} m².

The Tamarisk Member is composed primarily of massive, lithified anhydrite, including anhydrite 2, mudstone 3, and anhydrite 3. Testing of the Tamarisk at H-16 was unsuccessful. The estimated transmissivity of the Tamarisk at H-16 is one to two orders of magnitude lower than the least-transmissive unit successfully tested at H-16, which results in a permeability range from 4.6×10^{-20} to 4.6×10^{-19} m². Anhydrites in the Rustler have an approximate permeability of 1×10^{-19} m². The permeability of mudstone 3 is 1.5×10^{-19} m² (Brinster, 1991).

The Magenta is a dolomite that is typically less permeable than the Culebra. The Magenta Dolomite Member overlies the Tamarisk Member. The Magenta is an indurated, gypsiferous, arenaceous, dolomite that Holt and Powers (1990) classify as a dolarenite. The dolomite grains are primarily composed of silt to fine sand-sized clasts. Wavy to lenticular bedding and ripple cross laminae are prevalent through most of the Magenta. Holt and Powers (1990) estimate that inflow to the shaft from the Magenta during shaft mapping was less than 1 gal/min. The Magenta has a permeability of approximately 1.5×10^{-15} m² (Saulnier and Avis, 1988).

The Forty-niner Member is divided into three informal lithologic units. The lowest unit is anhydrite 4, a laminated anhydrite having a gradational contact with the underlying Magenta. Mudstone 4 overlies anhydrite 4 and is composed of multiple units containing mudstones, siltstones, and very fine sandstones. Anhydrite 5 is the uppermost informal lithologic unit of the Forty-niner Member. The permeability of mudstone 4, determined from the pressure responses in the Forty-niner interval of H-16 to the drilling of the AIS, is $3.9 \times 10^{-16} \text{ m}^2$ (referred to as the Forty-niner claystone by Avis and Saulnier, 1990).

The Salado Formation is a very low permeability formation that is composed of bedded halite, polyhalite, anhydrite, and mudstones. Inflows in the shafts have been observed over select intervals during shaft mapping, but flows are below the threshold of quantification. In some cases these weeps are individual, lithologically distinct marker beds, and in some cases they are not. Directly observable brine flow from the Salado Formation into excavated openings is a short-lived process. Table I2-1 lists the brine seepage intervals identified by Holt and Powers (1990) during their detailed mapping of the AIS. Seepage could be indicated by a wet rockface or by the presence of precipitate from brine evaporation on the shaft rockface. The zones listed in Table I2-1 make up less than 10% of the Salado section that is intersected by the WIPP shafts.

Table I2-1. Salado Brine Seepage Intervals⁽¹⁾

Stratigraphic Unit	Lithology	Thickness (m)
Marker Bed 103	Anhydrite	5.0
Marker Bed 109	Anhydrite	7.7
Vaca Triste	Mudstone	2.4
Zone A	Halite	2.9
Marker Bed 121	Polyhalite	0.5
Union Anhydrite	Anhydrite	2.3
Marker Bed 124	Anhydrite	2.7
Zone B	Halite	0.9
Zone C	Halite	2.7
Zone D	Halite	3.2
Zone E	Halite	0.6
Zone F	Halite	0.9
Zone G	Halite	0.6
Zone H	Halite	1.8
Marker Bed 129	Polyhalite	0.5
Zone I	Halite	1.7
Zone J	Halite	1.2

(1) After US DOE, 1995.

To gain perspective into the important stratigraphic units from a hydrogeologic view, the permeability and thickness of the units adjacent to the shafts can be compared. Table I2-2 lists the lithologic units in the Rustler and the Salado Formations with their best estimate

permeabilities and their thickness as determined from the AIS mapping. The stratigraphy of the units overlying the Rustler is not considered in Table I2-2 because these units are typically not saturated in the vicinity of the WIPP shafts. The overlying sediments account for approximately 25% of the stratigraphy column adjacent to the shafts.

Because permeability varies over several orders of magnitude, the log of the permeability is also listed to simplify comparison between units. Table I2-2 shows that by far the two most transmissive zones occur in the Rustler Formation; these are the Culebra and Magenta dolomites. These units are relatively thin when compared to the combined Rustler and Salado thickness adjacent to the shafts (3% of Rustler and Salado combined thickness). The Magenta and the Culebra are the only two units that are known to possess permeabilities higher than $1 \times 10^{-18} \text{ m}^2$.

Table I2-2. Permeability and Thickness of Hydrostratigraphic Units in Contact with Seals

Formation	Member/ Lithology	Undisturbed Permeability (m^2)	Thickness (m)
Rustler	Anhydrite ⁽¹⁾	1.0×10^{-19}	46.7
Rustler	Mudstone 4	3.9×10^{-16}	4.4
Rustler	Magenta	1.5×10^{-15}	7.8
Rustler	Mudstone 3	1.5×10^{-19}	2.9
Rustler	Culebra	2.1×10^{-14}	8.9
Rustler	Transition/ Bioturbated Clastics	2.2×10^{-18}	18.7
Salado	Halite	1.0×10^{-21}	356.6
Salado	Polyhalite	3.0×10^{-21}	10.9
Salado	Anhydrite	1.0×10^{-19}	28.2

(1) Anhydrite 5, Anhydrite 4, Anhydrite 3, and Anhydrite 2

The vast majority (97%) of the rocks adjacent to the shaft in the Rustler and the Salado Formations are low permeability ($< 1 \times 10^{-18} \text{ m}^2$). The conclusion that can be drawn from reviewing Table I2-2 is that the shafts are located hydrogeologically in a low permeability, low groundwater flow regime. Inflow measurements have historically been made at the shafts, and observable flow is attributed to leakage from the Rustler Formation.

Flow modeling of the Culebra has demonstrated that depressurization has occurred as a result of the sinking of the shafts at the site. Maximum estimated head drawdown in the Culebra at the centroid of the shafts was estimated by Haug et al. (1987) to be 33 m in the mid-1980s. This drawdown in the permeable units intersected by the shafts is expected because the shafts act as long-term constant pressure (atmospheric) sinks. Measurements of fluid flow into the WIPP shafts when they were unlined show a range from a maximum of 0.11 L/s (3,469 m^3/yr) measured in the Salt Handling Shaft on September 13, 1981 to a minimum of 0.008 L/s (252 m^3/yr) measured at the Waste Handling Shaft on August 6, 1987 (LaVenue et al., 1990).

The following summary of shaft inflow rates from the Rustler is based on a review of LaVenue et al. (1990) and Cauffman et al. (1990). Shortly after excavation and prior to grouting and liner installation, the inflow into the Salt Handling Shaft was 0.11 L/s (3,469 m^3/yr). The average flow

rate measured after shaft lining for the period from mid-1982 through October 1992 was 0.027 L/s (851 m³/yr). The average flow rate into the Waste Handling Shaft during the time when the shaft was open and unlined was about 0.027 L/s (851 m³/yr). Between the first and second grouting events (July 1984 to November 1987) the average inflow rate was 0.016 L/s (505 m³/yr). No estimates were found after the second grouting. Inflow to the pilot holes for the Exhaust Shaft averaged 0.028 L/s (883 m³/yr). In December 1984 a liner plate was grouted across the Culebra. After this time, a single measurement of inflow from the Culebra was 0.022 L/s (694 m³/yr). After liner plate installation, three separate grouting events occurred at the Culebra. No measurable flow was reported after the third grouting event in the summer of 1987. Flow into the AIS when it was unlined and draining averaged 0.044 L/s (1,388 m³/yr). Since the Rustler has been lined, flow into the AIS has been negligible.

The majority of the flow represented by these shaft measurements originates from the Rustler. This is clearly evident by the fact that lining of the WIPP shafts was found to be unnecessary in the Salado Formation below the Rustler/Salado contact. When the liners were installed, flow rates diminished greatly. Under sealed conditions, hydraulic gradients in rocks adjacent to the shaft will diminish as the far-field pressures approach ambient conditions. The low-permeability materials sealing the shaft combined with the reduction in lateral hydraulic gradients will likely result in flow rates into the shaft that are several orders of magnitude less than observed under open shaft or lined shaft conditions.

2.3.2 Observed Vertical Gradients

Hydraulic heads within the Rustler and between the Rustler and Salado Formations are not in hydrostatic equilibrium. Mercer (1983) recognized that heads at the Rustler Salado transition (referred to as the brine aquifer and not present in the vicinity of the WIPP shafts) indicate an upward hydraulic gradient from that zone to the Culebra. Later, with the availability of more head measurements within the Salado and Rustler members, Beauheim (1987) provided additional insight into the potential direction of vertical fluid movement within the Rustler. He reported that the hydraulic data indicate an upward gradient from the Salado to the Rustler.

Formation pressures in the Salado Formation have been decreased in the near vicinity of the WIPP underground facility. The highest, and thought to be least disturbed, estimated formation fluid pressure from hydraulic testing is 12.55 MPa estimated from interpretation of testing within borehole SCP01 in Marker Bed 139 (**MB139**) just below the underground facility horizon (Beauheim et al., 1993). The fresh-water head within MB139, based on the estimated static formation pressure of 12.55 MPa, is 1,663.6 m (5,458 ft) above mean sea level (**msl**).

Hydraulic heads in the Rustler have also been impacted by the presence of the WIPP shafts. Impacts in the Culebra were significant in the 1980s with a large drawdown cone extending away from the shafts in the Culebra (Haug et al., 1987). The undisturbed head of the Rustler Salado contact in the vicinity of the AIS is estimated to be about 936.0 m (3,071 ft) msl (Brinster, 1991). The undisturbed head in the Culebra is estimated to be approximately 926.9 m (3,041 ft) msl in the vicinity of the AIS (LaVenue et al., 1990). The undisturbed head in the Magenta is estimated to be approximately 960.1 m (3,150 ft) msl (Brinster, 1991).

The disturbed and undisturbed heads in the Rustler are summarized in Table I2-3. Also included is the freshwater head of MB139 based on hydraulic testing in the WIPP underground. Consistent with the vertical flow directions proposed by previous investigators, estimated

vertical gradients in the vicinity of the AIS before the shafts were drilled indicate a hydraulic gradient from the Magenta to the Culebra and from the Rustler/Salado contact to the Culebra. There is also the potential for flow from the Salado Formation to the Rustler Formation.

Table I2-3. Freshwater Head Estimates in the Vicinity of the Air Intake Shaft

Hydrologic Unit	Freshwater Head (m asl)		Reference
	Undisturbed	Disturbed	
Magenta Member	960.1 ¹	948.8 ² (H-16)	Brinster (1991) Beauheim (1987)
Culebra Member	926.9 ¹	915.0 ² (H-16)	LaVenue et al. (1990) Beauheim (1987)
Lower Unnamed Member	—	953.4 ² (H-16)	Beauheim (1987)
Rustler/Salado Contact	936.0 - 940.0 ¹	—	Brinster (1991)
Salado MB139	1,663.6 ²	—	Beauheim et al. (1993)

¹ Estimated from a contoured head surface plot based principally on well data collected prior to shaft construction.
² Measured through hydraulic testing and/or long-term monitoring.

2.4 Site Geochemical Setting

2.4.1 Regional and Local Geochemistry in Rustler Formation and Shallower Units

The Rustler Formation, overlying the Salado Formation, consists of interbedded anhydrite/gypsum, mudstone/siltstone, halite east of the WIPP site, and two layers of dolomite. Principal occurrences of NaCl/MgSO₄ brackish to briny groundwater in the Rustler at the WIPP site and to the north, west, and south are found (1) at the lower member near its contact with the underlying Salado and (2) in the two dolomite members having a variable fracture-induced secondary porosity. The mineralogy of the Rustler Formation is summarized in Table I2-4.

The five members of the Rustler Formation are described as follows: (1) The Forty-niner Member is similar in lithology to the other non-dolomitic units but contains halite east of the WIPP site. (2) The Magenta Member is another variably fractured dolomite/sulfate unit containing sporadic occurrences of groundwater near and west of the WIPP site. (3) The Tamarisk Member is dominantly anhydrite (locally altered to gypsum) with subordinate fine-grained clastics, containing halite to the east of the WIPP site. (4) The Culebra Dolomite Member is dominantly dolomite with subordinate anhydrite and/or gypsum, having a variable fracture-induced secondary porosity containing regionally continuous occurrences of groundwater at the WIPP site and to the north, west, and south. (5) An unnamed lower member consists of sandstone, siltstone, mudstone, claystone, and anhydrite locally altered to gypsum, and containing halite under most of the WIPP site and occurrences of brine at its base, mostly west of the WIPP site.

Table I2-4. Chemical Formulas, Distributions, and Relative Abundance of Minerals in the Rustler and Salado Formations (after Lambert, 1992)

Mineral	Formula	Occurrence/ Abundance
Amesite	$(\text{Mg}_4\text{Al}_2)(\text{Si}_2\text{Al}_2)\text{O}_{10}(\text{OH})_8$	S, R
Anhydrite	CaSO_4	SSS, RRR
Calcite	CaCO_3	S, RR
Carnallite	$\text{KMgCl}_3 \cdot 6\text{H}_2\text{O}$	SS ₊
Chlorite	$(\text{Mg}, \text{Al}, \text{Fe})_{12}(\text{Si}, \text{Al})_8\text{O}_{20}(\text{OH})_{16}$	S ₊ , R ₊
Corrensite	Mixed-layer chlorite/smectite	S ₊ , R ₊
Dolomite	$\text{CaMg}(\text{CO}_3)_2$	RR
Feldspar	$(\text{K}, \text{Na}, \text{Ca})(\text{Si}, \text{Al})_4\text{O}_8$	S ₊ , R ₊
Glauberite	$\text{Na}_2\text{Ca}(\text{SO}_4)_2$	S
Gypsum	$\text{CaSO}_4 \cdot 2\text{H}_2\text{O}$	S, RRR
Halite	NaCl	SSS, RRR
Illite	$\text{K}_{1-1.5}\text{Al}_4(\text{Si}_{7-6.5}\text{Al}_{1-1.5}\text{O}_{20})(\text{OH})_4$	S ₊ , R ₊
Kainite	$\text{KMgClSO}_4 \cdot 3\text{H}_2\text{O}$	SS ₊
Kieserite	$\text{MgSO}_4 \cdot \text{H}_2\text{O}$	SS ₊
Langbeinite	$\text{K}_2\text{Mg}_2(\text{SO}_4)_3$	S*
Magnesite	MgCO_3	S, R
Polyhalite	$\text{K}_2\text{Ca}_2\text{Mg}(\text{SO}_4)_4 \cdot 2\text{H}_2\text{O}$	SS, R
Pyrite	FeS_2	S, R
Quartz	SiO_2	S ₊ , R ₊
Serpentine	$\text{Mg}_3\text{Si}_2\text{O}_5(\text{OH})_4$	S ₊ , R ₊
Smectite	$(\text{Ca}_{1/2}, \text{Na})_{0.7}(\text{Al}, \text{Mg}, \text{Fe})_4(\text{Si}, \text{Al})_8\text{O}_{20}(\text{OH})_4 \cdot n\text{H}_2\text{O}$	S ₊ , R ₊
Sylvite	KCl	SS*

Key to Occurrence/Abundance notations:

S = Salado Formation; R = Rustler Formation; 3x = abundant, 2x = common, 1x = rare or accessory; * = potash-ore mineral (never near surface); † = potash-zone non-ore mineral; ‡ = in claystone interbeds.

The Dewey Lake Redbeds, overlying the Rustler Formation, are the uppermost Permian unit; they consist of siltstones and claystones locally transected by concordant and discordant fractures that may contain gypsum. The Dewey Lake Redbeds contain sporadic occurrences of groundwater that may be locally perched, mostly in the area south of the WIPP site. The Triassic Dockum Group (undivided) rests on the Dewey Lake Redbeds in the eastern half of the WIPP site and thickens eastward; it is a locally important source of groundwater for agricultural and domestic use.

The Gatuña Formation, overlying the Dewey Lake Redbeds, occurs locally as channel and alluvial pond deposits (sands, gravels, and boulder conglomerates). The pedogenic Mescalero caliche is commonly developed on top of the Gatuña Formation and on many other erosionally truncated rock types. Surficial dune sand, which may be intermittently damp, covers virtually all outcrops at and near the WIPP site. Siliceous alluvial deposits southwest of the WIPP site also

contain potable water. The geochemistry of groundwater found in the Rustler Formation and Dewey Lake Redbeds is summarized in Table I2-5.

Table I2-5. Major Solutes in Selected Representative Groundwater from the Rustler Formation and Dewey Lake Redbeds, in mg/L (after Lambert, 1992)

Well	Date	Zone	Ca	Mg	Na	K	SO ₄	Cl
WIPP-30	July 1980	R/S	955	2770	121,000	2180	7390	192,000
WIPP-29	July 1980	R/S	1080	2320	36,100	1480	12,000	58,000
H-5B	June 1981	Cul	1710	2140	52,400	1290	7360	89,500
H-9B	November 1985	Cul	590	37	146	7	1900	194
H-2A	April 1986	Cul	743	167	3570	94	2980	5310
P-17	March 1986	Cul	1620	1460	28,300	782	6020	48,200
WIPP-29	December 1985	Cul	413	6500	94,900	23,300	20,000	179,000
H-3B1	July 1985	Mag	1000	292	1520	35	2310	3360
H-4C	November 1986	Mag	651	411	7110	85	7100	8460
Ranch	June 1986	DL	420	202	200	4	1100	418

Key to Zone:

R/S = "basal brine aquifer" near the contact between the Rustler and Salado Formations; Cul = Culebra Member, Rustler Formation; Mag = Magenta Member, Rustler Formation; DL = Dewey Lake Redbeds.

2.4.2 Regional and Local Geochemistry in the Salado Formation

The Salado Formation consists dominantly of halite, interrupted at intervals of meters to tens of meters by beds of anhydrite, polyhalite, mudstone, and local potash mineralization (sylvite or langbeinite, with or without accessory carnallite, kieserite, kainite and glauberite, all in a halite matrix). Some uniquely identifiable non-halite units, 0.1 to 10 m thick, have been numbered from the top down (100 to 144) for convenience as marker beds to facilitate cross-basinal stratigraphic correlation. The WIPP facility was excavated just above Marker Bed 139 in the Salado Formation at a depth of about 655 m.

Although the most common Delaware Basin evaporite mineral is halite, the presence of less soluble interbeds (dominantly anhydrite, polyhalite, and claystone) and more soluble admixtures (e.g. sylvite, glauberite, kainite) has resulted in chemical and physical properties significantly different from those of pure NaCl. Under differential stress produced near excavations, brittle interbeds (anhydrite, polyhalite, magnesite, dolomite) may fracture, whereas under a similar stress regime pure NaCl would undergo plastic deformation. Fracturing of these interbeds has locally enhanced the permeability, allowing otherwise nonporous rock to carry groundwater (e.g., the fractured polyhalitic anhydrite of Marker Bed 139 under the floor of the WIPP excavations).

Groundwater in evaporites represents the exposure of chemical precipitates to fluids that may be agents (as in the case of dissolution) or consequences of postdepositional alteration of the evaporites (as in the cases of dehydration of gypsum and diagenetic dewatering of other minerals). Early in the geological studies of the WIPP site, groundwater occurrences that could be hydrologically characterized were identified.

- 1 Since the beginning of conventional mining in the Delaware Basin, relatively short-lived seeps
2 (pools on the floor, efflorescences on the walls, and stalactitic deposits on the ceiling) have
3 been known to occur in the Salado Formation where excavations have penetrated. These brine
4 occurrences are commonly associated with the non-halitic interbeds whose porosity is governed
5 either by fracturing (as in brittle beds) or mineralogical discontinuities (as in "clay" seams).
- 6 The geochemistry of brines encountered in the Salado Formation is summarized in Table I2-6.
7 The relative abundance of minerals was summarized in Table 2-4.

Table I2-6. Variations in Major Solutes in Brines from the Salado Formation, in mg/L (after Lambert, 1992)

Source of Brine	Date	Ca	Mg	K	Na	Cl	SO ₄
Room G Seep							
	Sep-87	278	14800	15800	99000	188000	29500
	Nov-87	300	18700	15400	97100	190000	32000
	Feb-88	260	18200	17100	94100	186000	36200
	Mar-88	280	17000	16200	92100	187000	34800
	Jul-88	292	13000	14800	96600	188000	29300
	Sep-88	273	14700	13700	86500	185000	28000
	Apr-91	240	14400	12900	95000	189000	28000
	Jul-91	239	14100	13100	93000	190000	27700
	Oct-91	252	14700	14100	95000	189000	27100
Marker Bed 139 (under repository)							
		300	18900	14800	67700	155900	14700
		300	17100	15600	72700	158900	13400
		300	17600	15800	71600	182200	14700
Room J							
		230	17700	13500	63600	167000	15100
		210	27400	22400	56400	168000	19600
		220	17900	15600	73400	165000	9300
		250	22200	18300	63000	165000	31100
		190	31000	19900	46800	170000	24600
		100	35400	27800	40200	173000	30000
		270	18900	14500	59900	166000	16200
		280	20200	17000	70400	165000	10600
Room Q							
		279	31500	22600	68000	205000	19400
		288	31100	24100	68000	203000	19200
		257	34000	26300	63000	205000	23500
AIS Sump (accumulation in bottom of sump)							
	Jul-88	960	1040	1720	118000	187000	6170
	May-89	900	500	600	83100	122700	7700
	May-89	1000	800	1100	82400	114200	8800
McNutt Potash Zone							
Duval mine		640	55400	30000	27500	236500	3650
Miss. Chem. mine		200	44200	45800	43600	226200	12050

3. Design Guidance

3.1 Introduction

The WIPP is subject to regulatory requirements contained in applicable portions of the New Mexico Hazardous Waste Act, specifically 20.4.1.500 NMAC and .900 (incorporating 40 CFR §264 and §270), and requirements contained in 40 CFR §191 and 40 CFR §194. The use of both engineered and natural barriers to isolate wastes from the accessible environment is required by 20.4.1.500 NMAC (incorporating 40 CFR §§264.111 and 264.601) and 40 CFR §191.14(d). The use of engineered barriers to prevent or substantially delay the movement of water, hazardous constituents, or radionuclides toward the accessible environment is required by 20.4.1.500 NMAC (incorporating 40 CFR §§264.111 and 264.601) and 40 CFR §194.44. Hazardous constituent release performance standards are specified in Permit Module V and 20.4.1.500 NMAC (incorporating 40 CFR §§264.111(b), 264.601(a), and 264 Subpart F). Quantitative requirements for potential releases of radioactive materials from the repository system are specified in 40 CFR §191. The regulations impose quantitative release requirements on the total repository system, not on individual subsystems of the repository system, for example, the shaft sealing subsystem.

3.2 Design Guidance and Design Approach

The guidance described for the design of the shaft sealing system addresses the need for the WIPP to comply with system requirements and to follow accepted engineering practices using demonstrated technology. The design guidance addresses the need to limit:

1. radiological or other hazardous constituents reaching the regulatory boundaries,
2. groundwater flow into and through the sealing system,
3. chemical and mechanical incompatibility,
4. structural failure of system components,
5. subsidence and accidental entry, and
6. development of new construction technologies and/or materials.

For each element of design guidance, a design approach has been developed. Table I2-7 contains qualitative design guidance and the design approach used to implement it.

Table I2-7. Shaft Sealing System Design Guidance

Qualitative Design Guidance	Design Approach
<i>The shaft sealing system shall limit:</i>	<i>The shaft sealing system shall be designed to meet the qualitative design guidance in the following ways:</i>
1. the migration of radiological or other hazardous constituents from the repository horizon to the regulatory boundary during the 10,000-year regulatory period following closure;	1. In the absence of human intrusion, brine migrating from the repository horizon to the Rustler Formation must pass through a low permeability sealing system.
2. groundwater flowing into and through the shaft sealing system;	2. In the absence of human intrusion, groundwater migrating from the Rustler Formation to the repository horizon must pass through a low permeability sealing system.
3. chemical and mechanical incompatibility of seal materials with the seal environment;	3. Brine contact with seal elements is limited and materials possess acceptable mechanical properties.
4. the possibility for structural failure of individual components of the sealing system;	4. State of stress from forces expected from rock creep and other mechanical loads is favorable for seal materials.
5. subsidence of the ground surface in the vicinity of the shafts and the possibility of accidental entry after sealing;	5. The shaft is completely filled with low-porosity materials, and construction equipment would be needed to gain entry.
6. the need to develop new technologies or materials for construction of the shaft sealing system.	6. Construction of the shaft sealing system is feasible using available technologies and materials.

4. Design Description

4.1 Introduction

The design presented in this section was developed based on (1) the design guidance outlined in Section 3.0, (2) past design experience, and (3) a desire to reduce uncertainties associated with the performance of the WIPP sealing system. The WIPP shaft sealing system design has evolved over the past decade from the initial concepts presented by Stormont (1984) to the design concepts presented in this document. The past designs are:

- the plugging and sealing program for the WIPP (Stormont, 1984),
- the initial reference seal system design (Nowak et al., 1990),
- the seal design alternative study (Van Sambeek et al., 1993),
- the WIPP sealing system design (DOE, 1995).

The present design changes were implemented to take advantage of knowledge gained from small-scale seals tests conducted at the WIPP (Knowles and Howard, 1996), advances in the ability to predict the time-dependent mechanical behavior of compacted salt rock (Callahan et al., 1996), large-scale dynamic salt compaction tests and associated laboratory determination of the permeability of compacted salt samples (Hansen and Ahrens, 1996; Brodsky et al., 1996), field tests to measure the permeability of the DRZ surrounding the WIPP AIS (Dale and Hurtado, 1996), and around seals (Knowles et al., 1996). A summary paper (Hansen et al., 1996) describing the design has been prepared.

The shaft sealing system is composed of seals within the Salado Formation, the Rustler Formation, and the Dewey Lake Redbeds and overlying units. All components of the sealing system are designed to meet Items 3, 4, and 6 of the Design Guidance (Table I2-7.); that is, all sealing system components are designed to be chemically and mechanically compatible with the seal environment, structurally adequate, and constructable using currently available technology and materials. The seals in the Salado Formation are also designed to meet Items 1 and 2 of the Design Guidance. These seals will limit fluid migration upward from the repository to the Rustler Formation and downward from the Rustler Formation to the repository. Migration of brine upward and downward is discussed in Sections 8.5 and 8.4 respectively. The seals in the Rustler Formation are designed to meet Item 2 in addition to Items 3, 4, and 6 of the Design Guidance. The seals in the Rustler Formation limit migration of Rustler brines into the shaft cross-section and also limit cross-flow between the Culebra and Magenta members. The principal function of the seals in the Dewey Lake Redbeds and overlying units is to meet Item 5 of the Design Guidance, that is, to limit subsidence of the ground surface in the vicinity of the shafts and to prevent accidental entry after repository closure. Entry of water (surface water and any groundwater that might be present in the Dewey Lake Redbeds and overlying units) into the sealing system is limited by restraining subsidence and by placing high density fill in the shafts.

4.2 Existing Shafts

The WIPP underground facilities are accessed by four shafts commonly referred to as the Waste, Air Intake, Exhaust, and Salt Handling Shafts. These shafts were constructed between 1981 and 1988. All four shafts are lined from the surface to just below the contact of the Rustler and Salado Formations. The lined portion of the shafts terminates in a substantial concrete structure called the "key," which is located in the uppermost portion of the Salado Formation. Drawings showing the configuration of the existing shafts are included in Appendix I2-E and

listed below in Table I2-8. Table I2-9 contains a summary of information describing the existing shafts.

The upper portions of the WIPP shafts are lined. The Waste, Air Intake, and Exhaust shafts have concrete linings; the Salt Handling Shaft has a steel lining with grout backing. In addition, during shaft construction, steel liner plates, wire mesh, and pressure grouting were used to stabilize portions of the shaft walls in the Rustler Formation and overlying units. Seepage of groundwater into the lined portions of the shafts has been observed. This seepage was expected; in fact, the shaft keys (massive concrete structures located at the base of each shaft liner) were designed to collect the seepage and transport it through a piping system to collection points at the repository horizon. In general, the seepage originates in the Magenta and Culebra members of the Rustler Formation and in the interface zone between the Rustler and Salado formations. It flows along the interface between the shaft liner and the shaft wall and through the DRZ immediately adjacent to the shaft wall. In those cases where seepage through the liner occurred, it happened where the liner offered lower resistance to flow than the interface and DRZ, for example, at construction joints. Maintenance grouting, in selected areas of the WIPP shafts, has been utilized to reduce seepage.

Table I2-8. Drawings Showing Configuration of Existing WIPP Shafts (Drawings are in Appendix I2-E)

Shaft	Drawing Title	Sheet Number of Drawing SNL-007
Waste	Near-Surface/Rustler Formation Waste Shaft Stratigraphy & As-Built Elements	2 of 28
Waste	Salado Formation Waste Shaft Stratigraphy & As-Built Elements	3 of 28
AIS	Near-Surface/Rustler Formation Air Intake Shaft Stratigraphy & As-Built Elements	7 of 28
AIS	Salado Formation Air Intake Shaft Stratigraphy & As-Built Elements	8 of 28
Exhaust	Near-Surface/Rustler Formation Exhaust Shaft Stratigraphy & As-Built Elements	12 of 28
Exhaust	Salado Formation Exhaust Shaft Stratigraphy & As-Built Elements	13 of 28
Salt Handling	Near-Surface/Rustler Formation Salt Handling Shaft Stratigraphy & As-Built Elements	17 of 28
Salt Handling	Salado Formation Salt Handling Shaft Stratigraphy & As-Built Elements	18 of 28

Table I2-9. Summary of Information Describing Existing WIPP Shafts

Shafts				
	Salt Handling	Waste	Air Intake	Exhaust
A. <u>Construction Method</u>				
i. Sinking method	Blind bored	Initial 6' pilot hole slashed by drill & blast (smooth wall blasting)	Raise bored	Initial 6' pilot hole slashed by drill & blast (smooth wall blasting)
ii. Dates of shaft sinking	7/81-10/81	Drilled 12/81-2/82 Slashed 10/83-6/84 Grouted 1984 & 1988	12/87-8/88	9/83-11/84
iii. Ground treatment in water-bearing zone	Grout behind steel liner during construction		Grouted 1993	Grouted 1985, 1986, & 1987
iv. Sump construction	Drill & blast	Drill & blast	No sump	No sump
B. <u>Upper Portion of Shaft *</u>				
i. Type of liner	Steel	Concrete	Concrete	Concrete
ii. Lining diameter (ID)	10'-0"	19'-0"	18'-0"/16'-7"	14'-0"
iii. Excavated diameter	11'-10"	20'-8" to 22'-4"	20'-3"	15'-8" to 16'-8"
iv. Installed depth of liner	838.5'	812'	816'	846'
C. <u>Key Portion of Shaft *</u>				
i. Construction material	Reinf. conc. w/chem. seals	Reinf. concrete w/chem. seals	Reinf. concrete w/chem. seals	Reinf. concrete w/chem. seals
ii. Liner diameter (ID)	10'-0"	19'-0"	16'-7"	14'-0"
iii. Excavated diameter	15'-0" to 18'-0"	27'-6" to 31'-0"	29'-3" to 35'-3"	21'-0" to 26'-0"
iv. Depth-top of Key	844'	836'	834'	846'
v. Depth-bottom of Key	883'	900'	897'	910'
vi. Dow Seal #1 depth	846' to 848'	846' to 849'	839' to 842'	853' to 856'
vii. Dow Seal #2 depth	853' to 856'	856' to 859'	854' to 857'	867' to 870'
viii. Dow Seal #3 depth	868 to 891'	NA	NA	NA
ix. Top of salt (Rustler/Salado contact)	851'	843'	841'	853'
D. <u>Lower Shaft (Unlined) *</u>				
i. Type of support	Unlined	Chain link mesh	Unlined	Chain link mesh
ii. Excavated diameter	11'-10"	20'-0"	20'-3"	15'-0"
iii. Depth-top of "unlined"	882'	900'	904'	913'
iv. Depth-bottom of "unlined"	2144'	2142'	2128'	2148'
E. <u>Station *</u>				
i. Type of support	Wire mesh		Wire mesh	Wire mesh
ii. Principal dimensions	21H x 31W	12H x 30W	25H x 36W	12H x 23W
iii. Depth-top of station	2144'	2142'	2128'	2148'
iv. Depth-floor of station	2162'	2160'	2150'	2160'
F. <u>Sump *</u>				
Depth-top of sump	2162'	2160'	No sump	No sump
Depth-bottom of sump	2272'	2286'		
G. <u>Shaft Duty</u>	Construction hoisting of excavated salt; personnel hoisting	Hoisting shaft for lowering waste containers; personnel hoisting until waste receipt	Ventilation shaft for intake (fresh) air; personnel hoisting	Exhaust air ventilation shaft

*This information is from the MOC drawings identified on Sheets 2, 3, 7, 8, 12, 13, 17, and 18 of Drawing SNL-007 (see Appendix I2-E).

4.3 Sealing System Design Description

This section describes the shaft sealing system design, components, and functions. The shaft sealing system consists of three essentially independent parts:

1. The seals in the Salado Formation provide the primary regulatory barrier. They will limit fluid flow into and out of the repository throughout the 10,000-year regulatory period.
2. The seals in the Rustler Formation will limit flow from the water-bearing members of the Rustler Formation and limit commingling of Magenta and Culebra groundwaters.
3. The seals in the Dewey Lake Redbeds and the near-surface units will limit infiltration of surface water and preclude accidental entry through the shaft openings.

The same sealing system is used in all four shafts. Therefore an understanding of the sealing system for one shaft is sufficient to understand the sealing system in all shafts. Only minor differences exist in the lengths of the components, and the component diameters differ to accommodate the existing shaft diameters.

The shaft liner will be removed in four locations in each shaft. All of these locations are within the Rustler Formation. Additionally, the upper portion of each shaft key will be eliminated. The portion of the shaft key that will be eliminated spans the Rustler/Salado interface and extends into the Salado Formation. The shaft liner removal locations are

1. from 10 ft above the Magenta Member to the base of the Magenta (removal distances vary from 34–39 ft because of different member thickness at shaft locations),
2. for a distance of 10 ft in the anhydrite of the Tamarisk Member,
3. through the full height of the Culebra (17–24 ft), and
4. from the top anhydrite unit in the unnamed lower member to the top of the key (67–85 ft).

Additionally, the concrete will be removed from the top of the key to the bottom of the key's lower chemical seal ring (23 to 29 ft). Drawing SNL-007, Sheets 4, 9, 14, and 19 in Appendix I2-E show shaft liner removal plans, and Sheet 23 shows key removal plans.

The decision to abandon portions of the shaft lining and key in place is based on two factors. First, no improvements in the performance of the sealing system associated with removal of these isolated sections of concrete have been identified. Second, because the keys are thick and heavily reinforced, their removal would be costly and time consuming. No technical problems are associated with the removal of this concrete; thus, if necessary, its removal can be incorporated in any future design.

The DRZ will be pressure grouted throughout the liner and key removal areas and for a distance of 10 ft above and below all liner removal areas. The pressure grouting will stabilize the DRZ during liner removal and shaft sealing operations. The grouting will also control groundwater seepage during and after liner removal. The pressure grouting of the DRZ has not been assigned a sealing function beyond the construction period. It is likely that this grout will seal the DRZ for an extended period of time. However, past experience with grout in the mining and tunneling industries demonstrates that groundwater eventually opens alternative pathways

through the media and reestablishes seepage patterns (maintenance grouting is common in both mines and tunnels). Therefore, post-closure sealing of the DRZ in the Rustler Formation has not been assumed in the design.

The compacted clay sealing material (bentonite) will seal the shaft cross-section in the Rustler Formation. In those areas where the shaft liner has been removed, the compacted clay will confine the vertical movement of groundwater in the Rustler to the DRZ. Sealing the shaft DRZ is accomplished in the Salado Formation. It is achieved initially through the interruption of the halite DRZ by concrete-asphalt waterstops and on a long-term basis through the natural process of healing the halite DRZ. The properties of the compacted clay are discussed in Section 5.3.2. The concrete-asphalt waterstops and DRZ healing in the Salado are discussed in Sections 7.6.1 and 7.5.2 respectively.

Reduction of the uncertainty associated with long-term performance is addressed by replacing the upper and lower Salado Formation salt columns used in some of the earlier designs with compacted clay columns and by adding asphalt sealing components in the Salado Formation. Use of disparate materials for sealing components reduces the uncertainty associated with a common-mode failure.

The compacted salt column provides a seal with an initial permeability several orders of magnitude higher than the clay or asphalt columns; however, its long-term properties will approach those of the host rock. The permeability of the compacted salt, after consolidation, will be several orders of magnitude lower than that of the clay and comparable to that of the asphalt. The clay provides seals of known low permeability at emplacement, and asphalt provides an independent low permeability seal of the shaft cross-section and the shaft wall interface at the time of installation. Sealing of the DRZ in the Rustler Formation during the construction period is accomplished by grouting, and initial sealing of the DRZ in the Salado Formation is accomplished by three concrete-asphalt waterstops.

In the following sections, each component of each of the three shaft segments is identified by name and component number (see Figure I2-5 for nomenclature). Associated drawings in Appendix I2-E are also identified. Drawings showing the overall system configurations for each shaft are listed in Table I2-10.

4.3.1 Salado Seals

The seals placed in the Salado Formation are composed of (1) consolidated salt, clay, and asphalt components that will function for very long periods, exceeding the 10,000-year regulatory period; and (2) salt saturated concrete components that will function for extended periods. The specific components that comprise the Salado seals are described below.

4.3.1.1 Compacted Salt Column

The compacted salt column (Component 10 in Figure I2-5, and shown in Drawing SNL-007, Sheet 25) will be constructed of crushed salt taken from the Salado Formation. The length of the salt column varies from 170 to 172 m (556 to 564 ft) in the four shafts. The compacted salt column is sized to allow the column and concrete-asphalt waterstops at either end to be placed between the Vaca Triste Unit and Marker Bed 136. The salt will be placed and compacted to a density approaching 90% of the average density of intact Salado salt. The effects of creep closure will cause this density to increase with time, further reducing permeability.

The salt column will offer limited resistance to fluid migration immediately after emplacement, but it will become less permeable as creep closure further compacts the salt. Salt creep increases rapidly with depth; therefore, at any time, creep closure of the shaft will be greater at greater depth. The location and initial compaction density of the compacted salt column were chosen to assure consolidation of the compacted salt column in the 100 years following repository closure. The state of salt consolidation, results of analyses predicting the creep closure of the shaft, consolidation and healing of the compacted salt, and healing of the DRZ surrounding the compacted salt column are presented in Sections 7.5 and 8.4 of this document. These results indicate that the salt column will become an effective long-term barrier within 100 years.

Table I2-10. Drawings Showing the Sealing System for Each Shaft (Drawings are in Appendix I2-E)

Shaft	Drawing Title	Sheet Number of Drawing SNL 007
Waste	Near-Surface/Rustler Formation Waste Shaft Stratigraphy & Sealing Subsystem Profile	4 of 28
Waste	Salado Formation Waste Shaft Stratigraphy & Sealing Subsystem Profile	5 of 28
AIS	Near-Surface/Rustler Formation Air Intake Shaft Stratigraphy & Sealing Subsystem Profile	9 of 28
AIS	Salado Formation Air Intake Shaft Stratigraphy & Sealing Subsystem Profile	10 of 28
Exhaust	Near-Surface/Rustler Formation Exhaust Shaft Stratigraphy & Sealing Subsystem Profile	14 of 28
Exhaust	Salado Formation Exhaust Shaft Stratigraphy & Sealing Subsystem Profile	15 of 28
Salt Handling	Near-Surface/Rustler Formation Salt Handling Shaft Stratigraphy & Sealing Subsystem Profile	19 of 28
Salt Handling	Salado Formation Salt Handling Shaft Stratigraphy & Sealing Subsystem Profile	20 of 28

4.3.1.2 Upper and Lower Salado Compacted Clay Columns

The upper and lower Salado compacted clay columns (Components 8 and 12 respectively in Figure I2-5) are shown in detail on Drawing SNL-007, Sheet 24. A commercial well-sealing grade sodium bentonite will be used to construct the upper and lower Salado clay columns. These clay columns will effectively limit fluid movement from the time they are placed and will provide an effective barrier to fluid migration throughout the 10,000-year regulatory period and thereafter. The upper clay column ranges in length from 102 to 107 m (335 to 351 ft), and the lower clay column ranges in length from 29 to 33 m (94 to 107 ft) in the four shafts. The locations for the upper and lower clay columns were selected based on the need to limit fluid migration into the compacting salt column. The lower clay column stiffness is sufficient to promote early healing of the DRZ, thus removing the DRZ as a potential pathway for fluids (Appendix D in the permit application, Section 5.2.1).

4.3.1.3 Upper, Middle, and Lower Concrete-Asphalt Waterstops

The upper, middle, and lower concrete-asphalt waterstops (Components 7, 9, and 11 respectively in Figure I2-5) are identical and are composed of three elements: an upper concrete plug, a central asphalt waterstop, and a lower concrete plug. These components are also shown on Drawing SNL-007, Sheet 22. The concrete specified is a specially developed salt-saturated concrete called Salado Mass Concrete (**SMC**). In all cases the component's overall design length is 15 m (50 ft).

The upper and lower concrete plugs of the concrete-asphalt waterstop are identical. They fill the shaft cross-section and have a design length of 7 m (23 ft). The plugs are keyed into the shaft wall to provide positive support for the plug and overlying sealing materials. The interface between the concrete plugs and the surrounding formation will be pressure grouted. The upper plug in each component will support dynamic compaction of the overlying sealing material if compaction is specified. Dynamic compaction of the salt column is discussed in Section 6.

The asphalt waterstop is located between the upper and lower concrete plugs. In all cases a kerf extending one shaft radius beyond the shaft wall is cut in the surrounding salt to contain the waterstop. The kerf is 0.3 m (1 ft) high at its edge and 0.6 m (2 ft) high at the shaft wall. The kerf, which cuts through the existing shaft DRZ, will result in the formation of a new DRZ along its perimeter. This new DRZ will heal shortly after construction of the waterstop, and thereafter the waterstop will provide a very low permeability barrier to fluid migration through the DRZ. The formation and healing of the DRZ around the waterstop are addressed in Section 7.6.1. The asphalt fill for the waterstop extends two feet above the top of the kerf to assure complete filling of the kerf. The construction procedure used assures that shrinkage of the asphalt from cooling will not result in the creation of voids within the kerf and will minimize the size of any void below the upper plug.

Concrete-asphalt waterstops are placed at the top of the upper clay column, the top of the compacted salt column, and the top of the lower clay column. The concrete-asphalt waterstops provide independent seals of the shaft cross-section and the DRZ. The SMC plugs (and grout) will fill irregularities in the shaft wall, bond to the shaft wall, and seal the interface. Salt creep against the rigid concrete components will place a compressive load on the salt and promote early healing of the salt DRZ surrounding the SMC plugs. The asphalt waterstop will seal the shaft cross-section and the DRZ.

The position of the concrete components was first determined by the location of the salt and clay columns. The components were then moved upward or downward from their initial design location to assure the components were located in regions where halite was predominant. This positioning, coupled with variations in stratigraphy, is responsible for the variations in the lengths of the salt and clay columns.

4.3.1.4 Asphalt Column

An asphalt-aggregate mixture is specified for the asphalt column (Component 6 in Figure I2-5). This column is 42 to 44 m (138 to 143 ft) in length in the four shafts, as shown in Drawing SNL-007, Sheet 23. The asphalt column is located above the upper concrete-asphalt waterstop; it extends approximately 5 m (16 ft) above the Rustler/Salado interface. A 6-m (20-ft) long concrete plug (part of the Rustler seals) is located just above the asphalt column.

The existing shaft linings will be removed from a point well above the top of the asphalt column to the top of the shaft keys. The concrete shaft keys will be removed to a point just below the lowest chemical seal ring in each key. The asphalt column is located at the top of the Salado Formation and provides an essentially impermeable seal for the shaft cross section and along the shaft wall interface. The length of the asphalt column will decrease slightly as the column cools. The procedure for placing the flowable asphalt-aggregate mixture is described in Section 6.

4.3.1.5 Shaft Station Monolith

A shaft station monolith (Component 13) is located at the base of the each shaft. Because the configurations of each shaft differ, drawings of the shaft station monoliths for each shaft were prepared. These drawings are identified in Table I2-11. The shaft station monoliths will be constructed with SMC. The monoliths function to support the shaft wall and adjacent drift roof, thus preventing damage to the seal system as the access drift closes from natural processes.

Table I2-11. Drawings Showing the Shaft Station Monoliths (Drawings are in Appendix I2-E)

Shaft	Drawing Title	Sheet Number of Drawing SNL-007
Waste	Waste Shaft Shaft Station Monolith	6 of 28
AIS	Air Intake Shaft Shaft Station Monolith	11 of 28
Exhaust	Exhaust Shaft Shaft Station Monolith	16 of 28
Salt Handling	Salt Handling Shaft Shaft Station Monolith	21 of 28

4.3.2 Rustler Seals

The seals in the Rustler Formation are composed of the Rustler compacted clay column and a concrete plug. The concrete plug rests on top of the asphalt column of the Salado seals. The clay column extends from the concrete plug through most of the Rustler Formation and terminates above the Rustler's highest water-bearing zone in the Forty-niner Member.

4.3.2.1 Rustler Compacted Clay Column

The Rustler compacted clay column (Component 4 in Figure I2-5) is shown on Drawing SNL-007, Sheet 27 for each of the four shafts. A commercial well-sealing-grade sodium bentonite will be used to construct the Rustler clay column, which will effectively limit fluid movement from the time of placement and provide an effective barrier to fluid migration throughout the 10,000-year regulatory period and thereafter. Design length of the Rustler clay column is about 71 m (234 to 235 ft) in the four shafts.

The location for the Rustler clay columns was selected to limit fluid migration into the shaft cross-section and along the shaft wall interface and to limit mixing of Culebra and Magenta waters. The clay column extends from above the Magenta Member to below the Culebra Member of the Rustler Formation. The Magenta and Culebra are the water-bearing units of the Rustler. The members above the Magenta (the Forty-niner), between the Magenta and Culebra (the Tamarisk), and below the Culebra (the unnamed lower member) are aquitards in the vicinity of the WIPP shafts.

4.3.2.2 Rustler Concrete Plug

The Rustler concrete plug (Component 5 in Figure I2-5) is constructed of SMC. The plugs for the four shafts are shown on Drawing SNL-007, Sheet 26. The plug is 6 m (20 ft) long and will fill the shaft cross-section. The plug is placed directly on top of the asphalt column of the Salado seals. The plug will be keyed into the surrounding rock and grouted. The plug permits work to begin on the overlying clay column before the asphalt has completely cooled. The option of constructing the overlying clay columns using dynamic compaction (present planning calls for construction using compressed clay blocks) is also maintained by keying the plug into the surrounding rock.

4.3.3 Near-Surface Seals

The near-surface region is composed of dune sand, the Mescalero caliche, the Gatuña Formation, the Santa Rosa Formation, and the Dewey Lake Redbeds. This region extends from the ground surface to the top of the Rustler Formation—a distance of about 160 m (525 ft). All but about 15 m (50 ft) of this distance is composed of the Dewey Lake Redbeds Formation. The near-surface seals are composed of two earthen fill columns and a concrete plug. The upper earthen fill column (Component 1) extends from the shaft collar through the surficial deposits downward to the top of the Dewey Lake Redbeds. The concrete plug (Component 2) is placed in the top portion of the Dewey Lake Redbeds, and the lower earthen fill column (Component 3) extends from the concrete plug into the Rustler Formation. These components are shown on Drawing SNL-007, Sheet 28.

This seal will limit the amount of surface water entering the shafts and will limit the potential for any future groundwater migration into the shafts. The near surface seals will also completely close the shafts and prevent accidental entry and excessive subsidence in the vicinity of the shafts. As discussed in Section 4.3.2, the existing shaft linings will be abandoned in place throughout the near-surface region.

4.3.3.1 Near-Surface Upper Compacted Earthen Fill

This component (Component 1 in Figure I2-5) will be constructed using locally available fill. The fill will be compacted to a density near that of the surrounding material to inhibit the migration of surface waters into the shaft cross-section. The length of this column varies from 17 to 28 m (56 to 92 ft) in the four shafts. In all cases, this portion of the WIPP sealing system may be modified as required to facilitate decommissioning of the WIPP surface facilities.

4.3.3.2 Near-Surface Concrete Plug

Current plans call for an SMC plug (Component 2 in Figure I2-5). However, freshwater concrete may be used if found to be desirable at a future time, and if approved by NMED through the Permit modification process specified in 20.4.1.900 NMAC (incorporating 40 CFR §270.42). The plug extends 12 m (40 ft) downward from the top of the Dewey Lake Redbeds. It is placed inside the existing shaft lining, and the interface is grouted.

4.3.3.3 Near-Surface Lower Compacted Earthen Fill

This component (Component 3 in Figure I2-5) will be constructed using locally available fill, which will be placed using dynamic compaction (the same method used to construct the salt column). The fill will be compacted to a density equal to or greater than the surrounding materials to inhibit the migration of surface waters into the shaft cross-section. The length of this column varies from 136 to 148 m (447 to 486 ft) in the four shafts.

5. Material Specification

Appendix I2-A provides a body of technical information for each of the WIPP shaft seal materials. The materials specification characterizes each seal material, establishes the adequacy of its function, states briefly the method of component placement, and quantifies expected characteristics (particularly permeability) pertinent to a WIPP-specific shaft seal design. The goal of the materials specifications is to substantiate why materials used in this seal system design will limit fluid flow within the shafts and thereby limit releases of hazardous constituents from the WIPP site at the regulatory boundary.

This section summarizes materials characteristics for shaft seal system components designed for the WIPP. The shaft seal system will not be constructed for decades; however, if it were to be constructed in the near term, materials specified could be placed in the shaft and meet performance specifications using current materials and construction techniques. Construction methods are described in Appendix I2-B. Materials specifications and construction specifications are not to be construed as the only materials or methods that would suffice to seal the shafts effectively. Undoubtedly, the design will be modified, perhaps simplified, and construction alternatives may prove to be advantageous during the years before seal construction proceeds. Nonetheless, a materials specification is necessary to establish a frame of reference for shaft seal design and analysis, to guide construction specifications, and to provide a basis for seal material parameters.

Design detail and other characteristics of the geologic, hydrologic, and chemical setting are provided in the text, appendices, and references. The four shafts will be entirely filled with dense materials possessing low permeability and other desirable engineering and economic attributes. Seal materials include concrete, clay, asphalt, and compacted salt. Other construction and fill materials include cementitious grout and earthen fill. Concrete, clay, and asphalt are common construction materials used extensively in sealing applications. Their descriptions, drawn from literature and site-specific references, are given in Appendix I2-A. Compaction and natural reconsolidation of crushed salt are uniquely applied here. Therefore, crushed salt specification includes discussion of constitutive behavior and sealing performance, specific to WIPP applications. Cementitious grout is also specified in some detail. Only rudimentary discussion of earthen fill is given here and in Appendices A and B. Specifications for each material are discussed in the following order:

- functions,
- material characteristics,
- construction,
- performance requirements,
- verification methods.

Seal system components are materials possessing high durability and compatibility with the host rock. The system contains functional redundancy and uses differing materials to reduce uncertainty in performance. All materials used in the shaft seal system are expected to maintain their integrity for very long periods. Some sealing components reduce fluid flow soon after placement while other components are designed to function well beyond the regulatory period.

5.1 Longevity

A major environmental advantage of the WIPP locale is an overall lack of groundwater to seal against. Even though very little regional water is present in the geologic setting, the seal system reflects great concern for groundwater's potential influence on the shaft seal system. If the hydrologic system sustained considerable fluid flow, brine geochemistry could impact engineered materials. Brine would not chemically change the compacted salt column, but mechanical effects of pore pressure are of concern to reconsolidation. The geochemical setting, as further discussed in Section 2.4, will have little influence on concrete, asphalt, and clay shaft seal materials. Each material is durable because the potential for degradation or alteration is very low.

Materials used to form the shaft seals are the same as those identified in the scientific and engineering literature as appropriate for sealing deep geologic repositories for radioactive wastes. Durability or longevity of seal components is a primary concern for any long-term isolation system. Issues of possible degradation have been studied throughout the international community and within waste isolation programs in the USA. Specific degradation studies are not detailed in this document because longevity is one of the over-riding attributes of the materials selected and degradation is not perceived to be likely. However, it is acknowledged here that microbial degradation, seal material interaction, mineral transformation, such as silicification of bentonite, and effects of a thermal pulse from asphalt or hydrating concrete are areas of continuing investigations.

Among longevity concerns, degradation of concrete is the most recognized. At this stage of the design, it is established that only small volumes of brine ever reach the concrete elements (see Section C4). Further analysis concerned with borehole plugging using cementitious materials shows that at least 100 pore volumes of brine in an open system would be needed to begin degradation processes. In a closed system, such as the hydrologic setting in the WIPP shafts, phase transformations create a degradation product of increased volume. Net volume increase owing to phase transformation in the absence of mass transport would decrease rather than increase permeability of concrete seal elements.

Asphalt has existed for thousands of years as natural seeps. Longevity studies specific to DOE's Hanford site have utilized asphalt artifacts buried in ancient ceremonies to assess long-term stability (Wing and Gee, 1994). Asphalt used as a seal component deep in the shaft will inhabit a benign environment, devoid of ultraviolet light or an oxidizing atmosphere. Additional assurance against possible microbial degradation in asphalt elements is provided with addition of lime. For these reasons, it is believed that asphalt components will possess their design characteristics well beyond the regulatory period.

Natural bentonite is a stable material that generally will not change significantly over a period of ten thousand years. Bentonitic clays have been widely used in field and laboratory experiments concerned with radioactive waste disposal. As noted by Gray (1993), three internal mechanisms, illitization, silicification and charge change, could affect sealing properties of bentonite. Illitization and silicification are thermally driven processes and, following discussion by Gray (1993), are not possible in the environment or time-frame of concern at the WIPP. The naturally occurring Wyoming bentonite which is the specified material for the WIPP shaft seal is well over a million years old. It is, therefore, highly unlikely that the metamorphism of bentonite enters as a design concern.

5.2 Materials

5.2.1 Mass Concrete

Concrete has low permeability and is widely used for hydraulic applications. The specification for mass concrete presents a special design mixture of a salt-saturated concrete called Salado Mass Concrete (SMC). Performance of SMC and similar salt-saturated mixtures has been established through analogous industrial applications and in laboratory and field testing. The documentation substantiates adequacy of SMC for concrete applications within the WIPP shafts.

The function of the concrete is to provide durable components with small void volume, adequate structural compressive strength, and low permeability. SMC is used as massive plugs, a monolith at the base of each shaft, and in tandem with asphalt waterstops. Concrete is a rigid material that will support overlying seal components while promoting natural healing processes within the salt DRZ. Concrete is one of the redundant components that protects the reconsolidating salt column. The salt column will achieve low permeabilities in fewer than 100 years, and concrete will no longer be needed at that time. However, concrete will continue to provide good sealing characteristics for a very long time.

Salt-saturated concrete contains sufficient salt as an aggregate to saturate hydration water with respect to NaCl. Salt-saturated concrete is required for all uses within the Salado Formation because fresh water concrete would dissolve part of the host rock. The concrete specified for the shaft seal system has been tailored for the service environment and includes all the engineering properties of high quality concrete, as described in Appendix I2-A. Among these are low heat of hydration, high compressive strength, and low permeability. Because SMC provides material characteristics of high-performance concrete, it will likely be the concrete of choice for all seal applications at the WIPP.

Construction involves surface preparation and slickline placement. A batching and mixing operation on the surface will produce a wet mixture having low initial temperatures. Placement uses a tremie line, where the fresh concrete exits the slickline below the surface level of the concrete being placed. Placed in this manner, the SMC will have low porosity (about 5%) with or without vibration. Tremie line placement is a standard construction method in mining operations.

Specifications of concrete properties include mixture proportions and characteristics before and after hydration. SMC strength is much greater than required for shaft seal elements, and the state of stress within the shafts is compressional with little shear stress developing. Volume stability of the SMC is also excellent; this, combined with salt-saturation, assures a good bond with the salt. Permeability of SMC is very low, consistent with most concrete (Pfeifle et al., 1996). Because of a favorable state of stress and isothermal conditions, the SMC will remain intact. Because little brine is available to alter concrete elements, minimal degradation is possible. These favorable attributes combine to assure concrete elements within the Salado will remain structurally sound and possess very low permeability (between 2×10^{-21} and 1×10^{-17} m²) for exceedingly long periods. A permeability distribution function and associated discussion are given in Appendix I2-A.

Standard ASTM specifications are made for the green and hydrated concrete properties. Quality control and a history of successful use in both civil construction and mining applications assure proper placement and performance.

5.2.2 Compacted Clay

Compacted clays are commonly proposed as primary sealing materials for nuclear waste repositories and have been extensively investigated against rigorous performance requirements. Advantages of clays for sealing purposes include low permeability, demonstrated longevity in many types of natural environments, deformability, sorptive capacity, and demonstrated successful utilization in practice for a variety of sealing purposes.

Compacted clay as a shaft sealing component functions as a barrier to brine flow and possibly to gas flow (see alternative construction methods in Appendix I2-B). Compacted bentonitic clay can generate swelling pressure and clays have sufficient rigidity to promote healing of any DRZ in the salt. Wetted swelling clay will seal fractures as it expands into available space and will ensure tightness between the clay seal component and the shaft walls.

The Rustler and Salado compacted clay columns are specified to be constructed of dense sodium bentonite blocks. An extensive experimental data base exists for the permeability of sodium bentonites under a variety of conditions. Many other properties of sodium bentonite, such as strength, stiffness, and chemical stability, are established. Bentonitic clays heal when fractured and can penetrate small fractures or irregularities in the host rock. Further, bentonite is stable in the seal environment. These properties, noted by international waste isolation programs, make bentonite a widely accepted seal material.

From the bottom clay component to the top earthen fill, different methods will be used to place clay materials in the shaft. Seal performance within the Salado Formation is far more important to regulatory compliance of the seal system than is performance of clay and earthen fill in the overlying formations. Therefore, more time and effort will be expended on placement of Salado clay components. Three potential construction methods could be used to place clay in the shaft, as discussed in Appendix I2-B: compacted blocks, vibratory roller, and dynamic compaction. Construction of Salado clay components specifies block assembly.

Required sealing performance of compacted clay elements varies with location. For example, Component 4 provides separation of water-bearing zones, while the lowest clay column (Component 12) limits fluid flow to the reconsolidating salt column. If liquid saturation in the clay column of 85% can be achieved, it would serve as a gas barrier. In addition, compacted clay seal components promote healing of the salt DRZ. To achieve low permeabilities, the dry density of the emplaced bentonite should be about 1.8 g/cm³. A permeability distribution function for performance assessment and the logic for its selection are given in Appendix I2-A.

Verification of specified properties such as density, moisture content, permeability, or strength of compacted clay seals can be determined by direct measurement during construction. However, indirect methods are preferred because certain measurements, such as permeability, are likely to be time consuming and invasive. Methods used to verify the quality of emplaced seals will include quality of block production and field measurements of density.

5.2.3 Asphalt

Asphalt is used to prevent water migration down the shaft in two ways: as an asphalt column near the Rustler/Salado contact and as a "waterstop" sandwiched between concrete plugs at three locations within the Salado Formation. Asphalt components of the WIPP seal design add assurance that minimal transport of brine down the sealed shaft will occur.

Asphalt is a widely used construction material because of its many desirable engineering properties. Asphalt is a strong cement, readily adhesive, highly waterproof, and durable. Furthermore, it is a plastic substance that is readily mixed with mineral aggregates. A range of viscosity is achievable for asphalt mixtures. It is highly resistant to most acids, salts, and alkalis. These properties are well suited to the requirements of the WIPP shaft seal system.

Construction of the seal components containing asphalt can be accomplished using a slickline process where low-viscosity heated material is effectively pumped into the shaft. The technology to apply the asphalt in this manner is available as described in the construction procedures in Appendix I2-B.

The asphalt components are required to endure for about 100 years and limit brine flow down the shaft to the compacted salt component. Since asphalt will not be subjected to ultraviolet light or an oxidizing environment, it is expected to provide an effective seal for centuries. Air voids less than 2% ensure low permeability. The permeability of the massive asphalt column is expected to have an upper limit $1 \times 10^{-18} \text{ m}^2$.

Sufficient construction practice and laboratory testing information is available to assure performance of the asphalt component. Laboratory validation tests to optimize viscosity may be desirable before final installation specifications are prepared. In general, verification tests would add quantitative documentation to expected performance values and have direct application to WIPP.

5.2.4 Compacted Salt Column

A reconsolidated column of natural WIPP salt will seal the shafts permanently. If salt reconsolidation is unimpeded by fluid pore pressures, the material will eventually achieve extremely low permeabilities approaching those of the native Salado Formation. Recent developments in support of the WIPP shaft seal system have produced confirming experimental results, constitutive material models, and construction methods that substantiate use of a salt column to create a low permeability seal component. Reuse of salt excavated in the process of creating the underground openings has been advocated since its initial proposal in the 1950s. Replacing the natural material in its original setting ensures physical, chemical, and mechanical compatibility with the host formation.

The function of the compacted and reconsolidated salt column is to limit transmission of fluids into or out of the repository for the statutory period of 10,000 years. The functional period starts within a hundred years and lasts essentially forever. After a period of consolidation, the salt column will almost completely retard gas or brine migration within the former shaft opening. A completely consolidated salt column will achieve flow properties indistinguishable from natural Salado salt.

1 The salt component is composed of crushed Salado salt with additional small amounts of water.
2 The total water content of the crushed salt will be adjusted to 1.5 wt% before it is tamped into
3 place. Field and laboratory tests have verified that natural salt can be compacted to significant
4 fractional density ($\rho \geq 0.9$) with addition of these moderate amounts of water.

5 Dynamic compaction is the specified construction procedure to tamp crushed salt in the shaft.
6 Deep dynamic compaction provides great energy to the crushed salt, is easy to apply, and has
7 an effective depth of compactive influence greater than lift thickness. Dynamic compaction is
8 relatively straightforward and requires a minimal work force in the shaft. Compaction itself will
9 follow procedures developed in a large-scale compaction demonstration, as outlined in
10 Appendix I2-B.

11 Numerical models of the shaft provide density of the compacted salt column as a function of
12 depth and time. Many calculations comparing models for consolidation of crushed salt were
13 performed to quantify performance of the salt column, as discussed in Appendix D of Appendix
14 I2 in the permit application and the references (Callahan et al., 1996; Brodsky et al., 1996).
15 From the density-permeability relationship of reconsolidating crushed salt, permeability of the
16 compacted salt seal component is calculated. In general, results show that the bottom of the
17 salt column consolidates rapidly, achieving permeability of $1 \times 10^{-19} \text{ m}^2$ in about 50 years. By 100
18 years, the middle of the salt column reaches similar permeability.

19 Results of the large-scale dynamic compaction demonstration suggest that deep dynamic
20 compaction will produce a sufficiently dense starting material. As with other seal components,
21 testing of the material in situ will be difficult and probably not optimal to ensure quality of the
22 seal element. This is particularly apparent for the compacted salt component because the
23 compactive effort produces a finely powdered layer on the top of each lift. It was demonstrated
24 (Hansen and Ahrens, 1996) that the fine powder is very densely compacted upon tamping the
25 superincumbent lifts. The best means to ensure that the crushed salt element is placed properly
26 is to establish performance through verification of quality assurance/quality control procedures.
27 If crushed salt is placed with a reasonable uniformity of water and compacted with sufficient
28 energy, long-term performance can be assured.

29 **5.2.5 Cementitious Grout**

30 Cementitious grouting is specified for all concrete members. Grouting is also used in advance of
31 liner removal to stabilize the ground and to limit water inflow during shaft seal construction.
32 Cementitious grout is specified because of its proven performance, nontoxicity, and previous
33 use at the WIPP.

34 The function of grout is to stabilize the surrounding rock before existing concrete liners are
35 removed. Grout will fill fractures within adjacent lithologies, thereby adding strength and
36 reducing permeability and, hence, water inflow during shaft seal construction. Grout around
37 concrete members of the concrete asphalt waterstop will be employed in an attempt to tighten
38 the interface and fill microcracks in the DRZ. Efficacy of grouting will be determined during
39 construction.

40 An ultrafine cementitious grout has been specifically developed for use at the WIPP (Ahrens
41 and Onofrei, 1996). This grout consists of Type 5 portland cement, pumice as a pozzolanic
42 material, and superplasticizer. The average particle size is approximately 2 microns. The

ultrafine grout is mixed in a colloidal grout mixer, with a water to components ratio (**W:C**) of 0.6:1.

Drilling and grouting sequences provided in Appendix I2-B follow standard procedures. Grout will be mixed on the surface and transported by slickline to the middle deck on the multi-deck stage (galloway). Grout pressures are specified below lithostatic to prevent hydrofracturing.

Performance of grout is not a consideration for compliance issues. Grouting of concrete elements is an added assurance to tighten interfaces. Grouting is used to facilitate construction by stabilizing any loose rock behind the concrete liner.

No verification of the effectiveness of grouting is currently specified. If injection around concrete plugs is possible, an evaluation of quantities and significance of grouting will be made during construction. Procedural specifications will include measurements of fineness and determination of rheology in keeping with processes established during the WIPP demonstration grouting (Ahrens et al., 1996).

5.2.6 Earthen Fill

A brief description of the earthen fill is provided in Appendix I2-A, and construction is summarized in Appendix I2-B. Compacted fill can be obtained from local borrow pits, or material excavated during shaft construction can be returned to the shaft. There are minimal design requirements for earthen fill and none that are related to WIPP regulatory performance.

5.3 Concluding Remarks

Materials specifications in Appendix I2-A provide descriptions of seal materials along with reasoning on their expected reliability in the WIPP setting. The specification follows a framework that states the function of the seal component, a description of the material, and a summary of construction techniques. The performance requirements for each material are detailed.

Materials chosen for use in the shaft seal system have several common desirable attributes: low permeability, high density, compatibility, longevity, low cost, constructability, availability, and supporting documentation.

6. Construction Techniques

Construction of the shaft sealing system is feasible. The described procedures utilize currently available technology, equipment, and materials to satisfy shaft sealing system design guidance. Although alternative methods are possible, those described satisfy the design guidance requirements listed in Table I2-7 and detailed in the appendices. Construction feasibility is established by reference to comparable equipment and activities in the mining, petroleum, and food industries and test results obtained at the WIPP. Equipment and procedures for emplacement of sealing materials are described below.

6.1 Multi-Deck Stage

A multi-deck stage (Figures I2-6 and I2-7) consisting of three vertically connected decks will be the conveyance utilized during the shaft sealing operation. Detailed sketches of the multi-deck stage appear in Appendix I2-E. The stage facilitates installation and removal of utilities and provides a working platform for the various sealing operations. A polar crane attached to the lower deck provides the mechanism required for dynamic compaction and excavation of the shaft walls. Additionally, the header at the bottom of the slickline is supported by a reinforced steel shelf, which is securely bolted to the shaft wall during emplacement of sealing materials. The multi-deck stage can be securely locked in place in the shaft whenever desired (e.g., during dynamic compaction, excavation of the salt walls of the shaft, grouting, liner removal, etc.). The multi-deck stage is equipped with floodlights, remotely aimed closed-circuit television, fold-out floor extensions, a jib crane, and range-finding devices. Similar stages are commonly employed in shaft sinking operations.

The polar crane can be configured for dynamic compaction (Figure I2-6) or for excavation of salt (Figure I2-7); a man cage or bucket can be lowered through the stage to the working surface below. Controlled manually or by computer, the crane and its trolley utilize a geared track drive. The crane can swiftly position the tamper (required for dynamic compaction) in the drop positions required (Figure I2-8) or accommodate the undercutter required for excavation of the shaft walls. The crane incorporates a hoist on the trolley and an electromagnet, enabling it to position, hoist, and drop the tamper. A production rate of one drop every two minutes during dynamic compaction is possible.

6.2 Salado Mass Concrete (Shaft Station Monolith and Shaft Plugs)

Salado Mass Concrete, described in Appendix I2-A, will be mixed on surface at 20°C and transferred to emplacement depth through a slickline (i.e., a steel pipe fastened to the shaft wall and used for the transfer of sealing materials from surface to the fill horizon) minimizing air entrainment and ensuring negligible segregation. Existing sumps will be filled to the elevation of the floor of the repository horizon, and emplacement of the shaft station monolith is designed to eliminate voids at the top (back) of the workings.

When excavating salt for waterstops or plugs in the Salado Formation, an undercutter attached to the trolley of the polar crane will be forced into the shaft wall by a combination of geared trolley and undercutter drives. Full circumferential cuts will be accomplished utilizing the torque developed by the geared polar crane drive.

The undercutter proposed is a modified version of those currently in use in salt and coal mines, where their performance is proven. Such modifications and applications have been judged feasible by the manufacturer.

The concrete-salt interface and DRZ around concrete plugs in the Salado Formation (and the one at the base of the Rustler Formation) will be grouted with ultrafine grout. Injection holes will be collared in the top of the plug and drilled downward at 45° below horizontal. The holes will be drilled in a “spin” pattern describing a downward opening cone designed to intercept both vertical and horizontal fractures (Figure I2-9). The holes will be stage grouted (i.e., primary holes will be drilled and grouted, one at a time). Secondary holes will then be drilled and grouted, one at a time, on either side of primaries that accepted grout.

6.3 Compacted Clay Columns (Salado and Rustler Formations)

Cubic blocks of sodium bentonite, 20.8 cm on the edge and weighing approximately 18 kg, will be precompacted on surface to a density between 1.8 and 2.0 gm/cm³ and emplaced manually. The blocks will be transferred from surface on the man cage. Block surfaces will be moistened with a fine spray of potable water, and the blocks will be manually placed so that all surfaces are in contact. Peripheral blocks will be trimmed to fit irregularities in the shaft wall, and remaining voids will be filled with a thick mortar of sodium bentonite and potable water. Such blocks have been produced at the WIPP and used in the construction of 0.9-m-diameter seals, where they performed effectively (Knowles and Howard, 1996). Alternatives, which may be considered in future design evaluations, are discussed in Appendix I2-B.

6.4 Asphalt Waterstops and Asphaltic Mix Columns

Neat asphalt is selected for the asphalt waterstops, and an asphaltic mastic mix (AMM) consisting of neat asphalt, fine silica sand, and hydrated lime will be the sealing material for the columns. Both will be fluid at emplacement temperature and remotely emplaced. Neat asphalt (or AMM, prepared in a pug mill near the shaft collar) will be heated to 180°C and transferred to emplacement depth via an impedance-heated, insulated tremie line (steel pipe) suspended from slips (pipe holding device) at the collar of the shaft.

This method of line heating is common practice in the mining and petroleum industries. This method lowers the viscosity of the asphalt so that it can be pumped easily. Remote emplacement by tremie line eliminates safety hazards associated with the high temperature and gas produced by the hot asphalt. Fluidity ensures that the material will flow readily and completely fill the excavations and shaft. Slight vertical shrinkage will result from cooling (calculations in Appendix D of Appendix I2 in the permit application), but the material will maintain contact with the shaft walls and the excavation for the waterstop. Vertical shrinkage will be counteracted by the emplacement of additional material.

6.5 Compacted WIPP Salt

Dynamic compaction of mine-run WIPP salt has been demonstrated (Ahrens and Hansen, 1995). The surface demonstration produced salt compacted to 90% of in-place rock salt density, with a statistically averaged permeability of 1.65×10^{-15} m². Additional laboratory consolidation of this material at 5 MPa confining pressure (simulating creep closure of the salt) resulted in increased compaction and lower permeability (Brodsky, 1994). Dynamic compaction was selected because it is simple, robust, proven, has excellent depth of compaction, and is applicable to the vertical WIPP shafts.

The compactive effect expanded laterally and downward in the demonstration, and observation during excavation of the compacted salt revealed that the lateral compactive effect will fill irregularities in the shaft walls. Additionally, the depth of compaction, which was greater than

that of the three lifts of salt compacted, resulted in the bottom lift being additionally compacted during compaction of the two overlying lifts. This cumulative effect will occur in the shafts.

Construction of the salt column will proceed in the following manner:

- Crushed and screened salt will be transferred to the fill elevation via slickline. Use of slicklines is common in the mining industry, where they are used to transfer backfill materials or concrete to depths far greater than those required at the WIPP. Potable water will be added via a fine spray during emplacement at the fill surface to adjust the moisture content to 1.5 ± 0.3 wt%, accomplished by electronically coordinating the weight of the water with that of the salt exiting the hose.
- Dynamic compaction will then be used to compact the salt by dropping the tamper in specific, pre-selected positions such as those shown in Figure I2-8.

6.6 Grouting of Shaft Walls and Removal of Liners

The procedure listed below is a common mining practice which will be followed at each elevation where liner removal is specified. If a steel liner is present, it will be cut into manageable pieces and hoisted to the surface for disposal, prior to initiation of grouting.

Upward opening cones of diamond drill holes will be drilled into the shaft walls in a spin pattern (Figure I2-10) to a depth ensuring complete penetration of the Disturbed Rock Zone (**DRZ**) surrounding the shaft. For safety reasons, no major work will be done from the top deck; all sealing activities will be conducted from the bottom deck. The ends of the holes will be 3 m apart, and the fans will be 3 m apart vertically, covering the interval from 3 m below to 3 m above the interval of liner removal. Tests at the WIPP demonstrated that the ultrafine cementitious grout penetrated more than 2 m from the injection holes (Ahrens et al., 1996).

Injection holes will be drilled and grouted one at a time, as is the practice in stage grouting. Primary holes are grouted first, followed by the grouting of secondary holes on either side of primaries that accepted grout. Ultrafine grout will be injected below lithostatic pressure to avoid hydrofracturing the rock, proceeding from the bottom fan upward. Grout will be mixed on surface and transferred to depth via the slickline.

Radial, horizontal holes will then be drilled on a 0.3-m grid, covering the interval to be removed. These will be drilled to a depth sufficient to just penetrate the concrete liner. A chipping hammer will be used to break a hole through the liner at the bottom of the interval. This hole, approximately 0.3 m in diameter, will serve as "free face," to which the liner can be broken. Hydraulically-actuated steel wedges will then be used in the pre-drilled holes to break out the liner in manageable pieces, beginning adjacent to the hole and proceeding upward. Broken concrete will be allowed to fall to the fill surface, where it will be gathered and hoisted to the surface for disposal. Chemical seal rings will be removed as encountered.

6.7 Earthen Fill

Local soil, screened to produce a maximum particle dimension of approximately 15 mm, will be the seal material. This material will be transferred to the fill surface via the slickline and emplaced in the same manner as the salt. After adjusting the moisture content of the earthen fill below the concrete plug in the Dewey Lake Redbeds to achieve maximum compaction, the fill

1 will be dynamically compacted, achieving a permeability as low as that of the enclosing
2 formation.

3 The portion of the earthen fill above the plug will be compacted with a vibratory-impact
4 sheepsfoot roller, a vibratory sheepsfoot roller, or a walk-behind vibratory plate compactor,
5 because of insufficient height for dynamic compaction.

6 **6.8 Schedule**

7 For discussion purposes, it has been assumed that the shafts will be sealed two at a time. This
8 results in the four shafts being sealed in approximately six and a half years. The schedules
9 presented in Appendix I2-B are based on this logic. Sealing the shafts sequentially would
10 require approximately eleven and a half years.

7. Structural Analyses of Shaft Seals

7.1 Introduction

The shaft seal system was designed in accordance with design guidance described in Section 3.2. To be successful, seal system components must exhibit desired structural behavior. The desired structural behavior can be as simple as providing sufficient strength to resist imposed loads. In other cases, structural behavior is critical to achieving desired hydrological properties. For example, permeability of compacted salt depends on the consolidation induced by shaft closure resulting from salt creep. In this example, results from structural analyses feed directly into fluid-flow calculations, which are described in Section 8, because structural behavior affects both time-dependent permeabilities of the compacted salt and pore pressures within the compacted salt. In other structural considerations, thermal effects are analyzed as they affect the constructability and schedule for the seal system. Thus a series of analyses, loosely termed structural analyses, were performed to accomplish three purposes:

1. to determine loads imposed on components and to assess both structural stability based on the strength of the component and mechanical interaction between components;
2. to estimate the influence of structural behavior of seal materials and surrounding rock on hydrological properties; and
3. to provide structural and thermal related information on construction issues.

For the most part, structural analyses rely on information and design details presented in the Design Description (Section 4), the Design Drawings (Appendix I2-E), and Material Specification (Section 5 and Appendix I2-A). Some analyses are generic, and calculation input and subsequent results are general in nature.

7.2 Analysis Methods

Finite-element modeling was the primary numerical modeling technique used to evaluate structural performance of the shaft seals and surrounding rock mass. Well documented finite-element computer programs, SPECTROM-32 and SPECTROM-41, were used in structural and thermal modeling, respectively. The computer program SALT_SUBSID was used in the subsidence modeling over the backfilled shaft-pillar area. Specific details of these computer programs as they relate to structural calculations are listed in Appendix D of Appendix I2 in the permit application, Section D2.

7.3 Models of Shaft Seals Features

Structural calculations require material models to characterize the behavior of (1) each seal material (concrete, crushed salt, compacted clay, and asphalt); (2) the intact rock lithologies in the near-surface, Rustler, and Salado formations; and (3) any DRZ within the surrounding rock. A general description of the material models used in characterizing each of these materials and features is given below. Details of the models and specific values of model parameters are given in Appendix D in the permit application, Section D3.

7.3.1 Seal Material Models

The SMC thermal properties required for the structural analyses (thermal conductivity, density, specific heat, and volumetric heat generation rate) were obtained from SMC test data. Concrete was assumed to behave as a viscoelastic material, based on experimental data, and the elastic

modulus of SMC was modeled as age-dependent. Strength properties of SMC were specified in the design (see Appendix I2-A).

For crushed salt, the deformational model included a nonlinear elastic component and a creep consolidation component. The nonlinear elastic modulus was assumed to be density-dependent, based on laboratory test data performed on WIPP crushed salt. Creep consolidation behavior of crushed salt was based on three candidate models whose parameters were obtained from model fitting to hydrostatic and shear consolidation test data performed on WIPP crushed salt. Creep consolidation models include functional dependencies on density, mean stress, stress difference, temperature, grain size, and moisture content.

Compacted clay was assumed to behave according to a nonlinear elastic model in which shear stiffness is negligible, and asphalt was assumed to behave as a weak elastic material. Thermal properties of asphalt were taken from literature.

7.3.2 Intact Rock Lithologies

Salado salt was assumed to be argillaceous salt that is governed by the Multimechanism Deformation Coupled Fracture (**MDCF**) model, which is an extension of the Munson-Dawson (**M-D**) creep model. A temperature-dependent thermal conductivity was necessary.

Salado interbeds were assumed to behave elastically. Their material strength was assumed to be described by a Drucker-Prager yield function, consistent with values used in previous WIPP analyses.

Deformational behavior of the near-surface and Rustler Formation rock types was assumed to be time-invariant, and their strength was assumed to be described by a Coulomb criterion, consistent with literature values.

7.3.3 Disturbed Rock Zone Models

Two different models were used to evaluate the development and extent of the DRZ within intact salt. The first approach used ratios of time-dependent stress invariants to quantify the potential for damage or healing to occur. The second approach used the damage stress criterion according to the MDCF model for WIPP salt.

7.4 Structural Analyses of Shaft Seal Components

7.4.1 Salado Mass Concrete Seals

Five analyses related to structural performance of SMC seals were performed, including (1) a thermal analysis, (2) a structural analysis, (3) a thermal stress analysis, (4) a dynamic compaction analysis, and (5) an analysis of the effects of clay swelling pressure. This section presents these analyses and evaluates the results in terms of the performance of the SMC seal. Details of these calculations are given in Appendix D in the permit application, Section D4.

7.4.1.1 Thermal Analysis of Concrete Seals

The objective of this calculation was to determine expected temperatures within (and surrounding) an SMC emplacement resulting from its heat of hydration. Results indicate that the concrete component temperature increases from ambient (27°C) to a maximum of 53°C at 0.02 year after emplacement. The maximum temperature in the surrounding salt is 38°C at

approximately the same time. The thermal gradient within the concrete is approximately 1.5°C/m. Most of the higher temperatures are contained within the concrete. At a radial distance of 2 m into the surrounding salt, the temperature rise is less than 1°C. These conditions are favorable for proper performance of the SMC components. A 26°C temperature rise and a 1.5°C/m temperature gradient are not large enough to cause thermal cracking as the concrete cools (Andersen et al., 1992).

7.4.1.2 Structural Analysis of Concrete Seals

The objectives of this calculation were to determine (1) expected stresses within the concrete components caused by restrained creep of the surrounding salt and (2) expected stresses in the concrete component from weight of overlying seal material.

In the upper concrete-asphalt waterstop, radial stresses increase (compression is positive) from zero at time of emplacement ($t = 0$) to 2.5 MPa at $t = 50$ years. Similarly, radial stresses in the middle concrete component range from 3.5 to 4.5 MPa at 50 years after emplacement. In the lower concrete-asphalt waterstop, radial stresses range from 4.5 to 5.5 MPa at $t = 50$ years. All the calculated stresses are well below the unconfined compressive strength of the concrete (30 MPa).

The upper, middle, and lower concrete-asphalt waterstops are located at depths of 300, 420, and 610 m, respectively. When performing these calculations, it was assumed that each concrete component must support the weight of the overlying materials between it and the next concrete component above it. Using an average overburden density of 0.02 MPa/m, stresses induced by the overlying material are significantly less than the strength of the concrete. The structural integrity of concrete components will not be compromised by either induced radial stress or imposed vertical stress.

7.4.1.3 Thermal Stress Analysis of Concrete Seals

The objectives of this calculation were (1) to determine thermal stresses in concrete components from the heat of hydration and (2) to determine thermal impact on the creep of the surrounding salt.

Thermoelastic stresses in the concrete were calculated based on a maximum temperature increase of 26°C and assuming a fully confined condition. Results of this calculation indicate that short-term compressive thermal stresses in the concrete will be less than 9.2 MPa. The temperature rise in the surrounding salt is insignificant in terms of producing either detrimental or beneficial effects. Based on these results, the structural integrity of concrete components will not be compromised by thermoelastic stresses caused by heat of hydration.

7.4.1.4 Effect of Dynamic Compaction on Concrete Seals

The objective of this calculation was to determine a required thickness of seal layers above concrete components to reduce the impact of dynamic compaction. Compaction depths for crushed salt and clay layers are 2.8 m and 2.2 m, respectively. Layers 3.7-m thick for crushed salt and 3-m thick for clay are to be emplaced before compaction begins, thus providing a layer about 30% thicker than the calculated compaction depths.

7.4.1.5 Effect of Clay Swelling Pressures on Concrete Seals

The objective of this calculation was to determine the increased stresses within concrete components as a result of clay swelling pressures. Test measurements on confined bentonite at an emplaced density of 1.8 g/cm^3 indicate that anticipated swelling pressures are on the order of 3.5 MPa. In order to fracture the salt surrounding the clay, the swelling pressures must exceed the lithostatic rock stress in the salt, which ranges from nominally 8.3 MPa at the upper clay seal to 14.4 MPa at the lower clay seal. The design strength of the concrete (31.0 MPa) is significantly greater than the swelling pressure of 3.5 MPa. Even in the unlikely event that the clay swelled to lithostatic pressures, the resulting state of stress in the concrete seal would lie well below any failure surface. Furthermore, the compressive tangential stress in the salt along the shaft wall, even after stress relaxation from creep, is always larger than lithostatic. Hence, radial fracturing from clay swelling pressure is not expected.

7.4.2 Crushed Salt Seals

Two analyses related to structural performance of crushed salt seals were performed, including (1) a structural analysis and (2) an analysis to determine effects of pore pressure on consolidation of crushed salt seals. This section presents the results of these analyses and evaluates the results in terms of performance of crushed salt seals. Details of these analyses are given in Appendix D in the permit application, Section D4.

7.4.2.1 Structural Analysis of Compacted Salt Seal

The objectives of this calculation were (1) to determine the fractional density of the crushed salt seal as a function of time and depth and, using these results, (2) to determine permeability of the crushed salt as a function of time and depth.

Results indicate that compacted salt will increase from its emplaced fractional density of 90% to a density of 95% approximately 40, 80, and 120 years after emplacement at the bottom, middle, and top of the shaft seal, respectively. Using the modified Sjaardema-Krieg creep consolidation model, the times required to fully reconsolidate the crushed salt to 100% fractional density are 70 years, 140 years, and 325 years at the bottom, middle, and top of the salt column, respectively. Based on these results, the desired fractional densities (hence, permeability) can be achieved over a substantial length of the compacted salt seal in the range of 50 to 100 years.

7.4.2.2 Pore Pressure Effects on Reconsolidation of Crushed Salt Seals

The objective of this calculation was to determine the effect of pore pressure on the reconsolidation of the crushed salt seal. Fractional densities of the crushed salt seal were calculated using the modified Sjaardema-Krieg consolidation model for a range of pore pressures (0, 2, and 4 MPa). Results indicate that times required to consolidate the crushed salt increase as the pore pressure increases, as expected. For example, for a pore pressure of 2 MPa, the times required to achieve a fractional density of 96% are about 90 years, 205 years, and 560 years at the bottom, middle, and top of the crushed salt column, respectively. A pore pressure of 4 MPa would effectively prevent reconsolidation of the crushed salt within a reasonable period ($<1,000$ years). The results of this calculation were used in the fluid flow calculations, and the impact of these pore pressures on the permeability of the crushed salt seal is described in Section 8 and Appendix C of Appendix I2 in the permit application.

7.4.3 Compacted Clay Seals

One analysis was performed to determine the structural response of compacted clay seals. The objective of this calculation was to determine stresses in the upper Salado compacted clay component and the lower Salado compacted clay component as a result of creep of the surrounding salt. Details of this calculation are given in Appendix D in the permit application, Section D4. Results of this calculation indicate that after 50 years the compressive stresses in the upper Salado compacted clay component are about 0.7 MPa, not including the effects of swelling pressures. Similarly, after 50 years the stresses in the lower Salado compacted clay component are approximately 2.6 MPa. Based on these results, the compacted clay component will provide some restraint to the creep of salt and induce a back (radial) stress in the clay seal, which will promote healing of the DRZ in the surrounding intact salt (see discussion about DRZ in Section 7.5.1).

7.4.4 Asphalt Seals

Three analyses were performed related to structural performance of the asphalt seals, including (1) a thermal analysis, (2) a structural analysis, and (3) a shrinkage analysis. This section presents the results of these analyses and evaluates the results in terms of the performance of the asphalt seal. Details of these analyses are given in Appendix D of Appendix I2 in the permit application Section D4.

7.4.4.1 Thermal Analysis

The objectives of this calculation were (1) to determine temperature histories within the asphalt seal and the surrounding salt and (2) to determine effects of the length of the waterstop.

Results indicate that the center of the asphalt column will cool from its emplaced temperature of 180°C to 83°C, 49°C, 31°C, and 26°C at times 0.1 year, 0.2 year, 0.5 year, and 1.0 year, respectively. Similarly, the asphalt/salt interface temperatures at corresponding times are 47°C, 38°C, 29°C, and 26°C. The time required for a waterstop to cool is significantly less than that required to cool the asphalt column. Based on these results, about 40 days are required for asphalt to cool to an acceptable working environment temperature. The thermal impact on enhanced creep rate of the surrounding salt is considered to be negligible.

7.4.4.2 Structural Analysis

The objective of this analysis was to calculate pressures in asphalt that result from restrained creep of the surrounding salt and to evaluate stresses induced on the concrete seal component by such pressurization.

Results indicate that pressures in the waterstops after 100 years are 1.8 MPa, 2.5 MPa, and 3.2 MPa for the upper, middle, and lower waterstops, respectively. Based on these results, the structural integrity of concrete components will not be compromised by imposed pressures, and the rock surrounding the asphalt will not be fractured by the pressure. The pressure from asphalt is enough to initiate healing of the DRZ surrounding the waterstop.

7.4.4.3 Shrinkage Analysis

The objective of this analysis was to calculate shrinkage of the asphalt column as it cools from its emplaced temperature to an acceptable working environment temperature. Results of this analysis indicate that the 42-m asphalt column will shrink 0.9 m in height as the asphalt cools from its emplaced temperature of 180°C to 38°C.

7.5 Disturbed Rock Zone Considerations

7.5.1 General Discussion of DRZ

Microfracturing leading to a DRZ occurs within salt whenever excavations are made. Laboratory and field measurements show that a DRZ has enhanced permeability. The body of evidence strongly suggests that induced fracturing is reversible and healed when deviatoric stress states created by the opening are reduced. Rigid seal components in the shaft provide a restraint to salt creep closure, thereby inducing healing stress states in the salt. A more detailed discussion of the DRZ is included in Appendix D in the permit application.

7.5.2 Structural Analyses

Three analyses were performed to determine the behavior of the DRZ in the rock mass surrounding the shaft. The first analysis considered time-dependent DRZ development and subsequent healing of intact Salado salt surrounding each of the four seal materials. The second analysis considered time-dependent development of the DRZ within anhydrite and polyhalite interbeds within the Salado Formation. The last analysis considered time-independent DRZ development within the near-surface and Rustler formations. These analyses are discussed below and given in more detail in Appendix D of Appendix I2 in the permit application, Section D5. Results from these analyses were used as input conditions for the fluid flow analysis presented in Section 8 and Appendix C of Appendix I2 in the permit application.

7.5.2.1 Salado Salt

The objective of this calculation was to determine time-dependent extent of the DRZ in salt, assuming no pore pressure effects, for each of the four shaft seal materials (i.e., concrete, crushed salt, compacted clay, and asphalt. The seal materials below a depth of about 300 m provide sufficient rigidity to heal the DRZ within 100 years. Asphalt, modeled as a weak elastic material, will not create a stress state capable of healing the DRZ because it is located high in the Salado.

7.5.2.2 Salado Anhydrite Beds

The objective of this calculation was to determine the extent of the DRZ within the Salado anhydrite and polyhalite interbeds as a result of creep of surrounding salt.

For all interbeds, the factor of safety against failure (shear or tensile fracturing) increases with depth into the rock surrounding the shaft wall. These results indicate that, with the exception of Marker Bed 117 (**MB117**), the factor of safety is greater than 1 (no DRZ will develop) for all interbeds. For MB117, the potential for fracturing is localized to within 1 m of the shaft wall.

7.5.2.3 Near-Surface and Rustler Formations

The objective of this calculation was to determine the extent of the DRZ surrounding the shafts in the near-surface and Rustler formations.

Rock types in near-surface and Rustler formations are anhydrite, dolomite, and mudstone. These rock types exhibit time-independent behavior. Results indicate that no DRZ will develop in anhydrite and dolomite (depths between 165 and 213 m). For mudstone layers, the radial extent of the DRZ increases with depth, reaching a maximum of 2.6 shaft radii at a depth of 223 m.

7.6 Other Analyses

This section discusses two structural analyses performed in support of design concerns, namely (1) the asphalt waterstops constructability and (2) benefits from shaft station backfilling. Analyses performed in support of these efforts are discussed below and given in more detail in Appendix D of Appendix I2 in the permit application, Section D6.

7.6.1 Asphalt Waterstops

The DRZ is a major contributor to fluid flows through a low permeability shaft seal system, regardless of the materials emplaced within the shaft. Therefore, to increase the confidence in the overall shaft seal, low permeability layers (termed radial waterstops) were included to intersect the DRZ surrounding the shaft. These waterstops are emplaced to alter the flow direction either inward toward the shaft seal or outward toward intact salt. Asphalt-filled waterstops will be effective soon after emplacement. The objectives of these structural calculations were to evaluate performance of the waterstops in terms of (1) intersecting the DRZ around the shaft, (2) inducing a new DRZ because of special excavation, and (3) promoting healing of the DRZ.

Results indicate that the DRZ from the shaft extends to a radial distance of less than one shaft radius (3.04 m). Waterstop excavation extends the DRZ radially to about 1.4 shaft radii (4.3 m). However, this extension is localized within the span of the concrete component and extends minimally past the waterstop edge. The DRZ extent reduced rapidly after the concrete and asphalt restrained creep of the surrounding salt. After 20 years, the spatial extent of the DRZ is localized near the asphalt-concrete interface, extending spatially into the salt at a distance of less than 2 m. Based on these results, construction of waterstops is possible without substantially increasing the DRZ. Furthermore, the waterstop extends well beyond the maximum extent of the DRZ surrounding the shaft and effectively blocks this flow path (within 2 years after emplacement), albeit over only a short length of the flow path.

7.6.2 Shaft Pillar Backfilling

The objective of this calculation was to assess potential benefits from backfilling a portion of the shaft pillar to reduce subsurface subsidence and thereby decrease the potential for inducing fractures along the shaft wall. The calculated subsidence without backfilling is less than one foot, due to the relatively low extraction ratio at the WIPP. Based on the results of this analysis, backfilling portions of the shaft pillar would result in only 10% to 20% reduction in surface subsidence. This reduction in subsidence from backfilling is not considered enough to warrant backfilling the shaft pillar area. The shaft seals within the Salado are outside the angle-of-draw for any horizontal displacements caused by the subsidence over the waste panels. Moreover, horizontal strains caused by subsidence induced by closures within the shaft pillar are compressive in nature and insignificant in magnitude to induce fracturing along the shaft wall.

8. Hydrologic Evaluation of the Shaft Seal System

8.1 Introduction

The design guidance in Section 3 presented the rationale for sealing the shaft seal system with low permeability materials, but it did not provide specific performance measures for the seal system. This section compares the hydrologic behavior of the system to several performance measures that are directly related to the ability of the seal system to limit liquid and gas flows through the seal system. The hydrologic evaluation is focused on the processes that could result in fluid flow through the shaft seal system and the ability of the seal system to limit any such flow. Transport of radiological or hazardous constituents will be limited if the carrier fluids are similarly limited.

The hydrologic performance models are fully described in Appendix C of Appendix I2 in the permit application. The analyses presented are deterministic. Quantitative values for those parameters that are considered uncertain and that may significantly impact the primary performance measures have been varied, and the results are presented in Appendix C of Appendix I2 in the permit application. This section summarizes the seal system performance analyses and discusses results within the context of the design guidance of Section 3. The results demonstrate that (1) fluid flows will be limited within the shaft seal system and (2) uncertainty in the conceptual models and parameters for the seal system are mitigated by redundancy in component function and materials.

8.2 Performance Models

The physical processes that could impact seal system performance are presented in detail in Appendix C of Appendix I2 in the permit application. These processes have been incorporated into four performance models. These models evaluate (1) downward migration of groundwater from the Rustler Formation, (2) gas migration and consolidation of the crushed salt seal component, (3) upward migration of brines from the repository, and (4) flow between water-bearing zones in the Rustler Formation. The first three are analyzed using numerical models of the Air Intake Shaft (**AIS**) seal system and the finite-difference codes SWIFT II and TOUGH28W. These codes are extensively used and well documented within the scientific community. A complete description of the models is provided in Appendix C of Appendix I2 in the permit application. The fourth performance model uses a simple, analytical solution for fluid flow. Results from the analyses are summarized in the following sections and evaluated in terms of the design guidance presented in Section 3.

Material properties and conceptual models that may significantly impact seal system performance have been identified, and uncertainty in properties and models have been addressed through variation of model parameters. These parameters include (1) the effective permeability of the DRZ, (2) those describing salt column consolidation and the relationship between compacted salt density and permeability, and (3) repository gas pressure applied at the base of the shaft seal system.

8.3 Downward Migration of Rustler Groundwater

The shaft seal system is designed to limit groundwater flowing into and through the shaft sealing system (see Section 3). The principal source of groundwater to the seal system is the Culebra Member of the Rustler Formation. The Magenta Member of this formation is also considered a groundwater source, albeit a less significant source than the Culebra. No

significant sources of groundwater exist within the Salado Formation; however, brine seepage has been noted at a number of the marker beds. The modeling includes the marker beds, as discussed in Appendix C of Appendix I2 in the permit application. Downward migration of Rustler groundwater must be limited so that liquid saturation of the compacted salt column salt column does not impact the consolidation process and to ensure that significant quantities of brine do not reach the repository horizon. Because it is clear that limitation of liquid flow into the salt column necessarily limits liquid flow to the repository, the volumetric flux of liquid into and through the salt column were selected as performance measures for this model.

Consolidation of the compacted salt column salt column will be most rapid immediately following seal construction. Simulations were conducted for the 200-year period following closure to demonstrate that, during this initial period, downward migration of Rustler groundwater will be insufficient to impact the consolidation process. Lateral migration of brine through the marker beds is also quantified in the analysis and shown to be nondetrimental to the function of the salt column.

8.3.1 Analysis Method

Seal materials will not, in general, be fully saturated with liquid at the time of construction. The host rock surrounding the shafts will also be partially desaturated at the time of seal construction. The analysis presented in this section assumes a fully saturated system. The effects of partial saturation of the shaft seal system are favorable in terms of system performance, as will be discussed in Section 8.3.2.

Seal material and host rock properties used in the analyses are discussed in Appendix C of Appendix I2 in the permit application, Section C3. Appendix I2-A contains a detailed discussion of seal material properties. A simple perspective on the effects of material and host rock properties may be obtained from Darcy's Law. At steady-state, the flow rate in a fully saturated system depends directly on the system permeability. The seal system consists of the component material and host rock DRZ. Low permeability is specified for the engineered materials; thus the system component most likely to impact performance is the DRZ. Rock mechanics calculations presented in Appendix D of Appendix I2 in the permit application predict that the DRZ in the Salado Formation will not be vertically continuous because of the intermittent layers of stiff anhydrites (marker beds). Asphalt waterstops are included in the design to minimize DRZ impacts. The effects of the marker beds and the asphalt waterstops on limiting downward migration are explicitly simulated through variation of the permeability of the layers of Salado DRZ.

Initial, upper, and lateral boundary conditions for the performance model are consistent with field measurements for the physical system. At the base of the shaft a constant atmospheric pressure is assumed.

8.3.2 Summary of Results

The initial pore volumes in the filled repository and the AIS salt column are approximately 460,000 m³ and 250 m³, respectively. The performance model predicts a maximum cumulative flow of less than 5 m³ through the sealed shafts for the 200 years following closure. If the marker beds have a disturbed zone immediately surrounding the shaft, the maximum flow is less than 10 m³ during the same period. Assuming the asphalt waterstops are not effective in interrupting the vertical DRZ, the volumetric flow increases but is still less than 30 m³ for the 200

years following closure. These volumes are less than 1/100 of 1% of the pore volume in the repository and less than 20% of the initial pore volume of the salt column.

Two additional features of the model predictions should also be considered. The first of these is that flow rates fall from less than 1 m³ / year in the first five years to negligible values within 10 years of seal construction. Therefore most of the cumulative flow occurs within a few years following closure. The second feature is the model prediction that the system returns to nearly ambient undisturbed pressures within two years. The repressurization occurs quickly within the model due to the assumption of a fully saturated flow regime because of brine incompressibility. As will be discussed in Section 8.4, the pore pressure in the compacted salt column is a critical variable in the analysis. The pressure profiles predicted by the model are an artifact of the assumption of full liquid saturation and do not apply to the pore pressure analysis of the salt column.

The magnitude of brine flow that can reach the repository through a sealed shaft is minimal and will not impact repository performance. The flow that reaches the salt column must be assessed with regard to the probable impacts on the consolidation process. Although the volume of flow to the salt column is a small percentage of the available pore volume, the saturation state and fluid pore pressure of this component are the variables of significance. These issues cannot be addressed by a fully saturated model. Instead it is necessary to include these findings in a multi-phase model that includes the salt column. This is the topic of Section 8.4.

The results of the fully saturated model will over-predict the flow rates through the sealed shaft. This analysis does not take credit for the time required for the system to resaturate, nor does it take credit for the sorptive capabilities of the clay components. The principal source of groundwater to the system is the Rustler Formation. The upper clay component is located below the Rustler and above the salt column and will be emplaced at a liquid saturation state of approximately 80%. Bentonite clays exhibit strong hydrophilic characteristics, and it is expected that the upper clay component will have these same characteristics. As a result, it is possible that a significant amount of the minimal Rustler groundwater that reaches the clay column will be absorbed and retained by this seal component. Although this effect is not directly included in the present analysis, the installation of a partially saturated clay component provides assurance that the flow rates predicted by the model are maximum values.

8.4 Gas Migration and Consolidation of Compacted Salt Column

The seal system is designed to limit the flow of gas from the disposal system through the sealed shafts. Migration of gas could impact performance if this migration substantially increases the fluid pore pressure of the compacted salt column. The initial pore pressure of the salt column will be approximately atmospheric. The sealed system will interact with the adjacent desaturated host rock as well as the far-field formation. Natural pressurization will occur as the system returns to an equilibrium state. This pressurization, coupled with seepage of brine through the marker beds, will also result in increasing fluid pore pressure within the compacted salt column. The analysis presented in this section addresses the issue of fluid pore pressure in the compacted salt column resulting from the effects of gas generation at the repository horizon and natural repressurization from the surrounding formation. A brief discussion on the impedance to gas flow afforded by the lower compacted clay column is also presented.

8.4.1 Analysis Method

A multi-phase flow model of the lower seal system was developed to evaluate the performance of components extending from the middle SMC component to the repository horizon. Rock mechanics calculations presented in Section 7 and Appendix D of Appendix I2 in the permit application predict that the compacted salt column will consolidate for a period of approximately 400 years if the fluid-filled pores of the column do not produce a backstress. Within the physical setting of the compacted salt column, three processes have been identified which may result in a significant increase in pore pressure: groundwater flow from the Rustler Formation, gas migration from the repository, and natural fluid flow and repressurization from the Salado Formation. The first two processes were incorporated into the model as initial and boundary conditions, respectively. The third process was captured in all simulations through modeling of the lithologies surrounding the shaft. Simulations were conducted for 200 years following closure to evaluate any effects these processes might have on the salt column during this initial period.

As discussed in Section 8.3.1, the host rock DRZ is an important consideration in seal system performance. A vertically continuous DRZ could exist in both the Rustler and Salado Formations. Concrete-asphalt waterstops are included in the design to add assurance that a DRZ will not adversely impact seal performance. The significance of a continuous DRZ and waterstops will be evaluated based on results of the performance model.

A detailed description of the model grid, assumptions, and parameters is presented in Appendix C of Appendix I2 in the permit application.

8.4.2 Summary of Results

The consolidation process is a function of both time and depth. The resultant permeability of the compacted salt column will similarly vary. To simplify the evaluation, an effective permeability of the salt component was calculated. This permeability is calculated by analogy to electrical circuit theory. The permeability of each model layer is equated to a resistor in a series of resistors. The equivalent resistance (i.e., permeability) of a homogeneous column of identical length is derived in this manner. Figure I2-11 illustrates this process.

Results of the performance model simulations are summarized in Table I2-12. The effective permeabilities were calculated by the model assuming that, as the salt consolidated, permeability was reduced pursuant to the best-fit line through the experimental data (Appendix I2-A, Figure I2A-7). From Table I2-12 it is clear that, for all simulated conditions, the salt column consolidates to very low values in 200 years. Differences in the effective permeability because of increased repository gas pressure and a vertically continuous DRZ were negligible. The DRZ around concrete components is predicted to heal (Appendix D of Appendix I2 in the permit application) within 25 years. If the asphalt waterstops do not function as intended, the DRZ in this region will still heal in 25 years, as compared to 2 years for effective waterstops. The effective permeability of the compacted salt column increases by about a factor of two for this condition. However, the resultant permeability is sufficiently low that the compacted salt columns will comprise permanent effective seals within the WIPP shafts.

Table I2-12. Summary of Results from Performance Model

Repository Pressure	Rustler Flow (m ³)	Continuous DRZ (Yes/No)	Concrete-Asphalt Waterstop Healing Time (Years)	Effective Permeability at 200 Years (m ²)
7 MPa in 100 Years	0	No	2	3.3×10^{-20}
14 MPa in 200 Years	0	No	2	3.3×10^{-20}
7 MPa in 100 Years	2.7	Yes	2	3.4×10^{-20}
7 MPa in 100 Years	17.2	Yes	25	6.0×10^{-20}

The relationship between the fractional density (i.e., consolidation state) of the compacted salt column and permeability is uncertain, as discussed in Appendix I2-A. Lines drawn through the experimental data (Figure A-7) provide a means to quantify this uncertainty but do not capture the actual physical process of consolidation. As observed through microscopy, consolidation is dominated by pressure solution and redeposition, a mechanism of mass movement facilitated by the presence of moisture on grain boundaries (Hansen and Ahrens, 1996). As this process continues, the connected porosity and hence permeability of the composite mass will reduce at a rate that has not been characterized by the data collected in WIPP experiments. The results of the multi-phase performance model presented in Table I2-12 used a best-fit line through the data. Additional simulations were conducted using a line that represents a 95% certainty that the permeability is less than or equal to values taken from this line. Model simulations that used the 95% line are not considered representative of the consolidation process. However, these results provide an estimation of the significance that this uncertainty may have on the seal system performance.

Figure I2-12 depicts the effective permeability of the salt column as a function of time using the 95% line. The consolidation process, and hence permeability reduction, essentially stopped at 75 years for this simulation. Although the model predicts that the fractional density at the base of the salt column will reach approximately 97% of the density of intact halite, the permeability remains several orders of magnitude higher than that of the surrounding host rock. As a result, repressurization occurs rapidly throughout the vertical extent of the compacted salt column, and consolidation ceases. Laboratory experiments have shown that permeability to brine should decrease to levels of 10^{-18} to 10^{-20} m² at the fractional densities predicted by the performance model. The transport of brine within the consolidating salt will reduce the permeability even further (Brodsky et al., 1995). The predicted permeability of 10^{-16} m² is still sufficiently low that brine migration would be limited (DOE, 1995). However, the results of this analysis are more valuable in terms of demonstrating the coupled nature of the mechanical and hydrological behavior of consolidating crushed salt.

A final consideration within this performance model relates to the lower compacted clay column. This clay column is included in the design to provide a barrier to both gas and brine migration from the repository horizon. The ability of the clay to prevent gas migration will depend upon its liquid saturation state (Section 5 and Appendix I2-A). The lower clay component has an initial liquid saturation of about 80%, and portions of the column achieve brine saturations of nearly 100% during the 200 year simulation period. If the clay component performs as designed, gas migration through this component should be minimal. An examination of the model gas

1 saturations indicates that, for all runs, gas flow occurs primarily through the DRZ prior to
2 healing. These model predictions are consistent with field demonstrations that brine-saturated
3 bentonite seals will prevent gas flow at differential pressures of up to 4 MPa (Knowles and
4 Howard, 1996).

5 **8.5 Upward Migration of Brine**

6 The performance model discussed in Section 8.3 was modified to simulate undisturbed
7 equilibrium pressures. As discussed in Appendix C of Appendix I2 in the permit application, the
8 Salado Formation is overpressurized with respect to the measured heads in the Rustler, and
9 upward migration of contaminated brines could occur through an inadequately sealed shaft.
10 Sections 8.3 and 8.4 demonstrated that the compacted salt column will consolidate to a low
11 permeability following repository closure. Appendix D of Appendix I2 in the permit application
12 and Section 7 show that the DRZ surrounding the long-term clay and crushed salt seal
13 components will completely heal within the first several decades. As a result, upward migration
14 at the base of the Salado salt is predicted to be approximately 1 m³ over the regulatory period.
15 At the Rustler/Salado contact, a total of approximately 20 m³ migrates through the sealed AIS
16 over the regulatory period. The only brine sources between these two depths are the marker
17 beds. It can therefore be concluded that most of the brine flow reaching the Rustler/Salado
18 contact originates in marker beds above the repository horizon. The seal system effectively
19 limits the flow of brine and gas from the repository through the sealed shafts throughout the
20 regulatory period.

21 **8.6 Intra-Rustler Flow**

22 The potential exists for vertical flow within water-bearing strata of the Rustler Formation. Flow
23 rates were estimated using a closed form solution of the steady-state saturated flow equation
24 (Darcy's Law). The significance of the calculated flow rates can be assessed in terms of the
25 width of the hydraulic disturbance (i.e., plume half-width) generated in the recipient flow field.
26 The plume half-width was calculated to be minimal for all expected conditions (Section C7).
27 Intra-Rustler flow is therefore concluded to be of such a limited quantity that (1) it will not affect
28 either the hydraulic or chemical regime in the Rustler and (2) it will not be detrimental to the seal
29 system.

9. Conclusions

The principal conclusion drawn from discussions in the previous sections and details provided in the appendices is that an effective, implementable design has been documented for the WIPP shaft sealing system. Specifically, the six elements of the Design Guidance, Table I2-12, are implemented in the design in the following manner:

1. The shaft sealing system shall limit the migration of radiological or other hazardous constituents from the repository horizon to the regulatory boundary during the 10,000-year regulatory period following closure.

Based on the analysis presented in Section 8.5, it was determined that this shaft sealing system effectively limits the migration of radiological or other hazardous constituents from the repository horizon to the regulatory boundary during the 10,000-year regulatory period following closure.

2. The shaft sealing system shall limit groundwater flowing into and through the shaft sealing system.

The combination of the seal components in the Salado Formation, the Rustler Formation, and above the Rustler combine to produce a robust system. Based on analysis presented in Section 8.3, it was concluded that the magnitude of brine flow that can reach the repository through the sealed shaft is minimal and will not impact repository performance.

3. The shaft sealing system shall limit chemical and mechanical incompatibility of seal materials with the seal environment.

The sealing system components are constructed of materials possessing high durability and compatibility with the host rock. Engineered materials including salt-saturated concrete, bentonite, clays, and asphalt are expected to retain their design properties over the regulatory period.

4. The shaft sealing system shall limit the possibility for structural failure of individual components of the sealing system.

Analysis of components has determined that: (a) the structural integrity of concrete components will not be compromised by induced radial stress, imposed vertical stress, temperature gradients, dynamic compaction of overlying materials, or swelling pressure associated with bentonite (Section 7.4.1); (b) the thermal impact of asphalt on the creep rate of the salt surrounding the asphalt waterstops is negligible (Section 7.4.4); and (c) the pressure from the asphalt element of the concrete-asphalt waterstops is sufficient to initiate healing of the surrounding DRZ within two years of emplacement (Section 7.6.1). The potential for structural failure of sealing components is minimized by the favorable compressive stress state that will exist in the sealed WIPP shafts.

5. The shaft sealing system shall limit subsidence of the ground surface in the vicinity of the shafts and the possibility of accidental entry after sealing.

The use of high density sealing materials that completely fill the shafts eliminates the potential for shaft wall collapse, eliminates the possibility of accidental entry after closure, and assures that local surface depressions will not occur at shaft locations.

6. The shaft sealing system shall limit the need to develop new technologies or materials for construction of the shaft sealing system.

1 The shaft sealing system utilizes existing construction technologies (identified in
2 Section 6) and materials (identified in Section 5).

3 The design guidance can be summarized as focusing on two principal questions: Can you build
4 it, and will it work? The use or adaptation of existing technologies for the placement of the seal
5 components combined with the use of available, common materials assure that the design can
6 be constructed. Performance of the sealing system has been demonstrated in the hydrologic
7 analyses that show very limited flows of gas or brine, in structural analyses that assure
8 acceptable stress and deformation conditions, and in the use of low permeability materials that
9 will function well in the environment in which they are placed. Confidence in these conclusions
10 is bolstered by the basic design approach of using multiple components to perform each
11 intended sealing function and by using extensive lengths within the shafts to effect a sealing
12 system. Additional confidence is added by the results of field and lab tests in the WIPP
13 environment that support the data base for the seal materials.

10. References

- Ahrens, E.H., and F.D. Hansen. 1995. *Large-Scale Dynamic Compaction Demonstration Using WIPP Salt: Fielding and Preliminary Results*. SAND95-1941. Albuquerque, NM: Sandia National Laboratories. (Copy on file in the Sandia WIPP Central Files, Sandia National Laboratories, Albuquerque, NM [SWCF] as WPO31104.)
- Ahrens, E.H., and M. Onofrei. 1996. "Ultrafine Cement Grout for Sealing Underground Nuclear Waste Repositories," *2nd North American Rock Mechanics Symposium (NARMS 96), Montreal, Quebec, June 19-21, 1996*. SAND96-0195C. Albuquerque, NM: Sandia National Laboratories. (Copy on file in the SWCF as WPO31251.)
- Ahrens, E.H., T.F. Dale, and R.S. Van Pelt. 1996. *Data Report on the Waste Isolation Pilot Plant Small-Scale Seal Performance Test, Series F Grouting Experiment*. SAND93-1000. Albuquerque, NM: Sandia National Laboratories. (Copy on file in the SWCF as WPO37355.)
- Andersen, P.J., M.E. Andersen, and D. Whiting. 1992. *A Guide to Evaluating Thermal Effects in Concrete Pavements*. SHRP-C/FR-92-101. Washington, DC: Strategic Highway Research Program, National Research Council. (Copy on file in the SWCF.)
- Avis, J.D., and G.J. Saulnier, Jr. 1990. *Analysis of the Fluid-Pressure Responses of the Rustler Formation at H-16 to the Construction of the Air-Intake Shaft at the Waste Isolation Pilot Plant (WIPP) Site*. SAND89-7067. Albuquerque, NM: Sandia National Laboratories. (Copy on file in the SWCF as WPO24168.)
- Bachman, G.O. 1987. *Karst in Evaporites in Southeastern New Mexico*. SAND86-7078. Albuquerque, NM: Sandia National Laboratories. (Copy on file in the SWCF as WPO24006.)
- Beauheim, R.L. 1987. *Interpretations of Single-Well Hydraulic Tests Conducted at and Near the Waste Isolation Pilot Plant (WIPP) Site, 1983-1987*. SAND87-0039. Albuquerque, NM: Sandia National Laboratories. (Copy on file in the SWCF as WPO27679.)
- Beauheim, R.L., R.M. Roberts, T.F. Dale, M.D. Fort, and W.A. Stensrud. 1993. *Hydraulic Testing of Salado Formation Evaporites at the Waste Isolation Pilot Plant Site: Second Interpretive Report*. SAND92-0533. Albuquerque, NM: Sandia National Laboratories. (Copy on file in the SWCF as WPO23378.)
- Brinster, K.F. 1991. *Preliminary Geohydrologic Conceptual Model of the Los Medaños Region Near the Waste Isolation Pilot Plant for the Purpose of Performance Assessment*. SAND89-7147. Albuquerque, NM: Sandia National Laboratories. (Copy on file in the SWCF as WPO27781.)
- Brodsky, N.S. 1994. *Hydrostatic and Shear Consolidation Tests with Permeability Measurements on Waste Isolation Pilot Plant Crushed Salt*. SAND93-7058. Albuquerque, NM: Sandia National Laboratories. Brodsky, N.S., D.H. Zeuch, and D.J. Holcomb. 1995. "Consolidation and Permeability of Crushed WIPP Salt in Hydrostatic and Triaxial Compression," *Rock Mechanics Proceedings of the 35th U.S. Symposium, University of*

1 Nevada, Reno, NV, June 5-7, 1995. Eds. J.J.K. Daemen and R.A. Schultz. Brookfield, VT: A.A.
2 Balkema. 497-502. (Copy on file in the SWCF as WPO22432.)

3 Brodsky, N.S., F.D. Hansen, and T.W. Pfeifle. 1996. "Properties of Dynamically Compacted
4 WIPP Salt," *4th International Conference on the Mechanical Behavior of Salt, Montreal,*
5 *Quebec, June 17-18, 1996.* SAND96-0838C. Albuquerque, NM: Sandia National Laboratories.
6 (Copy on file at the Technical Library, Sandia National Laboratories, Albuquerque, NM.)

7 Callahan, G.D., M.C. Loken, L.D. Hurtado, and F.D. Hansen. 1996. "Evaluation of Constitutive
8 Models for Crushed Salt," *4th International Conference on the Mechanical Behavior of Salt,*
9 *Montreal, Quebec, June 17-18, 1996.* SAND96-0791C. Albuquerque, NM: Sandia National
10 Laboratories. (Copy on file in the SWCF as WPO36449.)

11 Cauffman, T.L., A.M. LaVenue, and J.P. McCord. 1990. *Ground-Water Flow Modeling of the*
12 *Culebra Dolomite. Volume II: Data Base.* SAND89-7068/2. Albuquerque, NM: Sandia National
13 Laboratories. (Copy on file in the SWCF as WPO10551.)

14 Dale, T., and L.D. Hurtado. 1996. "WIPP Air-Intake Shaft Disturbed-Rock Zone Study," *4th*
15 *International Conference on the Mechanical Behavior of Salt, Montreal, Quebec, June 17-18,*
16 *1996.* SAND96-1327C. Albuquerque, NM: Sandia National Laboratories. (Copy on file in the
17 SWCF.)

18 DOE (U.S. Department of Energy). 1995. *Waste Isolation Pilot Plant Sealing System Design*
19 *Report.* DOE/WIPP-95-3117. Carlsbad, NM: U.S. Department of Energy, Waste Isolation Pilot
20 Plant. (Copy on file in the SWCF as WPO29062.)

21 EPA (Environmental Protection Agency). 1996a. *Criteria for the Certification and Re-*
22 *Certification of the Waste Isolation Pilot Plant's Compliance with the 40 CFR Part 191 Disposal*
23 *Regulations. Response to Comments Document for 40 CFR Part 194.* EPA 402-R-96-001.
24 Washington, DC: U.S. Environmental Protection Agency, Office of Radiation and Indoor Air.
25 (Copy on file in the Nuclear Waste Management Library, Sandia National Laboratories,
26 Albuquerque, NM.)

27 EPA (Environmental Protection Agency). 1996b. *Criteria for the Certification and Re-*
28 *Certification of the Waste Isolation Pilot Plant's Compliance with the 40 CFR Part 191 Disposal*
29 *Regulations. Background Information Document for 40 CFR Part 194.* EPA 402-R-96-002.
30 Washington, DC: U.S. Environmental Protection Agency, Office of Radiation and Indoor Air.
31 (Copy on file in the Nuclear Waste Management Library, Sandia National Laboratories,
32 Albuquerque, NM.)

33 Gray, M.N. 1993. *OECD/NEA International Stripa Project. Overview Volume III: Engineered*
34 *Barriers.* Stockholm, Sweden: SKB, Swedish Nuclear Fuel and Waste Management Company.
35 (Copy on file in the Nuclear Waste Management Library, Sandia National Laboratories,
36 Albuquerque, NM as TD898.2 .G73 1993.)

37 Hansen, F.D., and E.H. Ahrens. 1996. "Large-Scale Dynamic Compaction of Natural Salt," *4th*
38 *International Conference on the Mechanical Behavior of Salt, Montreal, Quebec, June 17-18,*

1996. SAND96-0792C. Albuquerque, NM: Sandia National Laboratories. (Copy on file in the SWCF as WPO39544.)

Hansen, F.D., E.H. Ahrens, A.W. Dennis, L.D. Hurtado, M.K. Knowles, J.R. Tillerson, T.W. Thompson, and D. Galbraith. 1996. "A Shaft Seal System for the Waste Isolation Pilot Plant," *Proceedings of SPECTRUM '96, Nuclear and Hazardous Waste Management, International Topical Meeting, American Nuclear Society/Department of Energy Conference, Seattle, WA, August 18-23, 1996*. SAND96-1100C. Albuquerque, NM: Sandia National Laboratories. (Copy on file in the SWCF as WPO39369.)

Haug, A., V.A. Kelley, A.M. LaVenue, and J.F. Pickens. 1987. *Modeling of Ground-Water Flow in the Culebra Dolomite at the Waste Isolation Pilot Plant (WIPP) Site: Interim Report*. SAND86-7167. Albuquerque, NM: Sandia National Laboratories. (Copy on file in the SWCF as WPO28486.) Hills, J.M. 1984. "Sedimentation, Tectonism, and Hydrocarbon Generation in [the] Delaware Basin, West Texas and Southeastern New Mexico," *American Association of Petroleum Geologists Bulletin*. Vol. 68, no. 3, 250-267. (Copy on file in the SWCF.)

Holt, R.M., and D.W. Powers. 1990. *Geologic Mapping of the Air Intake Shaft at the Waste Isolation Pilot Plant*. DOE-WIPP 90-051. Carlsbad, NM: Westinghouse Electric Corporation for U.S. Department of Energy. (Copy on file in the Nuclear Waste Management Library, Sandia National Laboratories, Albuquerque, NM.)

Knowles, M.K., and C.L. Howard. 1996. "Field and Laboratory Testing of Seal Materials Proposed for the Waste Isolation Pilot Plant," *Proceedings of the Waste Management 1996 Symposium, Tucson, AZ, February 25-29, 1996*. SAND95-2082C. Albuquerque, NM: Sandia National Laboratories. (Copy on file in the SWCF as WPO30945.)

Knowles, M.K., D. Borns, J. Fredrich, D. Holcomb, R. Price, D. Zeuch, T. Dale, and R.S. Van Pelt. 1996. "Testing the Disturbed Zone Around a Rigid Inclusion in Salt," *4th Conference on the Mechanical Behavior of Salt, Montreal, Quebec, June 17-18, 1996*. SAND95-1151C. Albuquerque, NM: Sandia National Laboratories. (Copy on file in the SWCF.)

Lambert, S.J. 1992. "Geochemistry of the Waste Isolation Pilot Plant (WIPP) Site, Southeastern New Mexico, U.S.A.," *Applied Geochemistry*. Vol. 7, no. 6, 513-531. (Copy on file in the SWCF as WPO26361.)

LaVenue, A.M., T.L. Cauffman, and J.F. Pickens. 1990. *Ground-Water Flow Modeling of the Culebra Dolomite. Volume I: Model Calibration*. SAND89-7068/1. Albuquerque, NM: Sandia National Laboratories. (Copy on file in the SWCF as WPO24085.)

Mercer, J.W. 1983. *Geohydrology of the Proposed Waste Isolation Pilot Plant Site, Los Medanos Area, Southeastern New Mexico*. Water-Resources Investigations Report 83-4016. Albuquerque, NM: U.S. Geological Survey, Water Resources Division. (Copy on file in the Nuclear Waste Management Library, Sandia National Laboratories, Albuquerque, NM.) (Copy on file in the SWCF.)

Mercer, J.W., and B.R. Orr. 1979. *Interim Data Report on the Geohydrology of the Proposed Waste Isolation Pilot Plant Site, Southeast New Mexico*. Water-Resources Investigations Report

1 79-98. Albuquerque, NM: U.S. Geological Survey, Water Resources Division. (Copy on file in
2 the SWCF.)

3 Nowak, E.J., J.R. Tillerson, and T.M. Torres. 1990. *Initial Reference Seal System Design:*
4 *Waste Isolation Pilot Plant*. SAND90-0355. Albuquerque, NM: Sandia National Laboratories.
5 (Copy on file in the SWCF as WPO23981.)

6 Pfeifle, T.W., F.D. Hansen, and M.K. Knowles. 1996. "Salt-Saturated Concrete Strength and
7 Permeability," *4th Materials Engineering Conference, ASCE Materials Engineering Division,*
8 *Washington, DC, November 11-18, 1996*. Albuquerque, NM: Sandia National Laboratories.)

9 Powers, D.W., S.J. Lambert, S-E. Shaffer, L.R. Hill, and W.D. Weart, eds. 1978. *Geological*
10 *Characterization Report Waste Isolation Plant (WIPP) Site, Southeastern New Mexico.*
11 SAND78-1596. Albuquerque, NM: Sandia National Laboratories. Vols. I-II. (Copy on file in the
12 SWCF as WPO5448, WPO26829-26830.)

13 Saulnier, G.J., Jr., and J.D. Avis. 1988. *Interpretation of Hydraulic Tests Conducted in the*
14 *Waste-Handling Shaft at the Waste Isolation Pilot Plant (WIPP) Site*. SAND88-7001.
15 Albuquerque, NM: Sandia National Laboratories. (Copy on file in the SWCF as WPO24164.)

16 Stormont, J.C. 1984. *Plugging and Sealing Program for the Waste Isolation Pilot Plant (WIPP).*
17 SAND84-1057. Albuquerque, NM: Sandia National Laboratories. (Copy on file in the SWCF as
18 WPO24698.)

19 Van Sambeek, L.L., D.D. Luo, M.S. Lin, W. Ostrowski, and D. Oyenuga. 1993. *Seal Design*
20 *Alternatives Study*. SAND92-7340. Albuquerque, NM: Sandia National Laboratories. (Copy on
21 file in the SWCF as WPO23445.)

22 Vine, J.D. 1963. *Surface Geology of the Nash Draw Quadrangle, Eddy County, New Mexico.*
23 Geological Survey Bulletin 1141-B. Washington, DC: U.S. Government Printing Office. (Copy on
24 file in the SWCF as WPO39558.)

25 Wing, N.R., and G.W. Gee. 1994. "Quest for the Perfect Cap," *Civil Engineering*. Vol. 64, no. 10,
26 38-41. (Copy on file in the SWCF as WPO21158.)

FIGURES

(This page intentionally blank)

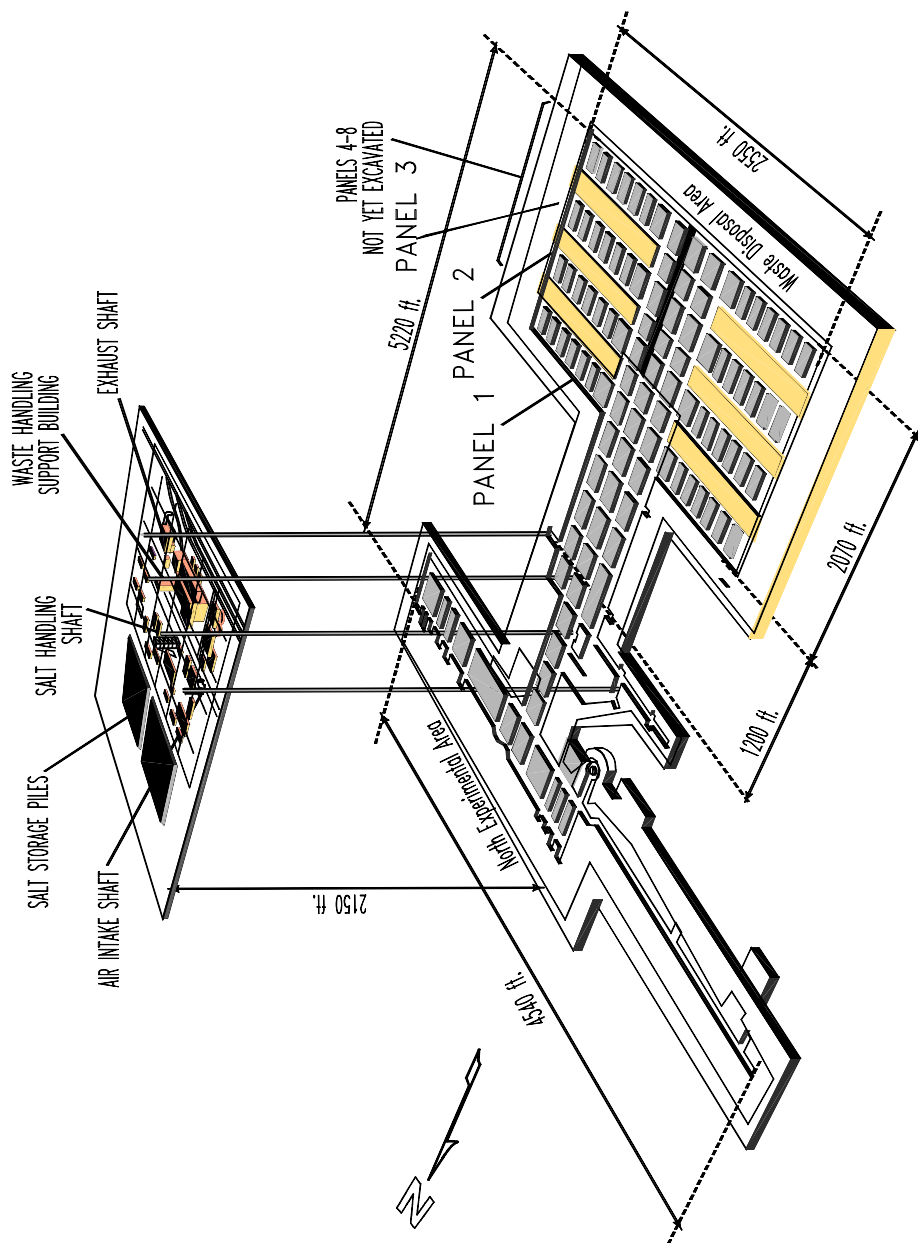


Figure I2-1
View of the WIPP underground facility

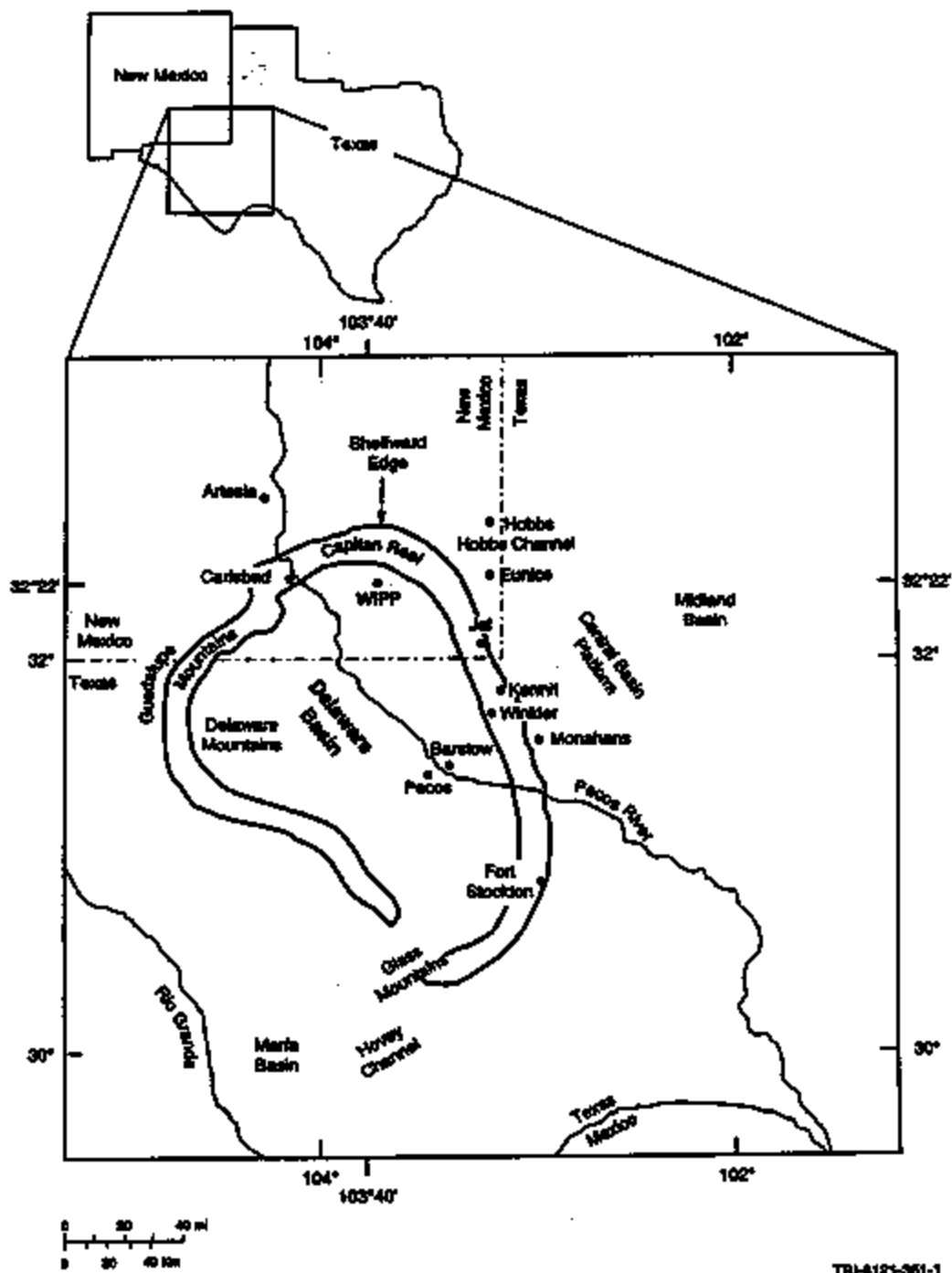


Figure I2-2
Location of the WIPP in the Delaware Basin

Erathem	System	Series	Lithostratigraphic Unit	Age Estimate (yr)
Cenozoic	Quaternary	Holocene	Windblown sand	
		Pleistocene	Mescalero caliche	~500,000
			Gatulia Formation	~600,000
	Tertiary	Pliocene		
			Ogallala Formation	5.5 million
		Miocene		24 million
		Oligocene	Absent in southeastern New Mexico	
		Eocene		
		Paleocene		66 million
	Cretaceous	Upper	Absent in southeastern New Mexico	
		Lower	Detritus preserved	144 million
Mesozoic	Jurassic		Absent in southeastern New Mexico	
				208 million
	Triassic	Upper	Dockum Group	
		Lower	Absent in southeastern New Mexico	245 million
Paleozoic	Upper	Ochoan	Dewey Lake Redbeds	
			Rustler Formation	
			Salado Formation	
	Permian		Castile Formation	
		Guadalupian	Capitan Limestone and Bell Canyon Formation	
	Lower			
	Leonardian	Bone Springs		
	Wolfcampian	Wolfcamp (informal)	286 million	

Modified from Bachman, 1987

Figure 12-5
Chart showing major stratigraphic divisions, southeastern New Mexico

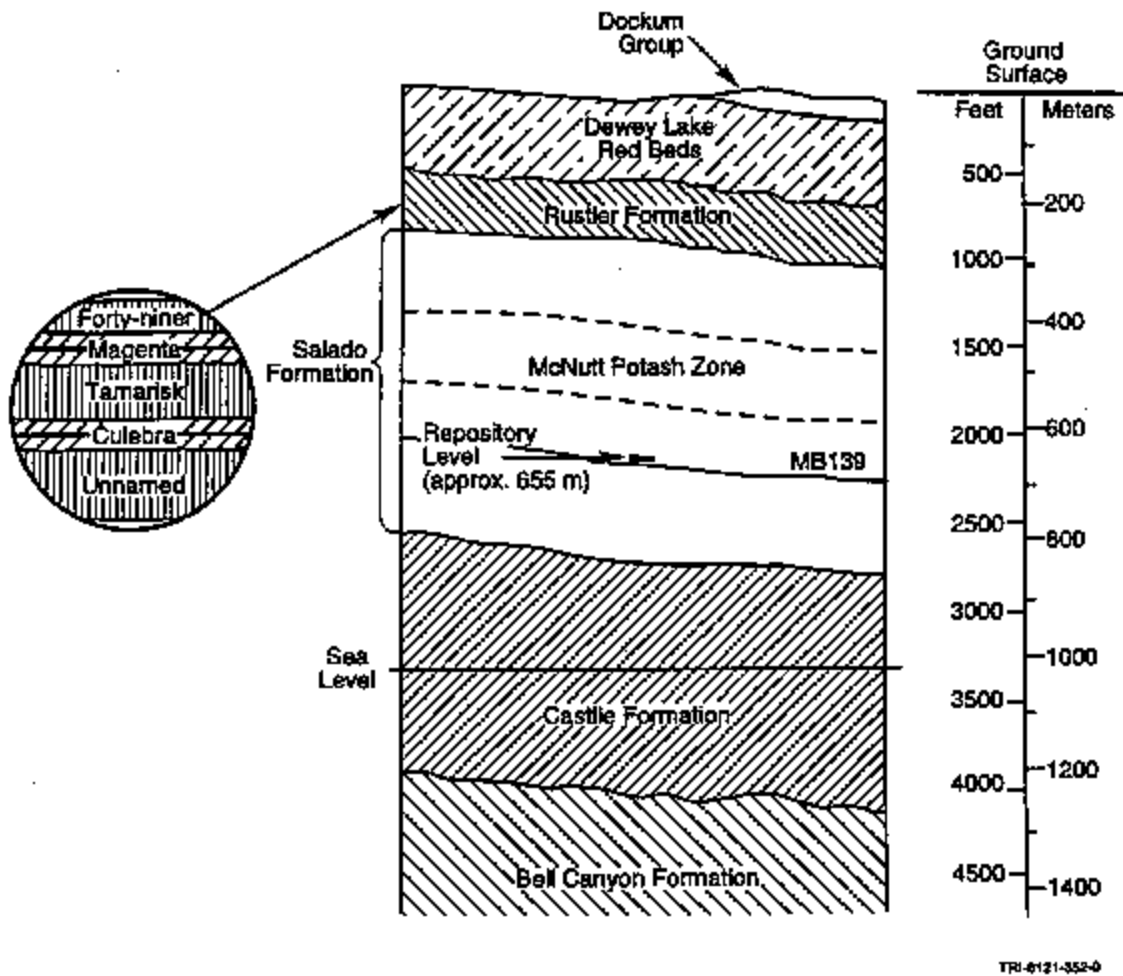


Figure I2-4
Generalized stratigraphy of the WIPP site showing repository level

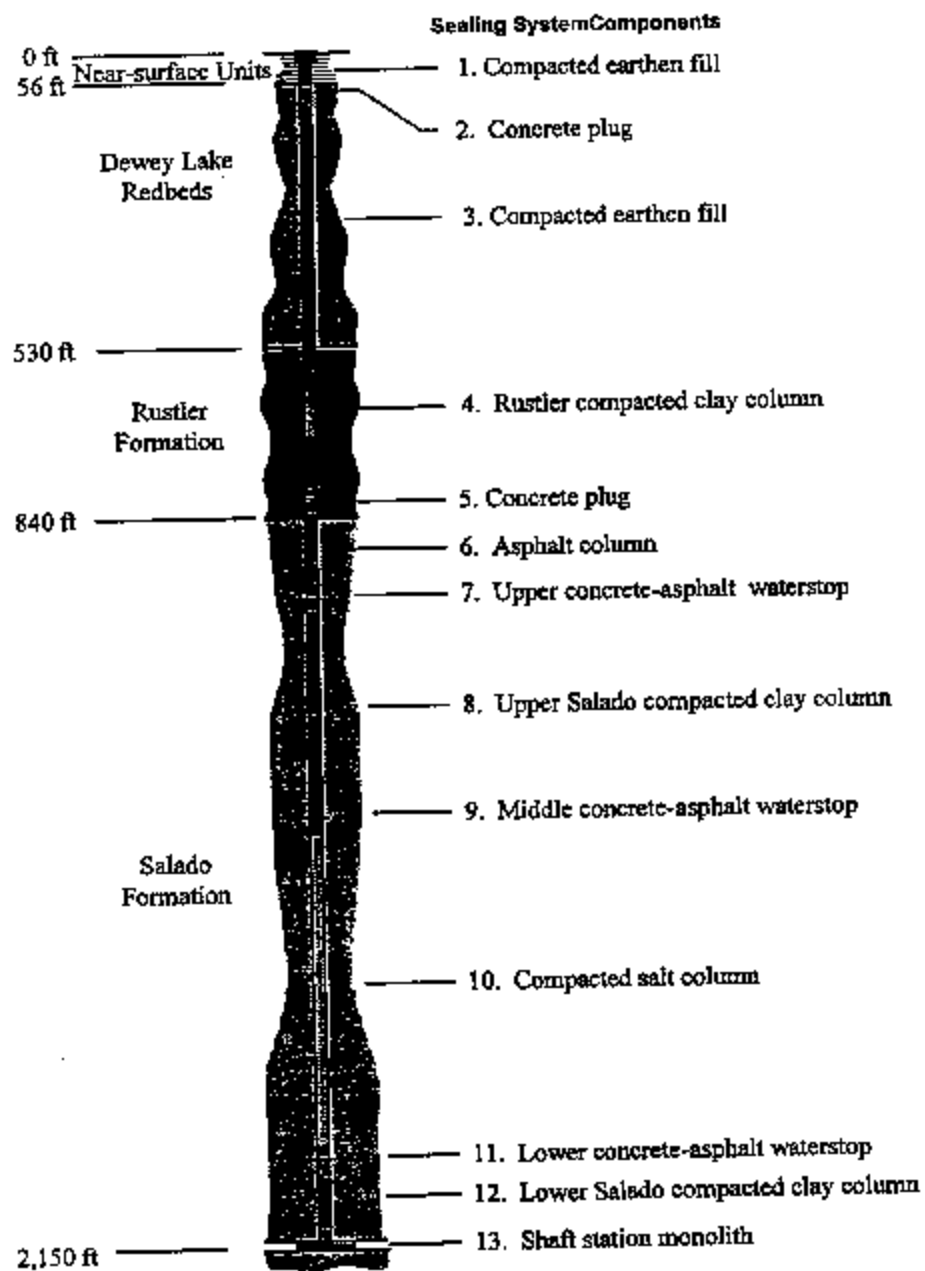


Figure I2-5
Arrangement of the Air Intake Shaft sealing system

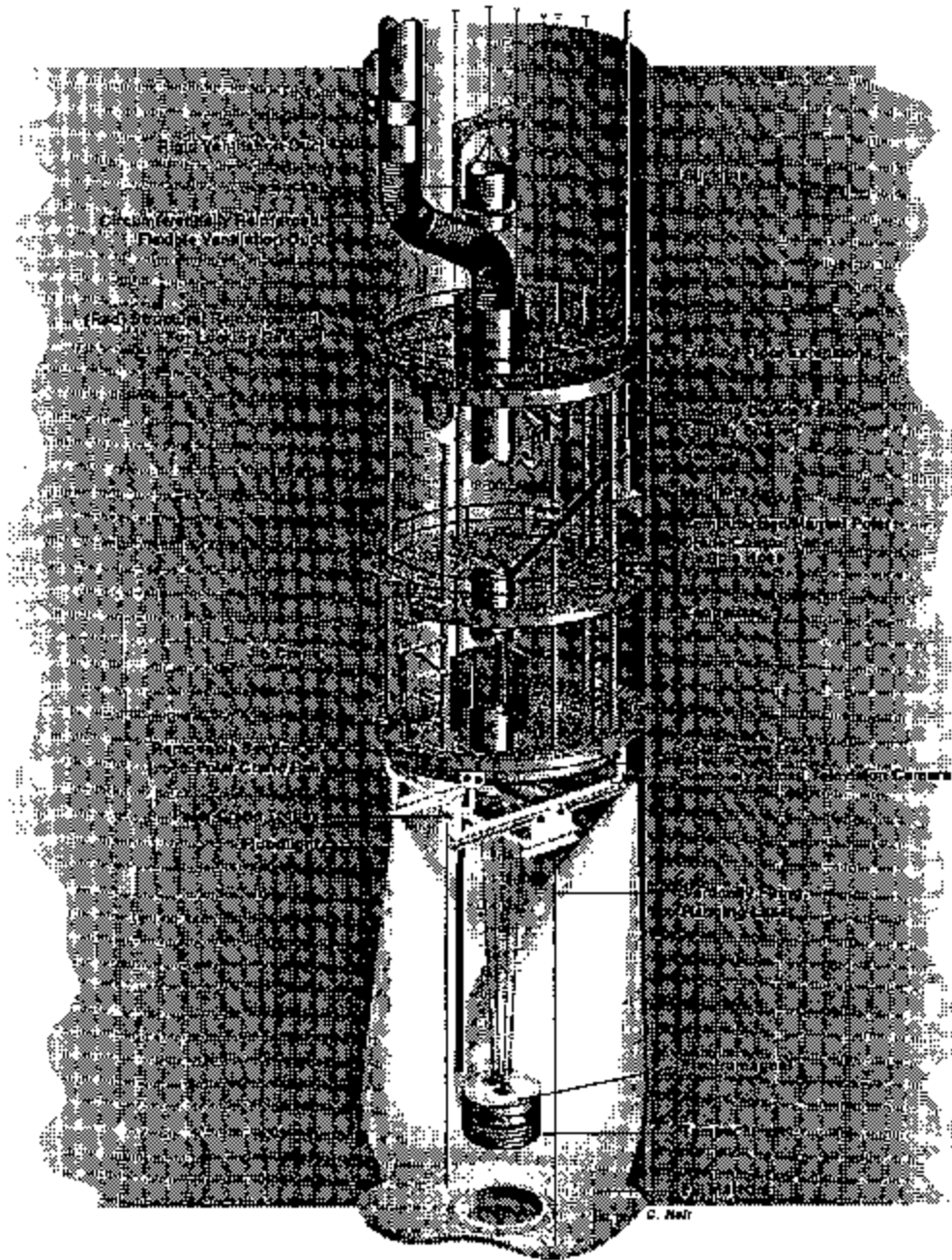


Figure I2-6
Multi-deck stage illustrating dynamic compaction

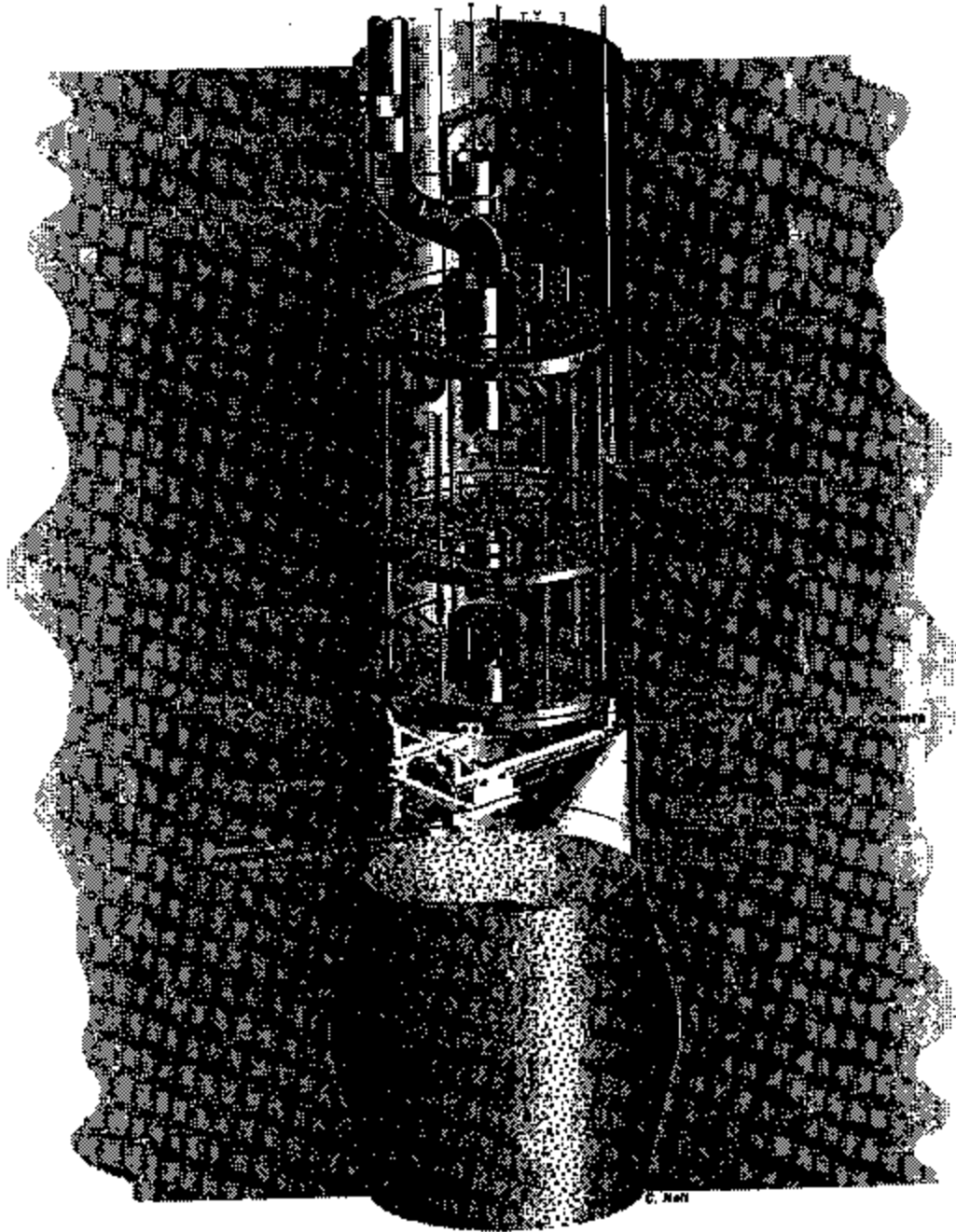
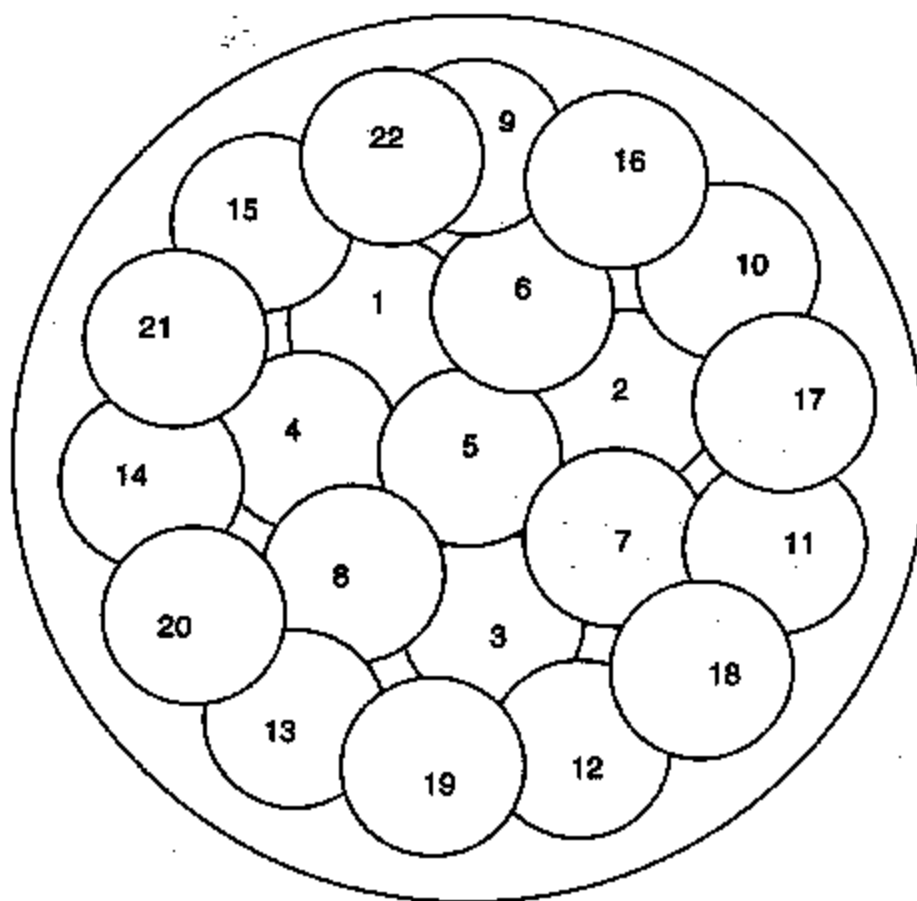


Figure I2-7
Multi-deck stage illustrating excavation for asphalt waterstop



Scale: 1" = 4'

TP-4121-376-0

Figure I2-8
Drop pattern for 6-m-diameter shaft using a 1.2-m-diameter tamper

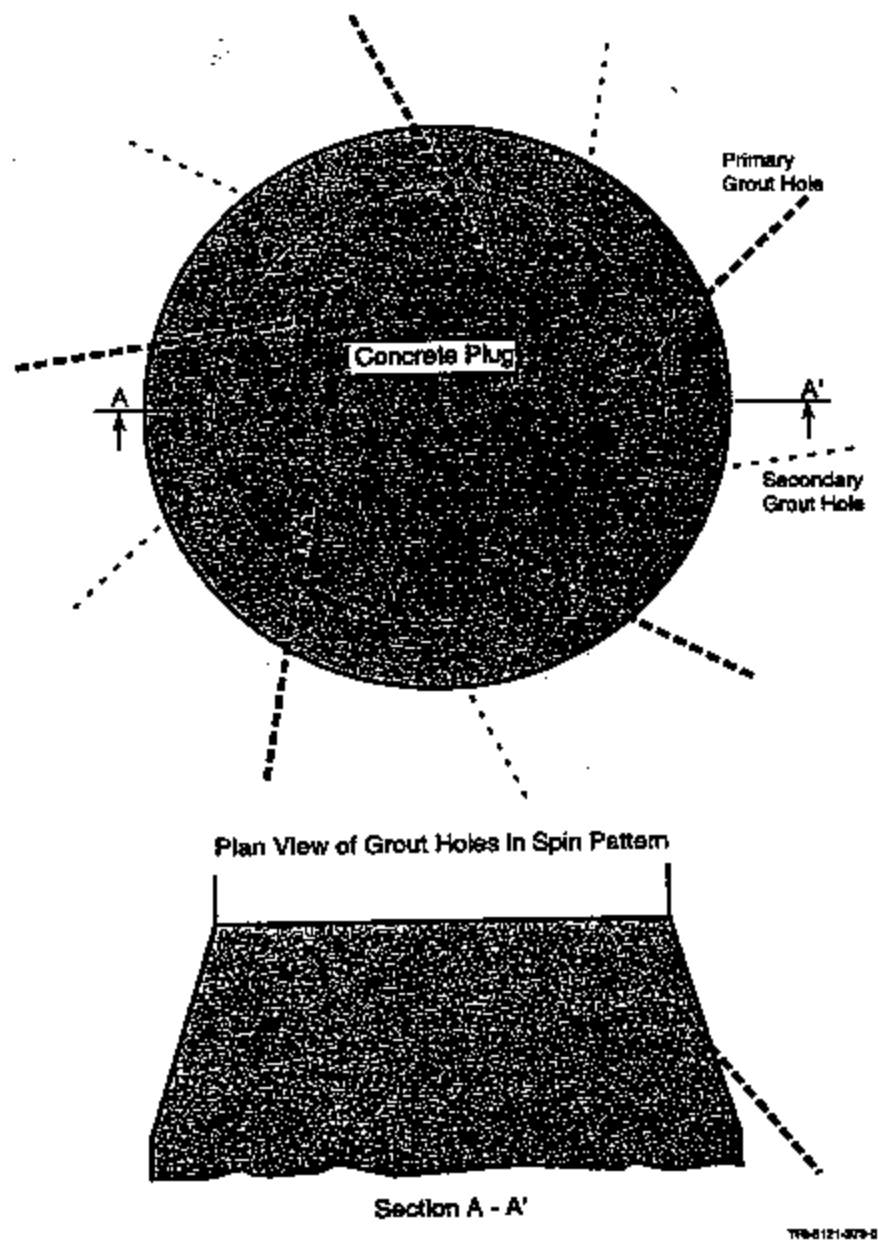
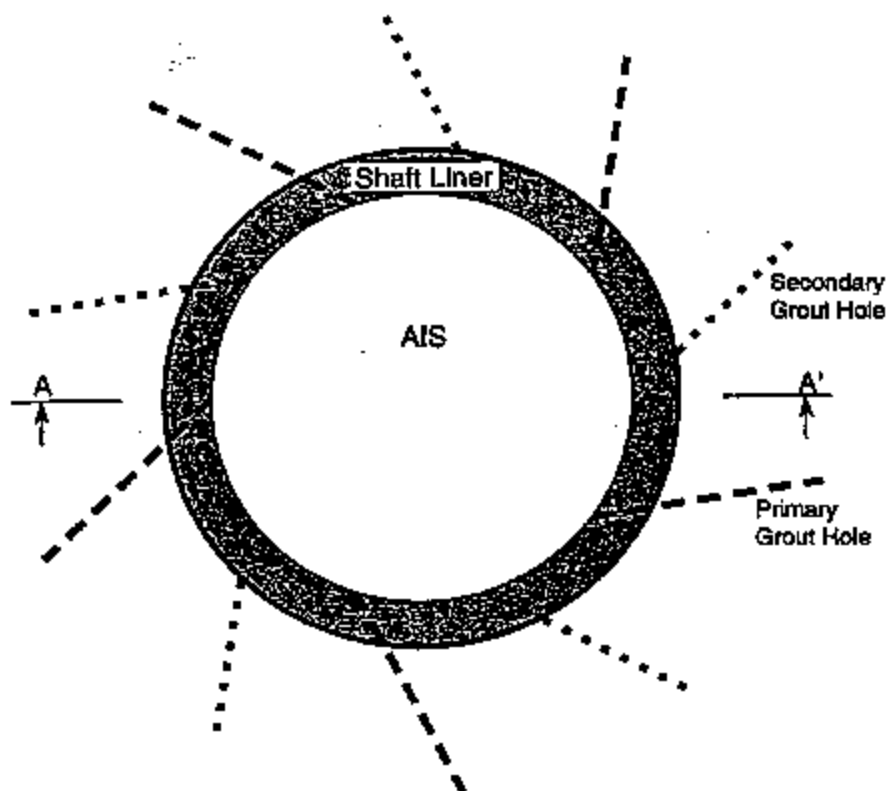


Figure I2-9
Plan and section views of downward spin pattern of grout holes



Plan View of Grout Holes in Spin Pattern



Section A - A'

TTR-6121-974-0

Figure I2-10
Plan and section views of upward spin pattern of grout holes

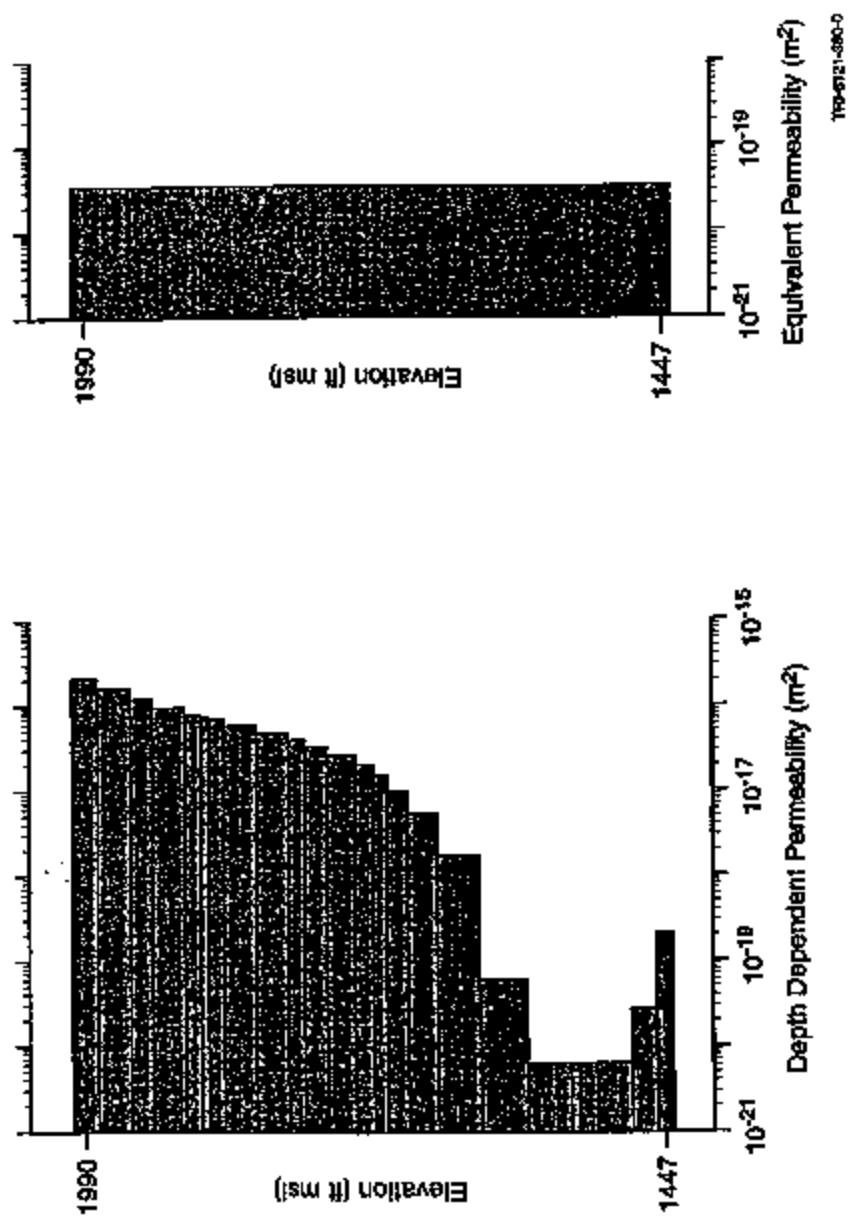


Figure I2-11
Example of calculation of an effective salt column permeability from the depth-
dependent permeability at a point in time

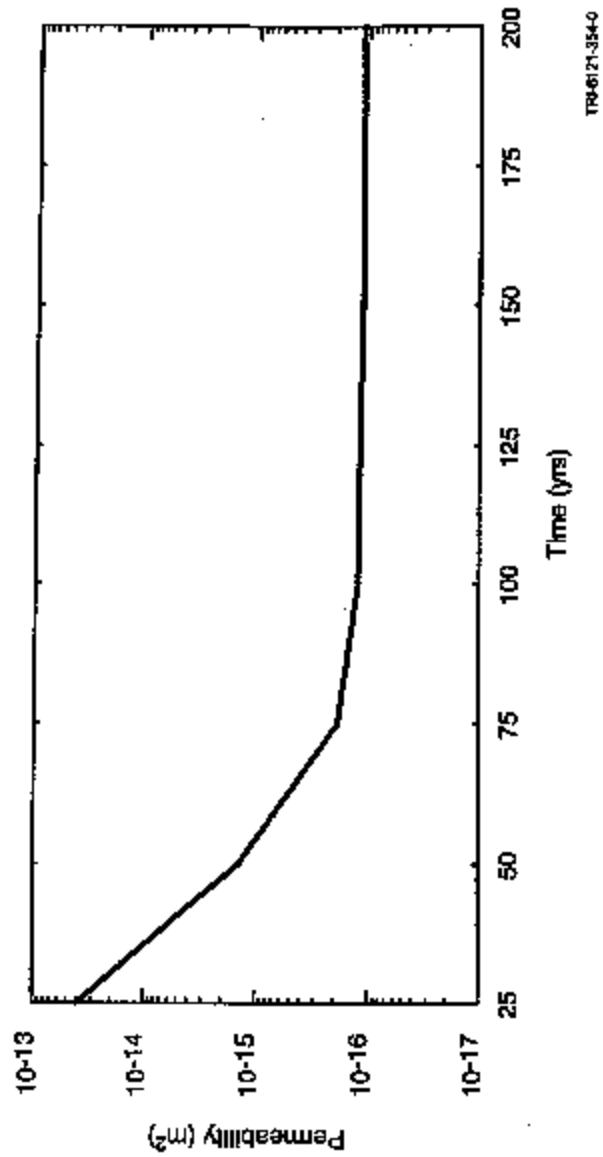


Figure I2-12
Effective permeability of the compacted salt column using the 95% certainty line